

# **Energy Harvesting Using Piezoelectric Elements to Power Microelectronic Devices**

*Thesis submitted in fulfilment of the requirements for the degree of*

**DOCTOR OF PHILOSOPHY**

By

**Ritendra Mishra**

Enrollment No. 126003

Under the Supervision of

**Dr. Shruti Jain**

**Dr. C Durgaprasad**



**DEPARTMENT OF ELECTRONICS AND COMMUNICATION  
ENGINEERING  
JAYPEE UNIVERSITY OF INFORMATION TECHNOLOGY  
WAKNAGHAT, SOLAN - 173234, INDIA**

**AUGUST-2016**

# TABLE OF CONTENTS

---

|   |                   |
|---|-------------------|
| <b>TABLE OF CONTENTS</b>                                      | <b><i>i</i></b>   |
| <b>DECLARATION BY CANDIDATE</b>                               | <b><i>iv</i></b>  |
| <b>SUPERVISOR'S CERTIFICATE</b>                               | <b><i>v</i></b>   |
| <b>ACKNOWLEDGMENT</b>   | <b><i>vi</i></b>  |
| <b>ABSTRACT</b>   | <b><i>ix</i></b>  |
| <b>LIST OF ABBREVIATIONS</b>                                  | <b><i>xi</i></b>  |
| <b>LIST OF FIGURES</b>  | <b><i>xii</i></b> |
| <b>LIST OF TABLES</b>   | <b><i>xvi</i></b> |
| <b>CHAPTER 1</b>  | <b><i>1</i></b>   |
| <b>INTRODUCTION</b>   | <b><i>1</i></b>   |
| <b>1.1 THE SOURCES OF AMBIENT ENERGY</b>                      | <b><i>3</i></b>   |
| 1.1.1 Natural sources   | <i>3</i>          |
| 1.1.2 Anthropogenic sources                                   | <i>5</i>          |
| <b>1.2 ENERGY HARVESTING – STATE OF THE ART</b>               | <b><i>6</i></b>   |
| <b>1.3 ENERGY HARVESTING METHODS</b>                          | <b><i>11</i></b>  |
| 1.3.1 Piezoelectricity  | <i>13</i>         |
| 1.3.2 Piezoelectric materials                                 | <i>14</i>         |
| 1.3.3 Piezoelectric Material Properties                       | <i>14</i>         |
| 1.3.4 Hard and Soft Piezoceramic Materials                    | <i>16</i>         |
| 1.3.5 Active and Passive Piezo Materials                      | <i>17</i>         |
| 1.3.6 Unimorphs and Bimorphs                                  | <i>17</i>         |
| <b>1.4 APPROACH</b>   | <b><i>18</i></b>  |
| <b>1.5 SUMMARY OF CONTRIBUTIONS</b>                           | <b><i>20</i></b>  |
| <b>CHAPTER 2</b>  | <b><i>22</i></b>  |
| <b>LITERATURE SURVEY</b>                                      | <b><i>22</i></b>  |
| <b>2.1 PIEZOELECTRIC ENERGY HARVESTING</b>                    | <b><i>23</i></b>  |
| <b>2.2 PIEZOELECTRIC ENERGY HARVESTING ELEMENTS</b>           | <b><i>25</i></b>  |
| <b>2.3 PIONEERING WORK ON ANTHROPOGENIC PIEZO HARVESTERS</b>  | <b><i>30</i></b>  |
| <b>2.4 FABRICATION OF A FLEXIBLE PIEZOCOMPOSITE GENERATOR</b> | <b><i>35</i></b>  |
| <b>2.5 CONCLUSION</b>   | <b><i>37</i></b>  |
| <b>CHAPTER 3</b>  | <b><i>38</i></b>  |

|  |            |
|--|------------|
| <b>DEVELOPMENT OF PIEZOELECTRIC ENERGY GENERATORS</b>  | <b>38</b>  |
| <b>3.1 EXPERIMENTAL TESTING OF PIEZO BUZZERS (HIGHER FREQUENCY LOW AMPLITUDE)</b>                  | <b>40</b>  |
| <b>3.2 RESULTS AND DISCUSSIONS</b>   | <b>44</b>  |
| 3.2.1 Effect of mechanical pre-stress on output voltage  | 44         |
| 3.2.2 Effect of mechanical pre-stress on resonance frequency                                       | 46         |
| 3.2.3 Power delivered to a resistive load  | 47         |
| <b>3.3 ASSEMBLY AND TESTING OF PIEZOCOMPOSITE DRUM HARVESTERS (HIGHER FREQUENCY LOW AMPLITUDE)</b> | <b>48</b>  |
| <b>3.4 EXPERIMENTAL PROCEDURE</b>  | <b>50</b>  |
| <b>3.5 RESULTS AND DISCUSSIONS</b>   | <b>53</b>  |
| <b>3.6 CONFIGURATION OF DRUM STACKS</b>  | <b>59</b>  |
| 3.6.1 Testing of the drum stacks with a custom footfall simulator                                  | 60         |
| 3.6.2 Results and discussions  | 62         |
| <b>3.7 SHOE-BASED ENERGY HARVESTERS</b>  | <b>64</b>  |
| 3.7.1 Experimental Procedure   | 67         |
| 3.7.2 Results and Discussions  | 67         |
| 3.7.3 Comparison of M1 and M2  | 73         |
| <b>3.8 CONCLUSION</b>  | <b>74</b>  |
| <b>CHAPTER 4</b>   | <b>76</b>  |
| <b>DEVELOPMENT OF ENERGY HARVESTING AND POWER CONDITIONING CIRCUITS</b>                            | <b>76</b>  |
| <b>4.1 AC TO DC CONVERSION</b>   | <b>79</b>  |
| 4.1.1 Standard Interface Analysis  | 79         |
| 4.1.2 MOSFET Bridge  | 81         |
| <b>4.2 NON-LINEAR PIEZOELECTRIC ENERGY HARVESTING CIRCUITS</b>                                     | <b>84</b>  |
| <b>4.3 CONCLUSION</b>  | <b>95</b>  |
| <b>CHAPTER 5</b>   | <b>96</b>  |
| <b>DEVELOPMENT OF ENERGY STORAGE MECHANISM</b>   | <b>96</b>  |
| <b>5.1 ANALYSIS OF ENERGY STORAGE ELEMENTS</b>   | <b>96</b>  |
| 5.1.1 Electrolytic capacitors  | 96         |
| 5.1.2 Supercapacitors  | 97         |
| 5.1.3 Lithium ion batteries  | 97         |
| 5.1.4 NiMH batteries   | 98         |
| <b>5.2 CHARGING OF CAPACITORS</b>  | <b>98</b>  |
| <b>5.3 CHARGING OF NiMH BATTERIES</b>  | <b>101</b> |
| <b>5.4 CONCLUSION</b>  | <b>103</b> |
| <b>CHAPTER 6</b>   | <b>104</b> |

|  |            |
|--|------------|
| <b>INTERFACING INTEGRATED ENERGY HARVESTING MODULE WITH<br/>SUITABLE APPLICATION</b> | <b>104</b> |
| <b>6.1 POWERING OF A MICROCONTROLLER</b>   | <b>105</b> |
| 6.1.1 Programming the Arduino Board  | 106        |
| 6.1.2 Flashing a LED   | 106        |
| <b>6.2 POWERING OF A RF TRANSMITTER</b>  | <b>107</b> |
| 6.2.1 RF Module  | 107        |
| 6.2.2 RF transmitter   | 108        |
| <b>6.3 CONCLUSION</b>  | <b>111</b> |
| <b>CHAPTER 7</b>   | <b>112</b> |
| <b>CONCLUSION AND FUTURE SCOPE</b>   | <b>112</b> |
| <b>PUBLICATIONS</b>  | <b>114</b> |
| <b>APPENDIX A</b>  | <b>127</b> |
| <b>APPENDIX B</b>  | <b>130</b> |
| <b>APPENDIX C</b>  | <b>133</b> |
| <b>APPENDIX D</b>  | <b>136</b> |

## DECLARATION BY CANDIDATE

---

I hereby declare that the work reported in the PhD thesis titled “**Energy Harvesting Using Piezoelectric Elements To Power Microelectronic Devices**” submitted at **Jaypee University of Information Technology, Wagnaghat, Solan, India** is an authentic record of my work carried out under the supervision of **Dr. Shruti Jain** and **Dr C. Durgaprasad**. I have not submitted this work partly or wholly elsewhere for the award of any other degree or diploma.

(Ritendra Mishra)

Department of Electronics & Communication Engineering

Jaypee University of Information Technology, Wagnaghat , India

Date:

## SUPERVISOR'S CERTIFICATE

---

This is to certify that the work reported in the PhD thesis titled “**Energy Harvesting Using Piezoelectric Elements To Power Microelectronic Devices**” submitted by **Ritendra Mishra** at **Jaypee University of Information Technology, Wagnaghat, Solan, India** is a bonafide record of his original work carried out under our supervision. This work has not been submitted elsewhere for any other degree or diploma.



Dr. Shruti Jain

Assistant Professor

Department of ECE

Jaypee University of Information  
Technology,

Wagnaghat , India

Date:

Dr. C Durgaprasad

Scientist ‘G’

Ceramics Division

Naval Materials Research  
Laboratory DRDO

Ambarnath , India

Date:

## ACKNOWLEDGMENT

---

*Hope is the thing with feathers; that perches on the soul,  
And sings the tune without the words; and never stops at all;  
And sweetest in the gale is heard; and sore must be the storm,  
That could abash the little bird, that kept so many warm;  
I've heard it in the chilliest land and on the strangest sea;  
Yet never, in extremity, it asked a crumb of me.*

My journey over the last 5 years has been one filled with hope and despair in equal measure. There were times of ecstasy and agony, elation as well as desolation. But it was hope that kept me moving forward. Along this journey I have met many people; some of whom were intrigued by my work, some who were skeptical, and many who derided it. I would like to express my gratitude to all of these people without whom my journey would be incomplete.

I would like to begin by expressing my profound gratitude towards my supervisor Dr. Shruti Jain who was always prompt in helping me out in any way she could even though we were far apart most of the time. She has been extremely supportive of me when it came to academics, familiarizing me with the nuances of the research world. She kept me on my toes for the whole duration of my PhD and it has been her perseverance that has enabled me to complete this work. I would also like to acknowledge Dr. P. K. Naik for his support.

It was an honor and pleasure working under my co-supervisor Dr. Chadalapaka Durgaprasad at NMRL. I will owe him a debt of gratitude forever for the care and

concern he has shown for me during my research work under him. Even though he was (and always is) extremely busy with work, he took out time daily to review my progress. He did not spare any resource at his disposal to help me out in my research. For that I'm thankful to him. Even while I was away from NMRL for several years, he would regularly enquire about my progress. It was his discipline and encouragement that helped me finish my thesis introduction years before I actually submitted it.

NMRL is one place of which I will always have fond memories. It's the place where I learnt a lot, including materials science. I made great acquaintances there and all of them were very helpful and appreciative of my work. I would like to thank Dr. Tapas Chongdar who facilitated my entry into NMRL and, without whom; I wouldn't be able to learn so much. He always had encouraging words and advice that were very helpful. Among others in the ceramics division, I would like to thank Mr. Subrat Sahu, Mr. Suresh Sonar, Mr. Dinesh for their technical guidance and help, Mr. Moses Jaisingh and Mr. Srinivas Rao for the regular discussions and provision of invaluable literature. I would like to thank the scientists from polymer division among whom Mr. Sangram Rath and Mr. Sivaraman were most helpful. I thank Mr. Jayendran and Mr. Shankar who were always forthcoming in providing me with any resource I needed. I would also like to thank the research scholars I had the good fortune of interacting with at NMRL who taught me lot. Finally, I would like to apologize if I have (because I have) missed out on a ton of other wonderful people's names who have been of great help at NMRL.

I would like to express my admiration and appreciation towards my supervisor at DIHAR Dr. Sunil Kumar Hota who, I believe, is one of the most dynamic people I've ever met. I am thankful to him for taking up quite a challenging project and giving me the opportunity to work in it. Every time I gave up hope, he had words of encouragement and advice with inspiring anecdotes from his own life and career. It was his "Live the dream, don't leave the dream" slogan that kept me going and, in a way, enabled me to finish what we had started. I also thank the former director of DIHAR Dr. R. B. Srivastava and the present director Dr. Bhuvnesh Kumar for their support.

I thank Mr. Navneet Bhagat, my CADD center trainer for teaching me simulation and modeling in a very engaging manner. He helped me out at a crucial time in my research when I was out of sorts trying to figure out how to complete my work. Even after my



course was over, he regularly lent a helping hand with any problem I faced related to my work.

I would like to thank all my peers (seniors and juniors alike) at DIHAR for their encouragement and support. Especially among them, I am indebted to Dr Saroj Kumar Das for nurturing me like an elder brother for the time we were together at DIHAR and even after that. I have learnt a lot from him. I thank Jagdish Arya, my batchmate, for giving me all those wonderful memories at Leh and elsewhere.

I am grateful to all my teachers from R D National College, especially Prof. Namrata Ajwani and Prof. Joga Rao, for instilling in us a culture of learning and moral values as much as (if not more than) my parents, which encouraged me to pursue a career in teaching and research.

Finally, I would like to express my utmost and heartfelt love and gratitude towards my family. Without their support, love and patience, I wouldn't be here. I would never be able to repay the debt I owe my mother who is the most selfless person I've ever known and who has always been there for me, from kindergarten to PhD, caring for me as her baby boy.

Date:

## ABSTRACT

---

As of 2013, the number of mobile electronic devices has surpassed the number of humans on the planet. Round-the-clock mobility and the need to stay connected have necessitated the development of a mobile and uninterrupted power source for these devices. Apart from mobile phones which are the fastest growing devices in the consumer electronics segment, wireless sensors networks are also a rapidly emerging area. They find application in defence, aerospace, structural health monitoring, environmental and wildlife monitoring, etc. Whereas the power requirements and size of these devices have shrunk drastically, the corresponding improvement in energy storage technology has not been at par. The reliance on batteries as the primary energy storage elements does not come without drawbacks. Batteries have limited storage capacities, need to be replaced and occupy unnecessary space. In many real world applications like medical implants and space exploration, it is not feasible to replace the batteries regularly. Such applications demand a self-contained power source that needs minimum maintenance and that can generate energy for long, indefinite periods of time.

Conventional energy sources are exhaustible, cause pollution and also alter and affect the environment adversely. In the near future, they will be exhausted and the possibility of an energy crisis may arise. Non-conventional energy sources, in particular renewable, present themselves as a very attractive and practicable alternative. Energy from the sun is almost inexhaustible and the world is increasingly relying on solar energy as a power source. Wind energy harvesting is also an emerging area. Advances in the area of energy harvesting have led to improvement in the technology and devices that can be used to capture these abundant sources of energy and utilize them. In addition to these macro sources, vibrations are also one of the most abundant sources of ambient energy and can be used as micro energy sources which can power microelectronic devices. The most common methods of vibration energy harvesting are the electromagnetic, electrostatic and piezoelectric methods. Each of these methods has advantages and drawbacks and finds suitability in select applications.

Human activity gives rise to dissipation of a lot of energy in the form of vibrations, impacts from human motion, machinery, etc. Active scavenging of this dissipated energy

can provide enough energy to power common microelectronic devices like mobile phones, smart wearables, medical implants, etc. as already demonstrated by many researchers, hobbyists and enthusiasts.

The present work attempts to design a generic energy harvester based on the piezoelectric method of energy harvesting. The aim is to fabricate a piezoelectric energy harvester that can be used to harvest energy from a variety of ambient vibration and impact energy sources. In particular, vibrations arising out of machines, buildings, household appliances, etc., which can range in frequency from less than 30 Hz to over 200 Hz but having low amplitude have been targeted. The suitability of the same energy harvesters as impact energy scavengers is also demonstrated by embedding them in shoes and harvesting energy from footfalls. The results indicate that useful amounts of energy can be obtained from commonly available piezoelectric buzzer elements that can be used to power microelectronic devices like microcontrollers and RF transmitter modules. Along with the development of a simple, low cost and durable energy harvester, a suitable energy harvesting circuit is also developed that suits different excitation profiles as described above. Finally, an energy storage element that can store the energy harvested and which is optimal for the present application is also employed. The comprehensive energy harvesting system is designed to work at sub-zero temperatures as one of the objectives of the present work was to develop an energy harvesting system for soldiers deployed at high altitude regions like Ladakh. The energy harvesting system is sensitive enough to be able to harvest energy from even small movements, keeping in mind that excessive movement is something inadvisable for troops in high altitude regions.

The methods described in the present work give a simple, efficient and affordable way to fabricate generic energy harvesters which can be used in a variety of environments and excitation profiles. The energy harvesting system designed herein has the potential to act as a supplementary power source for a variety of applications like emergency signalling, structural health monitoring, etc.

## LIST OF ABBREVIATIONS

---

|                |   |
|----------------|---|
| <b>DSSH</b>    | <b>Double Synchronized Switch Harvesting</b>  |
| <b>EAP/DEE</b> | <b>Electroactive Polymer/Dielectric Elastomer</b>                                   |
| <b>ID</b>      | <b>Internal Diameter</b>  |
| <b>MEMS</b>    | <b>Micro Electro Mechanical Systems</b>   |
| <b>MWCNT</b>   | <b>Multi-walled Carbon Nano tubes</b>   |
| <b>NIMH</b>    | <b>Nickel Metal Hydride</b>   |
| <b>PDMS</b>    | <b>Polydimethyl Siloxane</b>  |
| <b>PVDF</b>    | <b>Polyvinylidene Fluoride</b>  |
| <b>PWM</b>     | <b>Pulse Width Modulation</b>   |
| <b>PZT</b>     | <b>Lead Zirconate Titanate</b>  |
| <b>RF</b>      | <b>Radio Frequency</b>  |
| <b>SECE</b>    | <b>Synchronized Electric Charge Extraction</b>                                      |
| <b>SSDCI</b>   | <b>Synchronized<br/>Switching &amp; Discharge to Capacitor through<br/>Inductor</b> |
| <b>SSHI</b>    | <b>Synchronized Switch<br/>Harvesting On Inductor</b>                               |
| <b>THF</b>     | <b>Tetra Hydro Furan</b>  |
| <b>UVLO</b>    | <b>Under Voltage Lock Out</b>   |

## LIST OF FIGURES

| Figure No.  | Caption   | Page No. |
|-------------|---|----------|
| Figure 1.1  | Battery trends vs.other technologies [2] .....  | 2        |
| Figure 1.2  | Energy Harvesting Football (SOCKET) [19].....   | 8        |
| Figure 1.3  | Energy Harvesting Dance Floor [20] .....  | 9        |
| Figure 1.4  | Personal Energy Generator (PEG) that generates energy from human motion [21].....           | 9        |
| Figure 1.5  | Stockholm central station [22].....   | 10       |
| Figure 1.6  | Solar backpack [23].....  | 10       |
| Figure 1.7  | Piezoelectricity in quartz [31].....  | 13       |
| Figure 1.8  | (a) Unimorph..... (b) Bimorph [38] .....  | 18       |
| Figure 1.9  | Ambient sources for energy harvesting .....   | 19       |
| Figure 1.10 | Inclusive energy harvesting system interfaced with end application ...                      | 20       |
| Figure 2.1  | Piezoelectric energy conversion.....  | 24       |
| Figure 2.2  | Shoe generator designed by Paradiso & Co at MIT, (a) PVDF stave (b) PZT unimorph [68] ..... | 30       |
| Figure 2.3  | PZT bimorph shoe insert [69] .....  | 30       |
| Figure 2.4  | Shoe generator using EAP/DEE [70] .....   | 31       |
| Figure 2.5  | Quartz crystal powered shoe generator designed by Trevor Baylis .....                       | 32       |
| Figure 2.6  | Silicone embedded PZT 55] .....   | 32       |
| Figure 2.7  | Flexible barium titanate nanocomposite generator [57] .....                                 | 33       |
| Figure 2.8  | The PZT flexible composite .....  | 36       |
| Figure 2.9  | Stack of four Piezo Discs connected in parallel .....                                       | 37       |

|   |           |
|---|-----------|
| <b>Figure 3.1 Structure of a piezocomposite diaphragm [78]</b> .....  | <b>38</b> |
| <b>Figure 3.2 Piezoelectric buzzer elements</b> .....   | <b>39</b> |
| <b>Figure 3.3 Experimental setup for vibration analysis of piezo buzzers</b> .....  | <b>42</b> |
| <b>Figure 3.4 Voltage output without mechanical pre-stress for 35 mm buzzer</b> .....   | <b>44</b> |
| <b>Figure 3.5 Voltage output without mechanical pre-stress for 27 mm</b> .....  | <b>44</b> |
| <b>Figure 3.6 Voltage output with mechanical pre-stress for 35 mm buzzer</b> .....  | <b>45</b> |
| <b>Figure 3.7 Voltage output with mechanical pre-stress for 27 mm buzzer</b> .....  | <b>45</b> |
| <b>Figure 3.8 Frequency v/s weight (pre-stress) for 35 mm buzzer</b> .....  | <b>46</b> |
| <b>Figure 3.9 Frequency v/s weight (pre-stress) for 27 mm buzzer</b> .....  | <b>46</b> |
| <b>Figure 3.10 Power v/s load plot of 35 mm buzzer</b> .....  | <b>47</b> |
| <b>Figure 3.11 Power v/s load plot of 27 mm buzzer</b> .....  | <b>47</b> |
| <b>Figure 3.12 The piezoelectric buzzer elements with steel rings</b> .....   | <b>50</b> |
| <b>Figure 3.13 The drum harvesters</b> .....  | <b>51</b> |
| <b>Figure 3.14 Experimental setup for vibration analysis of drum harvesters</b> .....   | <b>52</b> |
| <b>Figure 3.15 Open circuit voltage of drum harvesters under excitation for different steel ring IDs (a), (b), (c) – 35 mm and (d), (e), (f) - 27 mm</b> .....                              | <b>53</b> |
| <b>Figure 3.16 Peak open circuit voltage comparison of experimental and simulated results for (a) 27 mm drum with steel ring ID 24 mm and (b) 35 mm drum with steel ring ID 32 mm</b> ..... | <b>55</b> |
| <b>Figure 3.17 Power output of drums vs.load resistance with different steel ring IDs (a), (b), (c) – 35 mm drum and (d), (e), (f) – 27 mm drum.</b> .....                                  | <b>56</b> |
| <b>Figure 3.18 Drum harvesters and (b) Drum stack</b> .....   | <b>59</b> |
| <b>Figure 3.19 (a) Drum harvesters with rubber discs adhered to them. (b) Stacks made using drum harvesters.</b> .....  | <b>59</b> |
| <b>Figure 3.20 Force under the foot while (a) walking and (b) running [2] [88]</b> .....  | <b>61</b> |
| <b>Figure 3.21 Footfall simulator</b> .....   | <b>61</b> |
| <b>Figure 3.22 Power output vs. increasing number of drums (D) (35 mm)</b> .....  | <b>62</b> |
| <b>Figure 3.23 Power output vs. increasing number of drums (D) (27 mm)</b> .....  | <b>62</b> |
| <b>Figure 3.24 Power output vs. increasing impact frequency for 35 mm drum stack</b>  | <b>63</b> |
| <b>Figure 3.25 Power output vs. increasing impact frequency for 27 mm drum stack</b>  | <b>64</b> |

|   |           |
|---|-----------|
| <b>Figure 3.26 DMS shoes with energy harvesting stacks embedded in the heel and forefoot sections (M1).</b> .....   | <b>65</b> |
| <b>Figure 3.27 Areas of maximum pressure under the foot [100].</b> .....  | <b>66</b> |
| <b>Figure 3.28 Insole made of polycarbonate sheet and drum harvesters (M2).</b> .....   | <b>66</b> |
| <b>Figure 3. 29 Model 1 open circuit voltage waveforms for 35 mm stack embedded in the heel (a) ID 31 mm (b) ID 32 mm and (c) ID 33 mm ( time = x axis &amp; voltage =y axis)</b> ..... | <b>68</b> |
| <b>Figure 3. 30 Model 1 open circuit voltage waveforms for 27 mm stack embedded in the heel (a) ID 23 mm (b) ID 24 mm and (c) ID 25 mm ( time = x axis &amp; voltage =y axis)</b> ..... | <b>70</b> |
| <b>Figure 3.31 Power curve at the heel for a walk</b> .....   | <b>71</b> |
| <b>Figure 3.32 Power curve at the forefoot for a walk</b> .....   | <b>71</b> |
| <b>Figure 3.33 Power curve at the heel for a run</b> .....  | <b>72</b> |
| <b>Figure 3.34 Power curve at the forefoot for a run</b> .....  | <b>72</b> |
| <b>Figure 3.35 Output power vs. load resistance for Model 1 and Model 2.</b> .....  | <b>73</b> |
| <br>  |           |
| <b>Figure 4.1 Electrical equivalent of a piezoelectric element.</b> .....   | <b>76</b> |
| <b>Figure 4.2 Equivalent circuit model of a piezoelectric element at very low frequencies</b> .....   | <b>78</b> |
| <b>Figure 4.3 Block diagram for a typical energy harvesting circuit interface for a piezoelectric vibration energy harvester</b> .....  | <b>78</b> |
| <b>Figure 4.4 The standard energy harvesting interface for a piezo energy harvester</b>   | <b>79</b> |
| <b>Figure 4.5 DC open circuit waveforms of 27 mm drum with diode bridge rectifier</b>   | <b>80</b> |
| <b>Figure 4.6 DC open circuit waveforms of 35 mm drum with diode bridge rectifier</b>   | <b>80</b> |
| <b>Figure 4.7 MOSFET Bridge rectifier</b> .....   | <b>81</b> |
| <b>Figure 4.8 MOSFET Bridge rectifier circuit for piezo drum harvesters</b> .....   | <b>82</b> |
| <b>Figure 4.9 DC open circuit waveform of 27 mm drum with MOSFET bridge rectifier</b> .....   | <b>82</b> |
| <b>Figure 4.10 DC open circuit waveform of 35 mm drum with MOSFET bridge rectifier</b> .....  | <b>83</b> |
| <b>Figure 4.11 Output power vs. load resistance for Model 1 and Model 2.</b> .....  | <b>83</b> |
| <b>Figure 4.12 Parallel SSHI</b> .....  | <b>85</b> |
| <b>Figure 4.13 Series SSHI</b> .....  | <b>85</b> |

|   |            |
|---|------------|
| <b>Figure 4.14 Hybrid SSHI.....</b>   | <b>86</b>  |
| <b>Figure 4.15 SSDCI .....</b>  | <b>86</b>  |
| <b>Figure 4.16 SECE.....</b>  | <b>87</b>  |
| <b>Figure 4.17 DSSH.....</b>  | <b>88</b>  |
| <b>Figure 4.18 Circuit for piezoelectric energy harvesting with LTC 3588 – 1 with<br/>output of 3.6 V .....</b>                     | <b>92</b>  |
| <b>Figure 4.19 LTC 3588 – 1 (a) Standard input/ output plots from datasheet (b)<br/>Results obtained with shoe harvesters .....</b> | <b>93</b>  |
| <b>Figure 4.20 Circuit for piezoelectric energy harvesting with LTC 3588 – 2 with<br/>output of 5 V .....</b>                       | <b>93</b>  |
| <b>Figure 4.21 LTC 3588 – 2 (a) Standard input/ output plots from datasheet (b)<br/>Results obtained with shoe harvesters .....</b> | <b>94</b>  |
| <br>  |            |
| <b>Figure 5.1 Charging curves of supercapacitors charged with piezo diaphragms....</b>  | <b>99</b>  |
| <b>Figure 5.2 Charging with 27 mm drum and 3 different steel ring IDs .....</b>   | <b>100</b> |
| <b>Figure 5.3 Charging with 35 mm drum and 3 different steel ring IDs .....</b>   | <b>100</b> |
| <b>Figure 5.4 Charging curve of a 22 mAh NiMH battery .....</b>   | <b>101</b> |
| <b>Figure 5.5 Charging curve of a 70 mAh NiMH battery .....</b>   | <b>102</b> |
| <b>Figure 5.6 Charging curve of a 160 mAh NiMH battery .....</b>  | <b>102</b> |
| <br>  |            |
| <b>Figure 6.1 Power available from energy harvesting vs.power requirement of<br/>electronic devices [114] .....</b>                 | <b>104</b> |
| <b>Figure 6.2 Arduino board powered by the charged supercapacitor .....</b>   | <b>107</b> |
| <b>Figure 6.3 Shoe-powered transmitter module and battery powered receiver module<br/>.....</b>                                     | <b>110</b> |



## LIST OF TABLES

---

| Table No. | Caption  | Page No. |
|-----------|--|----------|
| Table 1.1 | Power consumption of contemporary microelectronic components .....                       | 2        |
| Table 1.2 | Commonly used methods of vibration/kinetic energy harvesting .....                       | 12       |
| Table 1.3 | Comparison of commonly used piezoelectric materials .....                                | 14       |
| Table 2.1 | Comparison of properties relevant to use of piezoelectric materials as transducers ..... | 22       |
| Table 2.2 | Summary of maximum energy densities of three kinds of transducers ...                    | 23       |
| Table 2.3 | Commercially available piezoelectric elements .....                                      | 26       |
| Table 2.4 | Piezoelectric Cantilever Harvesters.....   | 27       |
| Table 2.5 | Flexible piezocomposite harvesters .....   | 27       |
| Table 2.6 | Circular piezocomposite harvesters for energy harvesting.....                            | 28       |
| Table 2.7 | Energy harvesting through human ambulation .....   | 34       |
| Table 3.1 | Dimensions of piezoelectric diaphragms used in the present work .....                    | 40       |
| Table 3.2 | Ambient vibration sources .....  | 41       |
| Table 3.3 | Comparison of resonant and impulse driven energy harvesting structures. ....             | 49       |
| Table 3.4 | Dimensions of the piezo buzzer elements used to make drum harvesters                     | 51       |
| Table 3.5 | Power output of drum harvesters at resonance. ....                                       | 57       |
| Table 3.6 | Power output v/s increasing number of drums .....  | 63       |
| Table 3.7 | Power output v/s impact frequency .....  | 64       |
| Table 3.8 | Power output vs. number of stacks in shoe.....   | 73       |
| Table 4.1 | Static capacitance of 27 mm and 35 mm drum harvesters.....                               | 77       |

|   |            |
|---|------------|
| <b>Table 5.1 Charging of various capacitors with the shoe-based harvesters.....</b> | <b>98</b>  |
| <b>Table 5.2 Supercapacitor charging with drum harvesters.....</b>                  | <b>100</b> |
| <b>Table 5.3 NiMH battery charging with shoe-harvesters .....</b>                   | <b>103</b> |
| <br>  |            |
| <b>Table 6.1 ATMEGA328 technical specifications.....</b>                            | <b>105</b> |

# CHAPTER 1

## INTRODUCTION

---

The Paris agreement on climate change in 2016 highlights the fact that, as well as causing the depletion of natural resources, the use of fossil fuels and other conventional energy sources is also irreversibly altering our environment. One of the ways of countering this change is the use of non-conventional and renewable energy sources.

Energy harvesting, also known variously as ambient energy harvesting or energy scavenging, is the conversion of energy extracted from ambient sources to useful forms like electricity and its storage for use in the operation of wireless autonomous devices like wearable electronics, wireless sensor nodes, etc. The ambient sources of energy include the sun, wind, tidal waves, geothermal energy, vibrations, human motion, electromagnetic sources, etc [1]. As humans are generally a mobile species and can traverse varied landscapes and terrains, there is an increasing need for portable energy generators that do not run on traditional fuels and can work in any environment and at the same time don't leave an adverse imprint on the natural environment.

Battery technologies have made significant strides but unfortunately have not kept pace with other technologies like the development of microprocessors, memory storage and wireless technology applications. Figure 1.1 shows the trends over a decade [2]. Batteries are unreliable and have a limited lifespan when it comes to critical applications like life support systems and remote unmanned locations (space exploration for example where maintenance cannot be done frequently).

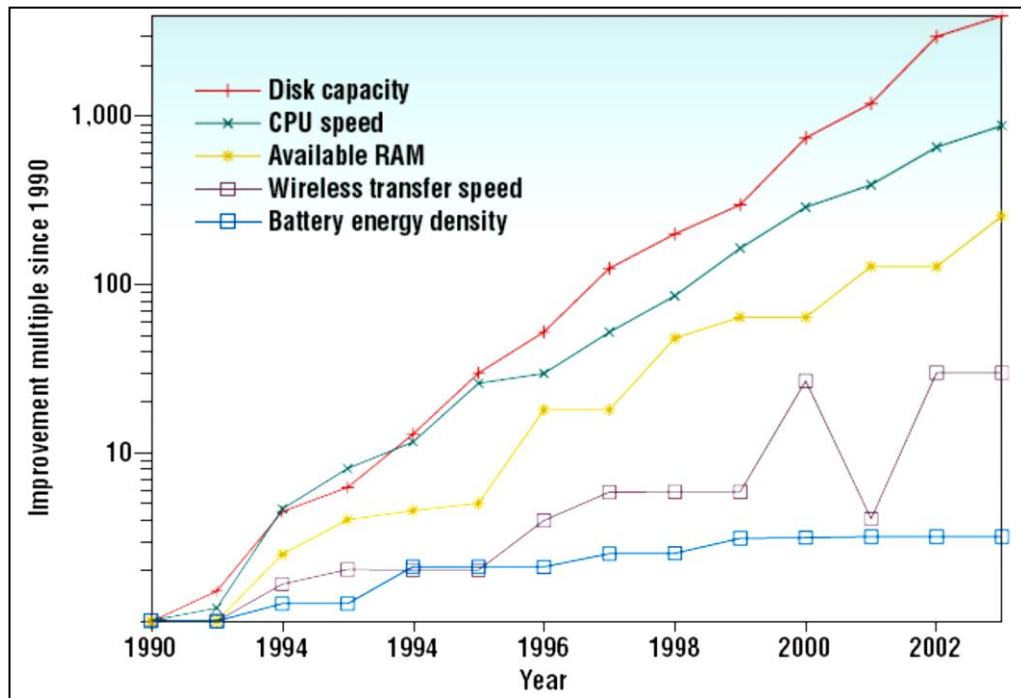


**Figure 1.1 Battery trends vs.other technologies [2]**

Technological advances have reduced the size of electronic devices across all fields and, in addition to making them portable, have also led to reduction in their power consumption. Table 1.1 gives the power consumption of some contemporary microelectronic components used in electronic devices.

**Table 1.1 Power consumption of contemporary microelectronic components**

| Device Name  | Current Consumption   | Operating Voltage              |
|--|---|--------------------------------|
| ICSENSE Smart power sensor interface chip [3]      | 2.4 $\mu$ A   | 0.9 – 4.2 V                    |
| STM8L/STM32L microcontrollers [4]                  | 0.3 $\mu$ A, 1.65 – 3 V (lowest power mode)                           | 1.65 – 3 V (lowest power mode) |
| CC2640 bluetooth module [5]                        | 5.9mA/ 1 $\mu$ A standby  | 1.8 – 3.8 V                    |
| MN-31540SH GPS module [6]                          | 18 (track)/21mA(acquire)  | 2.2 – 4.3 V                    |
| ZL70250 Ultra-Low-Power Sub-GHz RF Transceiver [7] | < 2 mA at -13dBm;< 5 mA at -2 dBm (TX); <1.9 mA (RX);< 500 nA (sleep) | 1.2 – 1.8 V                    |

## 1.1 THE SOURCES OF AMBIENT ENERGY

The sources of ambient energy can be broadly classified into two categories - natural and anthropogenic. Following is a brief look at the various sources that come under these two categories.

### 1.1.1 Natural sources

1. ***Waves and Tides*** – Waves are produced by winds blowing over the surface of water bodies like oceans. Tides on the other hand are caused by the gravitational pull of the moon and the sun. As most of earth is covered with water, this particular source is huge. Only difficulty that may arise is due to the geographical changes across the globe. To quote numbers, the United States receives 2,100 terawatt-hours of incident wave energy along its coastlines every year, and tapping just a fourth of this could generate as much energy as the complete U.S. hydropower system. Though currently there are very few active projects going on in this field around the world, the technology required is making great progress so that in the near future, we may see wave and tidal power generation become as common as, if not more than, hydroelectric power generation [8].
2. ***Geothermal energy*** – This is the heat energy available from the interior of the earth. It has been in use since thousands of years for cooking and heating. This thermal energy is contained in the rocks and fluids underneath the Earth's crust. It can be found from shallow ground to several miles below the surface, and even farther down to the extremely hot molten rock called magma. As per estimates geothermal energy can be used to generate electricity in the range of 35 to 2,000 GW. Present global installed capacity is 10,715 megawatts (MW), with the largest capacity in the United States (3,086 MW), Philippines and Indonesia. India has announced a plan to develop the country's first geothermal power plant in Chhattisgarh [9].
3. ***Wind energy*** – The power available from wind energy is plentiful, widely distributed throughout the globe and a clean source that does not pollute the environment. The Global Wind Energy Council (GWEC) reported that the wind industry installed more than 44,000 megawatts (MW) of new clean, reliable

wind power in 2012, bringing total installed global capacity to more than 280,000 MW. In percentage terms, wind power is currently the fastest-growing source of energy in the world. Serious commitments to reduce carbon dioxide have promoted wind power in Europe, while the ability to avoid constant imports of fuel has appealed to developing nations like India [10].

4. **Solar energy** – It's currently the most popular and most widely harvested form of ambient energy. The sun is an almost inexhaustible source of energy. The Earth receives 174 petawatts (PW) of incoming solar radiation at the upper atmosphere. Approximately 30% is reflected back to space while the rest is absorbed by clouds, oceans and land masses [11]. With advances in solar cell technology and energy storage systems, solar energy has the potential to take over from conventional energy sources.
5. **RF energy** - Electromagnetic waves permeate almost all of the space on earth. Be it visible light, AM/FM or radio waves, RF energy is omnipresent in the urban landscape. Either a large collection area or close proximity to the radiating wireless energy source is needed to get useful power levels from this source. The 'nantenna' is one proposed development which would overcome this limitation by making use of the abundant natural radiation (such as solar radiation). One idea is to deliberately broadcast RF energy to power remote devices: This is now commonplace in passive radio-frequency identification (RFID) systems [1].
6. **Earthquakes** - As an estimate,  $1.995262e+6$  Joules of energy are available from seismic waves emitted in a magnitude 1 earthquake [12]. Though this may seem farfetched as earthquakes are generally very destructive in nature, a jelly like energy harvester can be conceptualized that can harvest at least a part of the vibrations from the seismic waves. It will have to cover a large area of course and predicting the location of an earthquake is still difficult. These harvesters could be spread around earthquake prone zones and could be vital aids in detecting and forecasting earthquakes.

### 1.1.2 Anthropogenic sources

The word Anthropogenic may be defined as anything having its origin in the influence of human activity. The following are the anthropogenic sources of ambient energy.

1. ***Human physical and physiological processes*** – These include walking, breathing, body heat, blood pressure, upper limb motion, etc. In his momentous paper [13], Thad Starner gave an estimate of the amount of power available from these processes. According to his calculations, 3.7 – 6.4 W of power is available from body heat, 1 W from breathing, 0.93W from blood pressure, 24 W and 60 W from bicep curls and arm lifts respectively and finally 67W from walking. Thus the human body and it's processes are a store house of ambient energy. This energy, which is otherwise wasted, can be scavenged, though the issue is to do so as unobtrusively as possible. As an example, DARPA reportedly abandoned attempts to make a shoe powered generator due to the impracticality and the discomfort from the additional energy expended by a person wearing the shoes [14].
2. ***Machines*** – Human life has been made easy by the invention and use of machines. We use machines in almost all walks of life. These machines, ranging from a small air conditioner to huge cranes consume a lot of energy and dissipate quite a good proportion in the form of heat, vibrations, magnetic fields, electromagnetic waves, acoustic waves, etc. Each of these forms of dissipated energies can be scavenged again by designing suitable energy scavengers that can be attached to or near these sources. Stray magnetic fields that are generated by AC devices and propagate through earth, concrete, and most metals, including lead, can be the source of electric energy. The actual AC magnetic field strengths encountered within a given commercial building typically range from under 0.2 mG in open areas to several hundred near electrical equipment such as cardiac pace makers, CRT displays, oscilloscopes, motor vehicles (approximately up to 5 G max); computers, magnetic storage media, credit card readers, watches (approximately up to 10G max); magnetic power supply, liquid helium monitor (approximately up to 50 G max); magnetic wrenches, magnetic hardware, and other machinery (approximately up to 500 G max). Radio frequency waves and acoustic waves are also feasible sources [15].

## **1.2 ENERGY HARVESTING – STATE OF THE ART**

Scientific endeavours have taken a giant leap forward in the last century with space exploration, deep sea exploration and environmental monitoring becoming an essential part of research. These endeavours demand energy generators which can withstand the test of extreme and relatively unknown environments. These environments are not only physically challenging (at times unknown) but also the duration of operation of the devices in these places is uncertain and maintenance work is prohibitively difficult as well as expensive. Hence there is a need for an energy generator that should be low maintenance or maintenance free and can survive uncertain and long periods of time without the need for replacement.

There are possibly numerous applications of energy harvesting to civilian life. For example, a small wind system can be connected to the electric grid through the power provider or it can be a stand-alone system (off-grid). This makes small wind electric systems a good choice for rural areas that are not already connected to the electric grid [16]. Solar panels are already powering homes worldwide; be it for individual homes or entire cities. Microelectronic systems like mobile phones, medical implants, etc. can be powered on the go. For equipments installed in remote locations like mountains, deserts, underwater environment, outer space, etc., ambient energy sources can become the primary source of power.

The medical field will find energy harvesting extremely useful in remote and round the clock health monitoring of patients. Medical implants that run on electronics are growing in number by the day. Currently, they are battery-powered and the battery lifetime is about a decade. The inconvenience of undergoing regular surgery just to replace the battery can be avoided if the implants can be powered by harvesting energy from human physiological processes. For example, hypertension could be monitored and kept under control in patients even when the doctor is not around and they are on the go. Diagnosis could be done at the earliest and the requisite medication can be prescribed for a variety of diseases and disorders that need round the clock monitoring of vital physiological parameters which could be relayed in real time to the doctors who are away from the patient. The monitoring devices could be powered indefinitely by harvesting energy from physiological processes like blood pressure, heart beats, the motion of the diaphragm, the limbs, etc.



Energy harvesting is also finding application in structural health monitoring. Bridges, buildings and other similar vital installations can be monitored remotely using a feedback mechanism that relays the condition of these structures in real time and helps ease the maintenance work.

Environmental monitoring is another area which will find energy harvesting greatly helpful. Climate change and environmental pollution could be monitored using wireless sensor networks which are powered by scavenging ambient energy from the environment in which they are placed. Early warning systems working along similar lines could be placed to predict natural calamities like avalanches and earthquakes in advance and help prevent loss of lives. Wildlife monitoring is already an extensively undertaken activity to track endangered species. The tracking gadgets and gps could use the power from energy harvesting modules attached to the animals.

In the 21<sup>st</sup> century, warfare has become modernized too. Soldiers often have to traverse extreme and unknown terrains for uncertain periods of time carrying only limited power with them for their gadgets. This is where a portable generator that can harvest energy from ambient sources will come in very handy for survival and may be a potential life saver. The modernization of armed forces across the world has led to increased use of electronic equipment by soldiers in the field – from night-vision goggles, laptops, and communication devices to GPS and sensors. But there are significant technical and logistical challenges to efficiently equipping soldiers with the power they need to run this equipment. Because their devices must operate autonomously and indefinitely, soldiers typically have to carry up to 30 lbs of various primary and backup batteries, depending on the power requirements of their individual devices [17]. This adds considerably to the weight of the equipment and provisions they pack. But what if soldiers could carry a single lightweight power-conversion device that is able to adapt to the power needs of all their equipment? Such a power-conversion device should enable them to use any available power source in the field – generators, field chargers, solar panels, fuel cells, and so on – to recharge their batteries. Having a wearable energy harvester that can supplement their power source will be a very useful tool to have and give a strategic advantage.

Alternative energy sources are a means of extending the life of an industrial system. As an alternative to accessing the system to change batteries or hardwire power, having a

different type of energy source enables the application to be positioned in otherwise inaccessible areas and operate longer without requiring maintenance. One of the key applications for energy harvesting is wireless sensors. These are already deployed in many areas, specifically for smart meters, but the applications are growing as the technology develops and new ways to use the power are devised.

Energy harvesting is a fast growing industry. It is estimated that energy harvesting components will exceed \$4 billion by 2020, which is momentous considering that the market was \$79.5 million in 2009 resulting in an average annual growth rate of over 73%. The present market leaders are Europe, North America, Japan and China. There are several reasons why companies are investing in energy harvesting. Some are looking to lessen the cost associated with powering systems. Depending on the life expectancy of the system an upfront cost to use energy harvesting could pay off in the long run, even if the energy generated is not substantial [18].

A few examples of commercially available as well as prototype energy harvesters designed by various researchers, hobbyists, entrepreneurs and enthusiasts are as follows:

1. By kicking the SOCKET ball around shown in Fig 1.2, players can generate enough electricity in a 30 minute game to power a LED lamp for three hours. The ball has a pendulum kind of a mechanism which stores kinetic energy and can be used later [19].



**Figure 1.2 Energy Harvesting Football (SOCKET) [19]**

2. The Sustainable Dance Floor (SDF) uses the movement of people as source of energy. This kinetic energy is transformed into electricity which powers the dance floor's LED lights that create the disco atmosphere. In that way the floor shown in Fig 1.3 is reacting to the public and engages people in an interactive

dance experience. The electricity can also be fed back to the electricity grid, be used for energy applications that create a unique Energy Experience, or power other customized local systems [20].



**Figure 1.3 Energy Harvesting Dance Floor [20]**

3. The nPower PEG is a light-weight, titanium encased portable generator that can recharge a handheld device (phone, media player, camera, GPS etc.) when one is away from the power supply grid. It is different from other mobile power solutions in that no fuel is needed. The US\$150 PEG, which is 9 inches long and weighs 9 ounces, is shown in Fig 1.4 and harvests kinetic energy as you move about daily. It can be put in backpacks, bumbags, handbags, brief cases or gloveboxes and it will collect and store energy from movements [21].



**Figure 1.4 Personal Energy Generator (PEG) that generates energy from human motion [21]**

4. Sweden's largest train station, Stockholm's Central Station shown in Fig 1.5, is already harvesting the body heat of the 250,000 passengers who pass through

every day [22]. The effort has enabled them to cut down on electricity bills for the office block by 25 percent.



**Figure 1.5 Stockholm central station [22]**

5. Indian startup Lumos Design Technology has designed and is already selling solar backpacks shown in Fig 1.6. The components incorporated were a rectangular piece of solar fabric, which has a thin film of solar cells fused together, and a battery fitted inside. The battery takes in solar energy from the fabric and stores the power, which can then be fed to a phone or laptop through any USB [23].



**Figure 1.6 Solar backpack [23]**

### **1.3 ENERGY HARVESTING METHODS**

With rapid strides in the field of microelectronics, electronic devices are shrinking in size by the day. Additionally, their power requirements are shrinking too. As these devices are predominantly mobile, an increasing need is being felt to have a portable power source that can power these devices, independent of conventional power sources such as batteries, domestic power supplies, etc., and which could be universally accessible [24, 25]. A lot of research has been carried out previously to convert different forms of ambient energy into usable electrical energy. There are basically three common mechanisms used for energy scavenging applications which are electrostatic, electromagnetic and piezoelectric [26]. In the 90s, researchers turned their attention towards anthropomorphic energy scavenging, which, in simple terms, means the extraction of energy unobtrusively from human activities and processes such as walking, breathing, body heat, etc. Power generation by body heat, breathing or motion can potentially power a computer [27]. A comparison of different energy harvesting methods is shown in Table 2.6 [28]. The phenomenon that has shown immense promise in the area of energy harvesting is piezoelectricity. Piezoelectric materials are most suitable for anthropogenic energy harvesting owing to their high energy density (Table 2.6), high electromechanical conversion efficiency and their ability to be fabricated into different forms like films, sheets and other flexible structures that can be incorporated unobtrusively into body wear. Piezoelectricity is the phenomenon by which certain materials convert mechanical energy into electrical energy (direct piezoelectric effect). Naturally occurring materials such as quartz, Rochelle salt, etc exhibit this phenomenon. Man-made materials viz. ceramics like lead zirconate titanate (PZT), polymers like polyvinylidene fluoride (PVDF) also show evidence of this phenomenon. The reverse effect, that is change in shape of the material in response to application of electric current, also exists. Piezoelectric materials are so versatile that they find application in a diverse range of gadgets from the simple gas lighter and telephone buzzers to ultrasonic cleaners and missiles.

Vibrations are one of the most abundant sources of ambient energy and as such can be used for harvesting useful amounts of energy which can power microelectronic devices. The most common methods of vibration/ kinetic energy harvesting explored

scientifically and exploited commercially are the piezoelectric, electromagnetic and electrostatic methods. Table 1.2 [28, 29] gives a comparison of these three methods based on their power density as well as their advantages and drawbacks.

**Table 1.2 Commonly used methods of vibration/kinetic energy harvesting**

| <b>Method</b>   | <b>Energy density (mJ/ cm<sup>3</sup>)</b> | <b>Advantages</b>   | <b>Disadvantages</b>   |
|-----------------|--|---|--|
| Electromagnetic | 24.8                                       | <ol style="list-style-type: none"> <li>1. High output current</li> <li>2. Variety of configurations and materials can be used</li> </ol>  | <ol style="list-style-type: none"> <li>1. Low output voltage</li> <li>2. Design problems due to poor magnet properties and limited number of turns of coil</li> </ol>    |
| Electrostatic   | 4  | <ol style="list-style-type: none"> <li>1. Easily realizable in MEMS</li> </ol>  | <ol style="list-style-type: none"> <li>1. Need initial charge</li> <li>2. Low output current</li> <li>3. High output voltages</li> </ol>                                 |
| Piezoelectric   | 35.4                                       | <ol style="list-style-type: none"> <li>1. No need for external accrements</li> <li>2. No start-up charge required</li> <li>3. Can be fabricated in various shapes</li> <li>4. Integrable into various structures</li> </ol> | <ol style="list-style-type: none"> <li>1. Low output currents</li> <li>2. Overall performance and lifetime are limited</li> <li>3. Brittle nature of material</li> </ol> |

Piezoelectric materials have been a popular choice for researchers in the area of energy harvesting for a few decades now. They have an inherent ability to convert mechanical energy into electrical energy. Piezoelectric elements can be repetitively deformed to generate energy and power devices, with characteristic applications being sensors and industrial equipment [30]. A key advantage of these materials is that they can be

optimised to suit specific applications using well established fabrication techniques. Owing to these advantages of piezoelectric materials over other methods, the present research work employs the piezoelectric method for ambient energy harvesting.

### 1.3.1 Piezoelectricity

Piezoelectricity is a type of coupling between the mechanical and electrical behaviours of a certain class of materials. It is the electric charge that accumulates in some solid materials (such as crystals, certain ceramics, and biological matter such as bone, DNA and various proteins) in response to applied mechanical stress. The process is reversible in that materials that exhibit the direct piezoelectric effect (the internal generation of electrical charge resulting from an applied mechanical force) also exhibit the converse piezoelectric effect (the internal generation of a mechanical strain resulting from an applied electrical field). The first demonstration of the direct piezoelectric effect was in 1880 by the brothers Pierre Curie and Jacques Curie [14]. The converse piezoelectric effect was mathematically deduced from the fundamental principles of thermodynamics by Gabriel Lippman in 1881 and then confirmed experimentally by the Curie brothers. These two effects generally coexist in a piezoelectric material. Figure 1.7 shows the piezoelectric effect in quartz [31].

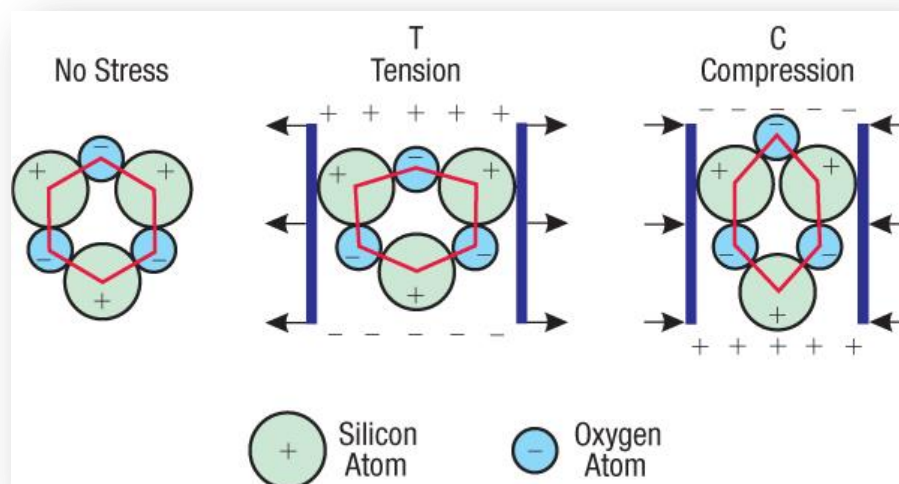


**Figure 1.7 Piezoelectricity in quartz [31]**

### 1.3.2 Piezoelectric materials

There are naturally occurring as well as synthetic piezoelectric materials. The natural materials include quartz, Rochelle salt, topaz, sucrose, etc. Other natural materials that exhibit this phenomenon are silk, dna, tendons, wood, enamel, dentin.

In order to be practically useful in engineering applications, the coupling between the electrical and mechanical behaviours of a piezoelectric material has to be adequately strong. For this reason man-made piezoceramics were developed in the second half of the 20th century. The most popular of all engineering ceramics, PZT (lead zirconate titanate) was developed at the Tokyo Institute of Technology in the 1950s and various versions of it (particularly PZT-5A and PZT-5H) are today the most commonly used engineering piezoceramics. As far as energy harvesting research is concerned, PZT-5A and PZT-5H are the most widely used piezoceramics according to the literature available in this field [32]. Other synthetic materials include barium titanate, lead titanate, lithium niobate, zinc oxide, etc. to name a few. There are also some polymers like polyvinlydene fluoride (PVDF) which are piezoelectric.

### 1.3.3 Piezoelectric Material Properties

The properties of these materials that are considered vital for energy harvesting are known as the piezoelectric charge constants ( $d_{31}$  &  $d_{33}$ ), the piezoelectric voltage constants ( $g_{31}$  &  $g_{33}$ ) and the coupling coefficients  $k$  giving the electromechanical conversion efficiency. The figure of merit of a piezoelectric material is the product of  $d$  and  $g$ . A piezoelectric material suitable for energy harvesting is characterized by the large magnitude of product of the  $g$  and  $d$  [15]. The temperature beyond which the piezoelectric characteristic breaks down is known as the Curie temperature. Table 1.3 gives a comparison of the four most commonly used synthetic piezoelectric materials [33, 34].

**Table 1.3 Comparison of commonly used piezoelectric materials**

| <b>Property</b> | <b>PZT – 5H</b> | <b>PZT – 5A</b> | <b>BaTiO<sub>3</sub></b> | <b>PVDF</b> |
|-----------------|-----------------|-----------------|--------------------------|-------------|
|                 |                 |                 |                          |             |



|  |      |       |      |      |
|--|------|-------|------|------|
| $d_{33}$ (pC/N)                                    | 593  | 374   | 149  | 33   |
| $g_{33}$ (Vm/N)                                    | 19.7 | 24.8  | 14.1 | 330  |
| $d_{31}$ (pC/N)                                    | -274 | -171  | -78  | -23  |
| $g_{31}$ (Vm/N)                                    | -9.1 | -11.4 | 5    | 216  |
| $k_{33}$   | 0.75 | 0.71  | 0.48 | 0.15 |
| $k_{31}$   | 0.39 | 0.31  | 0.21 | 0.12 |
| Curie Temp. ( $^{\circ}$ C)                        | 195  | 365   | 120  | 110  |
| Relative permittivity<br>( $\epsilon/\epsilon_0$ ) | 3400 | 1700  | 1700 | 12   |

Piezoelectric ceramics, which at the present time are based mainly on Lead Zirconate-Lead Titanate compounds, are subject to an exemption from the EU directive to reduce hazardous substances (RoHS) and can therefore be used without hesitation [35]. Nevertheless, concern over the environmental impact of lead has driven researchers to look out for lead free piezoelectric materials analogous to PZT. In recent times, there has been stress on utilization of lead-free materials in domestic and medical applications. Out of all the possible choices for lead-free ceramics, (Na,K)NbO<sub>3</sub> (KNN)-based ceramics such as KNN-LiNbO<sub>3</sub>, KNN-LiTaO<sub>3</sub>, KNN-LiSbO<sub>3</sub>, KNN-Li(Nb, Ta, Sb)O<sub>3</sub>, KNN-BaTiO<sub>3</sub> (BT), KNN-SrTiO<sub>3</sub>, and KNN-CaTiO<sub>3</sub> have gained prominence mainly for two reasons: (i) piezoelectric properties exist over a wide range of temperature and (ii) there are several options for additions and substitutions [15].

### **1.3.4 Hard and Soft Piezoceramic Materials**

Internationally, the convention is to divide piezoelectric ceramics into two groups. The terms "soft" and "hard" PZT ceramics point to the mobility of the dipoles or domains and consequently to the polarization and depolarization behaviour.

"Hard" or hard doped PZT materials have the ability to withstand high electrical and mechanical stresses. Their properties change only slightly under these conditions which makes them particularly ideal for high-power applications. The advantages of these PZT materials are moderate permittivity, large piezoelectric coupling factors, high qualities and great stability under high mechanical loads and operational fields. Low dielectric losses facilitate their uninterrupted use in resonance mode with only low intrinsic warming of the element. These piezo elements are used in ultrasonic cleaning (typically kHz frequency range), for example, the machining of materials (ultrasonic welding, bonding, drilling, etc.), in sonicators to disperse liquid media, in the medical field (ultrasonic tartar removal, surgical instruments etc.) as well as in sonar technology [35]. Examples include Navy type I and Navy type III.

Characteristic features of soft piezo ceramics include comparably elevated domain mobility and the consequent "soft ferroelectric" behaviour, i.e. they are comparatively easy to polarize. The advantages of the "soft" PZT materials are their large piezo- electric charge coefficient, moderate permittivities and high coupling factors. Important fields of application for "soft" piezo ceramics are actuators for micropositioning and nanopositioning, sensors such as conventional vibration pickups, ultrasonic transmitters and receivers for flow or level measurement, for example, object identification or monitoring as well as electro-acoustic applications as sound transducers and microphones, to their use as sound pickups on musical instruments [36]. Examples include PZT-5A and PZT-5H. For the application of energy harvesting, therefore, soft PZT is the natural choice.

### 1.3.5 Active and Passive Piezo Materials

Piezoelectric elements can be used in applications both as active and passive elements. The direct piezoelectric effect, for example, enables a transducer to act as a passive sound receiver or pickup by the conversion of acoustic energy into an electrical signal. Applications comprise hydrophones used to detect low frequency noises under water, and microphones. The converse piezoelectric effect allows a transducer to act as an active sound transmitter or loudspeaker. Particularly, a piezo-tweeter is an audio speaker component used to generate high frequency sounds [36]. Thus, piezo actuators are active elements and piezo transducers are passive elements.

In some applications, the same element can be used as both an active as well as a passive device. For example, smart skis have been developed which use piezoelectric materials. These materials embedded on the skis in parts which experience the most vibrations act as both sensors and actuators. They act to control the unnecessary vibrations and keep the skis on the snow irrespective of whether it is hard or soft, the speed (high or low) or if the surface is uneven [37].

### 1.3.6 Unimorphs and Bimorphs

A piezoelectric **unimorph** has one active (i.e. piezoelectric) layer and one inactive (i.e. non-piezoelectric) layer.

In general application, a unimorph is a cantilever (or any generic piezoelectric element) that consists of one active layer and one inactive layer shown in Fig 1.8 (a). Where active layer is piezoelectric, deformation in that layer may be brought about by the application of an electric field which induces a bending displacement in the cantilever. The inactive layer may be fabricated from a non-piezoelectric material. The direct piezoelectric effect also applies, in which case, a deformation generates a voltage [38].

Along similar lines, a bimorph has two active layers. It works with one layer expanding and the other contracting as shown in Fig 1.8 (b).

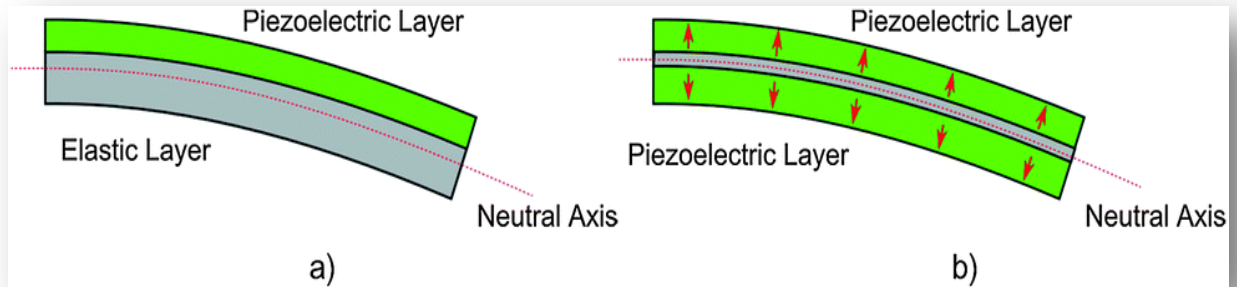


**Figure 1.8 (a) Unimorph (b) Bimorph [38]**

## 1.4 APPROACH

In accordance with DIHAR's mandate to ensure food, health and energy security for troops stationed in the Ladakh sector, there was a specific requirement for the development of a power generator for troops during patrolling operations. The qualitative requirements of such a generator are as follows:

- a) Self-contained portable energy generator.
- b) Power output of around 100 mW sufficient to act as a supplementary power source for handheld gadgets like mobile phones, walkie talkies, emergency signalling devices, etc.
- c) Ability to operate in sub-zero temperatures.
- d) Minimum of moving parts and unobtrusive.
- e) Life of at least 6 months.

To power such a generator, a source of energy is needed and that source has to be ambient. Figure 1.9 depicts the common sources of ambient energy with their drawbacks and advantages.

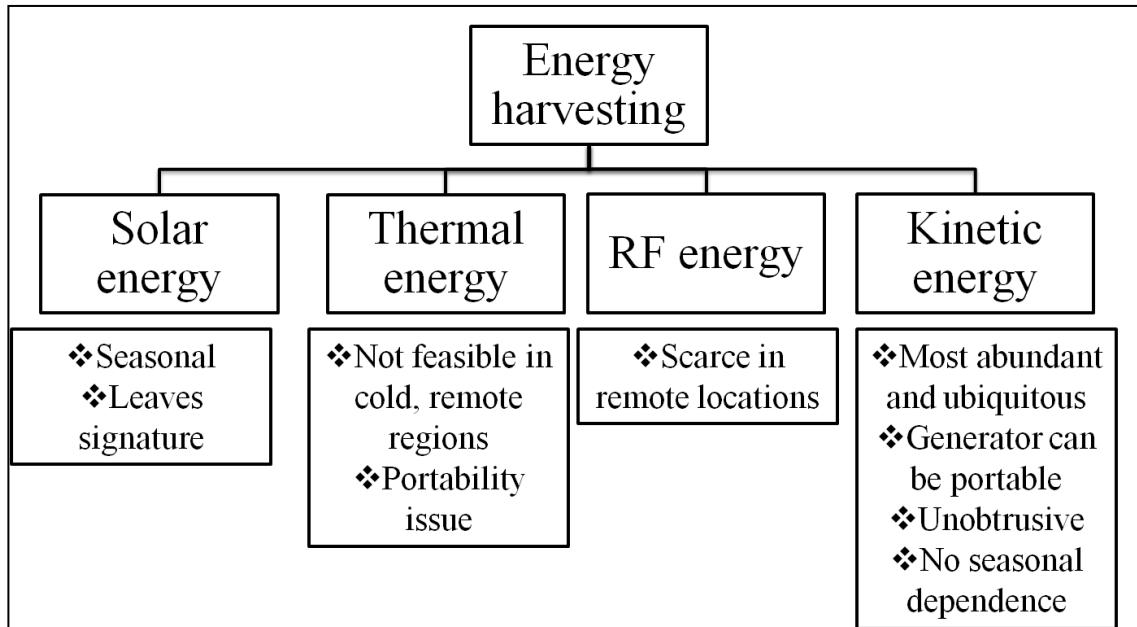


**Figure 1.9 Ambient sources for energy harvesting**

Harvesting kinetic energy from a wearable would be the best way to scavenge energy as then the generator could be made truly portable and unobtrusive. Since walking is a very common activity and, as already mentioned earlier, since a large amount of energy is available in footfalls, the generator could be made a part of shoes. Hence, the present research work explores shoe-based piezoelectric energy harvesters. In addition, the suitability of those same harvesters as vibration energy scavengers is also explored.

The present work, therefore, is aimed towards designing and developing an inclusive energy harvesting system which will then be interfaced with a suitable end application. Figure 1.10 shows a block diagram of the complete energy harvesting system interfaced with the application.

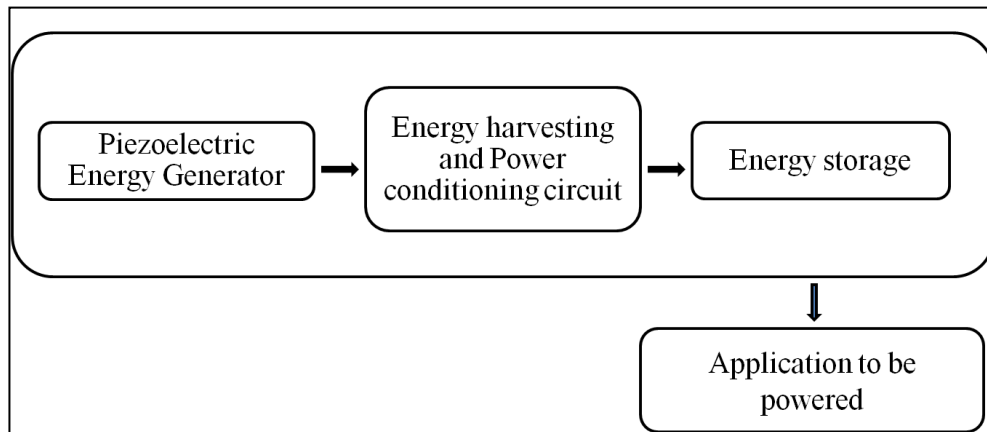


**Figure 1.10 Inclusive energy harvesting system interfaced with end application**

## 1.5 SUMMARY OF CONTRIBUTIONS

**Chapter 2** gives a summary of the literature surveyed in the present work. It starts with a comparison of various piezoelectric elements, their uses, relevant electrical and mechanical properties. It also describes pioneering work and existing literature on piezoelectric energy harvesting elements, the various experimental setups, mechanisms and power obtained. Further it describes prior art as far as shoe-based energy harvesting is concerned. The chapter ends with the description of flexible piezocomposite generators and a novel attempt to fabricate the same in the present work.

**Chapter 3** is related to the analysis of piezocomposite diaphragms and drum harvesters under low amplitude, higher frequency excitation profile as well as high amplitude low frequency impacts. It elucidates the material selection criteria and the basic electromechanical model of a piezoelectric element. The effect of pre-stress on the

power output of the piezocomposite diaphragms is studied. A simple method for the assembly of drum harvesters made using piezocomposite elements is described. A novel microcontroller-based bench testing setup to test the drums under a high amplitude and low frequency impact excitation profile is designed. A stack structure is also designed using the modified drum harvesters. The drums and the stack are tested using the footfall simulator under different conditions to study the power output. Shoe-based drum harvesters are also analyzed under different conditions. A comparison of existing shoe-based energy harvesting systems with their mechanisms, applications and drawbacks is carried out. Further, the modification of drum harvesters fabricated in chapter 3 to make them suitable for embedding in shoes is described. Fabrication of shoe-based energy harvesters and analysis with walking and running experiments in a real time environment are discussed.

**Chapter 4** Different energy harvesting circuits in conjunction with the shoe-based harvesters are analyzed in this chapter. Various non-linear methods of piezoelectric energy harvesting are discussed with their advantages and drawbacks. A comparison between the power outputs of two different bridge rectifiers is carried out. Finally, two commercially available variants of energy harvesting IC LTC 3588 are tested as potential energy harvesting solutions for vibration and impact energy harvesting.

**Chapter 5** discusses the analysis of different energy storage elements for their suitability for storing the energy generated with the piezoelectric generators designed in the present work. The advantages and drawbacks of these elements are elucidated.

**Chapter 6** discusses the potential applications of the energy harvesters analyzed in the present work. Specifically, two different applications are demonstrated. Firstly, the powering of a microcontroller board with the energy harvested from vibration using drum harvesters is described. Secondly, the powering of a RF transmitter is demonstrated. A battery-less/battery-powered RF transmission module is designed, assembled and successfully tested.

## CHAPTER 2

### LITERATURE SURVEY

---

Piezoelectric energy harvesters are essentially transducers made using materials that can be broadly classified into one of the three categories viz. ceramics, polymers and composites. Table 2.1 gives a comparison of the properties of these materials with respect to their use as transducers [39].

**Table 2.1 Comparison of properties relevant to use of piezoelectric materials as transducers**

| <b>Parameter</b>    | <b>Ceramic</b> | <b>Polymer</b> | <b>Composite</b> |
|---------------------|----------------|----------------|------------------|
| Acoustic impedance  | High (-)       | Low (+)        | Low (+)          |
| Coupling factor     | High (+)       | Low (-)        | High (+)         |
| Spurious modes      | Many (-)       | Few (+)        | Few (+)          |
| Dielectric constant | High (+)       | Low (-)        | Medium (+)       |
| Flexibility         | Stiff (-)      | Flexible (+)   | Flexible (+)     |
| Cost                | Cheap(+)       | Expensive (-)  | Medium (+)       |

**(+) = Favorable, (-) = Unfavourable**

Piezoelectric power generators have many advantages over other conversion methods. Owing to their simplicity, these generators can even be fabricated on the scale of micro electromechanical systems (MEMS). Another benefit is that the lifespan of the system is nearly unlimited if the applied force and external temperature are within the operational range. Unlike power generation methods that rely on heat conversion, a piezoelectric generator presents no problems such as heat isolation. In addition, the mechanical energy required for conversion can conceivably be obtained from the



environment. Even with these advantages, piezoelectric elements have been neglected for power generation because of the considerably small electrical output [40].

## 2.1 PIEZOELECTRIC ENERGY HARVESTING

As discussed earlier (chapter 1), piezoelectric energy harvesting is a much better way of vibration energy harvesting due to its advantages over other methods. Table 2.2 gives a comparison of the three most commonly used methods of vibration energy harvesting based on their energy density [28].

**Table 2.2 Summary of maximum energy densities of three kinds of transducers**

| Type            | Energy density (mJcm <sup>-3</sup> ) | Equation   | Assumptions                     |
|-----------------|--------------------------------------|--|---------------------------------|
| Piezoelectric   | 35.4                                 | $\left(\frac{1}{2}\right) \frac{\sigma_y^2 k^2}{2c}$ | PZT 5 H                         |
| Electromagnetic | 24.8                                 | $\left(\frac{1}{2}\right) \frac{B^2}{\mu_0}$         | 0.25T                           |
| Electrostatic   | 4                                    | $\left(\frac{1}{2}\right) \varepsilon_0 E^2$         | $3 \times 10^7 \text{ Vm}^{-1}$ |

$\sigma_y$  is the yield stress,  $k$  is the coupling coefficient,  $c$  is the elastic constant,  $B$  is the magnetic field,  $\mu_0$  is the permeability of free space,  $\varepsilon_0$  is the permittivity of free space, and  $E$  is the electric field.

Piezoelectric materials convert mechanical energy from pressure, vibrations or force into electricity. They are capable of generating electrical charge when a mechanical load is applied on them. This property of piezoelectric materials has prompted researchers to develop various piezoelectric harvesters such as ENERCHIP, ultrasonic actuators, accelerometers in order to power and control different applications. Due to their inherent ability to convert mechanical energy into electrical energy, piezoelectric materials have become a viable ambient energy scavenging source. Currently a wide

variety of piezoelectric materials are available and the appropriate choice for sensing, actuating or harvesting energy depends on their characteristics. Polycrystalline ceramic is a common piezoelectric material. With their anisotropic characteristics, the properties of the piezoelectric material differ depending upon the direction of forces and orientation of the polarization and electrodes. However, using piezoelectric materials to harvest energy requires a mechanism of storing the energy generated. This means we can either implement a circuit to store the energy harvested for using it later or develop a circuit to utilise the energy as it is harvested. Moreover, the energy harvested can be stored in rechargeable batteries instead of using capacitors.

Out of many manmade piezoelectric materials, the most popular is PZT. PZT-based transducers can be used for ambient vibration energy harvesting. This energy can be stored and used to power up electrical and electronic devices. With recent advancements in micro and nano-scale devices, PZT power generation can provide a conventional alternative to traditional power sources used to operate certain types of sensors/actuators, telemetry and micro electromechanical systems (MEMS) devices. The major application of MEMS technology is in sensors which include sensors for medical (blood pressure), automotive (pressure, accelerometer) and industrial (pressure, mass air flow) applications. Among all the MEMS energy harvesting devices, piezoelectric MEMS have attracted a lot of research interest for their simplicity. Under vibrational stimulus, piezoelectric material will generate electrical energy. The source of vibration can be easily obtained from our daily activities. It can be fabricated in dimensions of the order of a few millimeters which is a perfect solution for providing free continuous power output for low power microelectronic devices. Figure 2.1 shows the basic idea of energy conversion of a piezoelectric element [41].

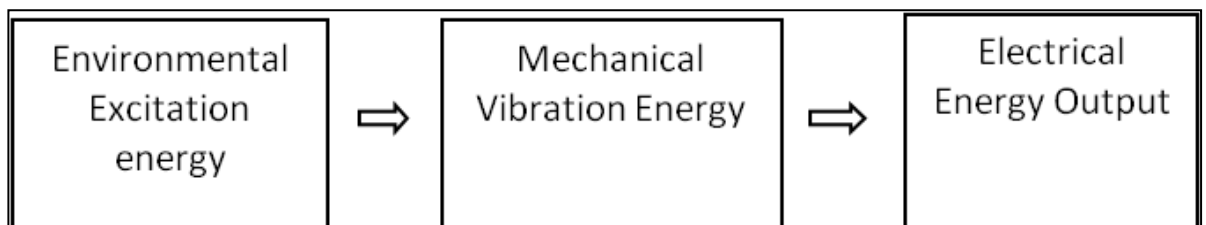


**Figure 2.1 Piezoelectric energy conversion**

We hypothesized that these piezoelectric materials could be utilized to generate electricity at a place where there is no conventional sources of electricity. As an example, our army soldiers are stationed at high altitude posts like Siachen, Khardungla, Kargil which are situated between 14,000 and 18,000 feet above MSL where there is no source of electricity. These are regions of extremely low pressure and temperature. Moreover, the oxygen content in the air is low. The temperature falls below  $-30\text{ }^{\circ}\text{C}$  in peak winter. Soldiers are generally stationed at these locations for a considerable duration and face many natural hardships due to the extreme climatic conditions, which force them to be covered from head to foot. At some places they also have to carry oxygen cylinders. The frequently occurring problems are frostbite, snow blindness, sunburn. Therefore, there is a need for a portable generator that gives enough energy to run microelectronic devices that they use and help them in mitigating the severe conditions. Of all anthropogenic activities, human ambulation (walking) has drawn special interest in the area of energy harvesting. About 67 watts of power is reportedly available from the heel strike [13] of which 5 watts can be extracted by an appropriately shaped piezoelectric insert [2].

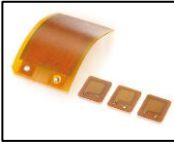


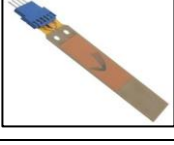

## **2.2 PIEZOELECTRIC ENERGY HARVESTING ELEMENTS**

Researchers have comprehensively reviewed energy harvesting using piezoelectric materials with respect to different materials, configurations, efficiencies, ambient energy sources like vibrations, biomechanical sources, natural sources, machines, harvesting electronics, etc. Sodano et al. [42] discuss power harvesting using different systems and their application to the real world. In Anton et al. [43], various shapes and configurations of piezo harvesters and factors affecting the power output are discussed. Mitcheson [44] reviews the principles and state-of-art in motion-driven miniature energy harvesters and discusses trends, suitable applications, and possible future developments. Goldfarb [45] analyses the efficiency of piezoelectric ceramics for electric power generation. Gambier and co. [46] describe a hybrid energy harvesting system employing piezoelectric, solar and thermal generators.

Table 2.3 gives a comparison of the various commercially available piezo harvesters that were explored in this work. There are different types of piezoelectric elements available commercially like cantilevers, discs, diaphragms, rings, patches, etc.

Although any piezoelectric material can act as an electromechanical generator, the choice of an energy harvester depends on the usable power that can be obtained and its suitability to serve the needs of a particular application. Some of the harvesters (patches) shown in the table could not be obtained for testing as they were very expensive and required import, while some (cantilever) were obtained as free samples.

**Table 2.3 Commercially available piezoelectric elements**

|   | <b>Element</b> | <b>Application</b>   |
|---|----------------|--|
|    | Patches        | <ol style="list-style-type: none"> <li>1. Sensors</li> <li>2. Actuators</li> </ol>                               |
|    | Rings          | <ol style="list-style-type: none"> <li>1. Actuators</li> <li>2. Motors</li> </ol>                                |
|  | Discs          | <ol style="list-style-type: none"> <li>1. Actuators</li> <li>2. Ultrasonics</li> </ol>                           |
|  | Cantilever     | <ol style="list-style-type: none"> <li>1. Sensors</li> <li>2. Energy harvesting</li> </ol>                       |
|  | Diaphragms     | <ol style="list-style-type: none"> <li>1. Acoustics</li> <li>2. Sensors</li> <li>3. Energy harvesting</li> </ol> |

Piezoelectric cantilever energy harvesters have been a popular choice of researchers and commercial manufacturers and have been the subject of a lot of research. Coated on a cantilever beam, piezoceramics allow simple energy harvesting without additional mechanical structures. Relatively small external excitations result in output of several volts [47]. The cantilever configuration offers large average strain in the piezoelectric material for a given applied force and low resonant frequencies can be achieved due to the low stiffness of the structure [23]. However, these energy harvesters are not suitable

for low frequency high amplitude applications. Table 2.4 lists research carried out with piezoelectric cantilever elements.

**Table 2.4 Piezoelectric Cantilever Harvesters**

| <b>Reference</b>        | <b>Peak Power<br/>(mW)</b> | <b>Resonance<br/>Frequency<br/>(Hz)</b> | <b>Acceleration<br/>(m/s<sup>2</sup>)</b> | <b>Resistive<br/>Load at<br/>resonance<br/>(kΩ)</b> |
|-------------------------|----------------------------|---|---|---|
| Roundy et al [48]       | 0.375                      | 120                                     | 2.5                                       | -   |
| Sodano et al [49]       | 1.5 – 2                    | 0 – 250                                 | 2   | 1   |
| Zheng et al [50]        | 0.325                      | 150                                     | 4.8                                       | 98  |
| Glynne-Jones et al [51] | 0.003                      | 80                                      | -   | 333   |
| Eichhorn et al [52]     | 0.003 – 0.006              | 115                                     | 3.4                                       | -   |
| Leon et al [53]         | 1.85                       | -                                       | 2   | -   |
| Song et al [54]         | 0.106                      | 16.1                                    | 10  | 600   |

In recent years, researchers have turned their attention towards lead-free and flexible piezoelectric energy harvesters. Table 2.5 outlines research on flexible piezoelectric energy harvesters.

**Table 2.5 Flexible piezocomposite harvesters**

| <b>Inventor</b>         | <b>Year</b> | <b>Peak Power</b> | <b>Application<br/>demonstrated</b> |
|-------------------------|-------------|-------------------|-------------------------------------|
| Mc Alpine & Co.<br>[55] | 2010        | NA                | NA                                  |
| X Chen & Co. [56]       | 2010        | 0.00003 μW        | NA                                  |

|                     |      |    |                 |
|---------------------|------|----|-----------------|
| Z L Wang & Co. [57] | 2012 | NA | Flashing an LED |
|---------------------|------|----|-----------------|

Circular piezoelectric energy harvesters, in particular piezocomposite diaphragms, have been analyzed by researchers in various setups and excitation profiles. Table 2.6 gives a comparison of such harvesters.

**Table 2.6 Circular piezocomposite harvesters for energy harvesting**

| Reference            | Dimensions (mm)      | Thickness (mm)         | Power    | Frequency (Hz) | Force/ Pressure / Acceleration (as applicable) | Resistive Load at resonance (k $\Omega$ ) |
|----------------------|----------------------|------------------------|----------|----------------|--|---|
| X-Chen et al [58]    | 25 (P)<br>30 (S)     | 0.2 (P)*<br>0.2 (S)*   | 12 mW    | 113            | 1.2 N  | 33  |
| Minazara el al [59]  | 12.5 (P)<br>20.5 (S) | 0.23 (P)<br>0.4 (S)    | 1.7 mW   | 1710           | 80 N   | 5.6                                       |
| Wischke et al [60]   | 25 (P)<br>35 (S)     | 120 (P)<br>100 (S)     | 1.3 mW   | 1              | 10 N   | -   |
| Kim et al [61]       | 25 (P)<br>30 (S)     | 0.127 (P)<br>0.508 (S) | 0.029 mW | 0.3            | 10 kPa   | -   |
| Palosaari et al [62] | 34.5 (P)             | 0.191 (P)              | 1.08 mW  | 0.96           | (0-24.5) N                                     | 1.2                                       |

|                                |                      |                     |  |       |                       |   |
|--------------------------------|----------------------|---------------------|--|-------|-----------------------|---|
|                                | 45.5 (S)             | 0.100 (S)           |  |       |                       |   |
| W Wang et al<br>[63]           | 25 (P)<br>40 (S)     | 0.2 (P)<br>0.2 (S)  | 28 mW<br>(series)<br><br>27 mW<br>(parallel) | 150   | 0.8 N                 | 160<br>(series)<br><br>11<br>(parallel) |
| Ericka et al [64]              | 12.5 (P)<br>20.5 (S) | 0.23 (P)<br>0.4 (S) | 1.8 mW                                       | 2.58k | 19.6 m/s <sup>2</sup> | 56                                      |
| Cymbal - H W<br>Kim et al [65] | 29 (P)               | 1 (P)               | 30 mW  | 100   | 7.8 N                 | 5                                       |
| Drum – S Wang<br>et al [66]    | 20 (P)<br>15 (S)     | 0.2 (P)<br>0.2 (S)  | 11 mW  | 590   | 0.7 N                 | 18                                      |

**\* (P) denotes piezo and (S) indicates the metal substrate**

It is clear from the above table that circular piezoelectric diaphragm harvesters generate useful amounts of energy in a wide range of vibration profiles (wide frequency as well as force range). They can be used in combination to increase the power further and a drum harvester is the best configuration of increasing the number of piezo elements in a harvester setup, and hence the power. There is the possibility of getting nearly double the power using a drum harvester compared to a single diaphragm element as it uses two elements that work in tandem. Additionally, a drum harvester is able to work with large excitation amplitudes as well. A device employing several drum harvesters connected in series/parallel can be conceptualized and one aim of the present research is to fabricate such a device and use it to harvest energy from real world vibration environments. The energy thus harvested will be used to power microelectronic devices.

## 2.3 PIONEERING WORK ON ANTHROPOGENIC PIEZO HARVESTERS

One of the first attempts at investigating the harvesting of energy from human ambulation using piezoelectric materials was by Antaki et al. [67]. Another notable attempt at designing a shoe powered piezoelectric generator was at MIT by Paradiso and Co. In the paper ‘Parasitic Power Harvesting in Shoes’ [68], Kymissis et al. described the design of a shoe powered piezoelectric generator in which two kinds of piezo materials were used viz. PVDF and PZT shown in figure 2.2. A PVDF stave was inserted in the insole and a PZT unimorph was inserted in the heel. The average powers produced by the stave and the unimorph were 1 mW and 2 mW respectively with the collective power being enough to power a RF encoder which could be used to give the location of a person.

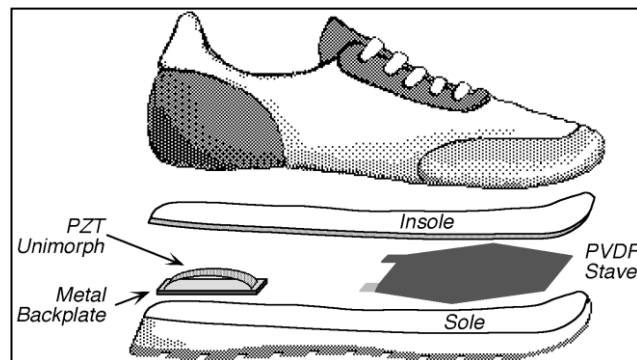


**Figure 2.2 Shoe generator designed by Paradiso & Co at MIT, (a) PVDF stave (b) PZT unimorph [68]**

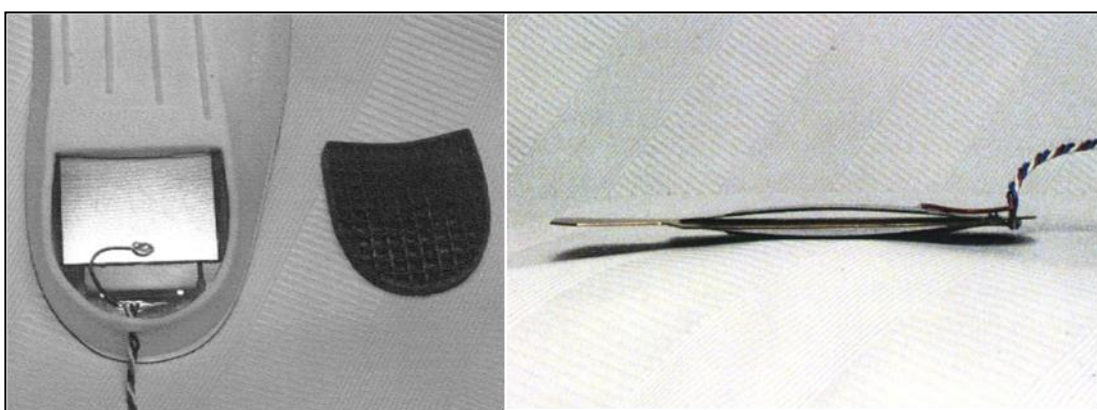


**Figure 2.3 PZT bimorph shoe insert [69]**



Later, the same group also designed another piezo generator shoe insert shown in figure 2.3 [69]. This time it was a customized bimorph made using two unimorphs. The average power obtained was 1.8 mW for a vertical displacement of 4.8 mm.

Around the same time, research was also carried out on materials known as electroactive polymers (EAP) or dielectric elastomers (DEE) which demonstrated a similar ability as piezoelectric materials but had a different mechanism. DARPA in collaboration with SRI International designed a shoe generator using such a material which was able to generate 800 mW of power at two steps per second for a heel compression of 3 mm (figure 2.4). The energy density of this prototype was measured as 0.4 J/gm. The prototype received a patent in 2004 [70].

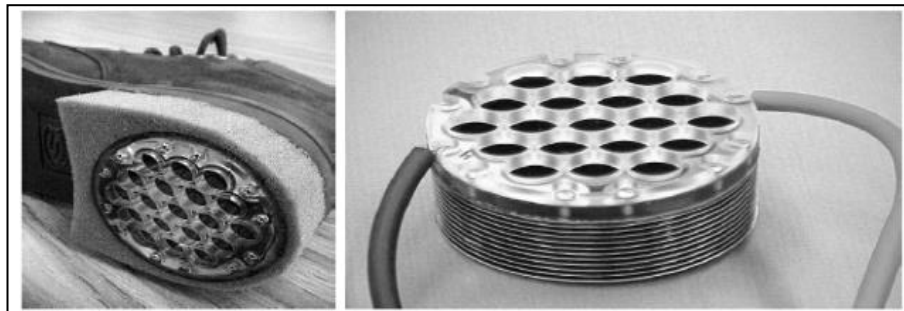


**Figure 2.4 Shoe generator using EAP/DEE [70]**

In 2001, well known British inventor Trevor Bayliss trekked the Namibian desert for 100 miles wearing prototype piezo generator shoes developed in collaboration with the Defense Evaluation Research Agency of the UK Ministry of Defense. This prototype was reportedly able to generate about 150 mW of power. The partial charging of a mobile phone was demonstrated [71].



**Figure 2.5 Quartz crystal powered shoe generator designed by Trevor Baylis**

In 2010, McAlpine et al. described a method to manufacture flexible nanogenerators. The team fabricated PZT nanofibers and transferred them onto a silicone substrate to get a highly flexible nanogenerator (figure 2.6). The advantage of such a generator is that it can be used as a universal, implantable generator. It is flexible and removes the drawbacks arising due to rigidity and brittleness of PZT sheets. Applications may include implants inside the human body (using lead free materials) to power life support devices like pacemakers [55].

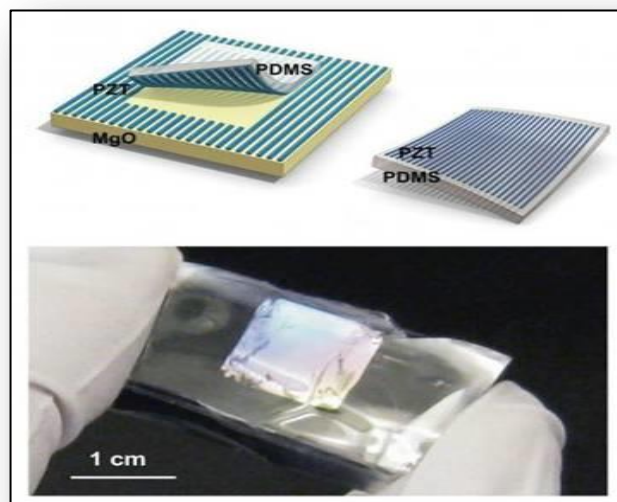


**Figure 2.6 Silicone embedded PZT [55]**

Dr. Zhong Lin Wang of the Korea Advanced Institute of Science and Technology in collaboration with Georgia Institute of Technology has made quite a few breakthroughs in flexible nanogenerator technology. Dr. Wang and his team have worked on zinc oxide, studying its piezoelectric and semiconductive properties. They fabricated ZnO

nanowires, nanobelts, etc. In vivo experiments were conducted by implanting the nanowires into the heart and diaphragm of rats where 30 pA at 3 mV and 4 pA at 2 mV were generated respectively [72, 73]. Wang and co workers next attempted to fabricate a lead-free flexible nanogenerator [57]. A nanocomposite generator (NCG) was fabricated using a simple low cost method (figure 2.7). The materials used were barium titanate nanoparticles, carbon nanotubes and silicone. The advantage of the method used besides being simple and low cost is that a large area generator can be fabricated. NCG is giving consistent output. Outputs with finger compression and foot compression were measured with the outputs being 4 nA at 150 mV and 150 nA at 1.5 V respectively. The prototype was used to charge a capacitor bank which was used successfully to light a LED. Table 2.7 summarizes different shoe-based energy harvesters.

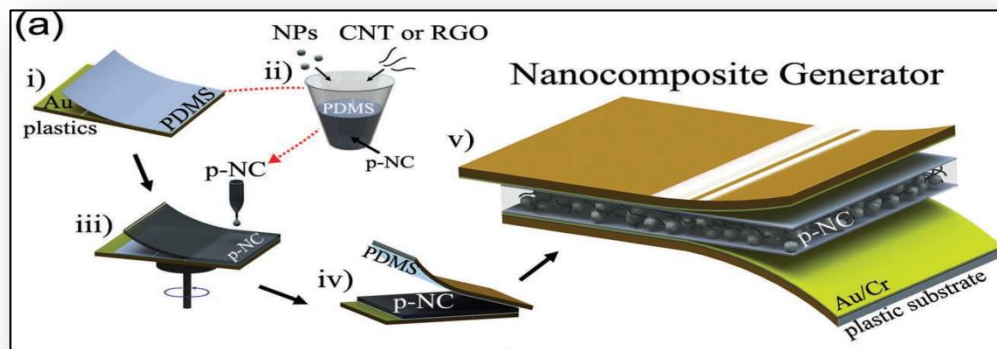


**Figure 2.7 Flexible barium titanate nanocomposite generator [57]**

**Table 2.7 Energy harvesting through human ambulation**

| <b>Inventor</b> | <b>Year</b> | <b>Output power (mW)</b> | <b>Material</b> | <b>Mechanism</b>                             | <b>Application (reported)</b>          | <b>Drawbacks/ Limitations</b> |
|-----------------|-------------|--------------------------|-----------------|--|--|-------------------------------|
| Antaki [67]     | 1995        | 23 / kg body weight      | PZT             | Hydraulic system                             | Battery charging for artificial organs | Very heavy                    |
| Shenck [69]     | 1998        | 1 -2                     | PZT             | Curved patch and flexible stave              | RF encoder                             | Low power output              |
| Pelrine [70]    | 2001        | 800                      | EAP             | Bellows                                      | Gadget powering for soldiers           | Gait affected                 |
| Baylis [71]     | 2001        | 150                      | Quartz Crystal  | -  | Mobile phone charging                  | For demo only                 |
| Von Buren [74]  | 2006        | 0.005-0.025              | Electromagnetic | Rotary generator                             | Body worn sensor networks              | Low power output              |
| Liu [75]        | 2012        | 1.6                      | Electromagnetic | Magnet coil and pendulum arrangement         | Charging of battery                    | Low power output              |
| J Zhao [76]     | 2014        | 1                        | PVDF            | Multilayer PVDF film in a sandwich structure | Low power wearable sensors             | Low power                     |
| Leinonen [77]   | 2012        | 0.081 / step             | PZT             | Moonie                                       | --                                     | Low power                     |

## **2.4 FABRICATION OF A FLEXIBLE PIEZOCOMPOSITE GENERATOR**

In the present work, initially an attempt to fabricate flexible piezocomposite generators was made. What follows is the description of a novel method to achieve the same.

The following materials were used to fabricate a flexible Piezocomposite material:

1. PZT 5H powder (3  $\mu$  and 1  $\mu$  particle size)
2. Multiwalled carbon nano tubes (MWCNT) (diameter 5–20 nm, length upto 10  $\mu$ )
3. Polydimethyl siloxane (PDMS) synthetic silicone rubber
4. Solvents THF, chloroform

Two types of composites were fabricated. One contained only PZT and PDMS. The other contained MWCNTs in addition to the two components mentioned earlier. Different techniques were used for mixing of the ceramic (PZT) in the polymer (PDMS). To begin with, a composite was made using a shear mixer (muller). 10 gm of PDMS and 1 gm of PZT powder (3  $\mu$ ) were shear mixed at a rotation speed of 100 rpm in the muller. Curing agent was added to the composite in the ratio 10:1 and the composite was mixed thoroughly. A film was cast using the composite in a Petri dish. It took 24 hrs for the composite to cure fully and attain a rubber-like consistency.

To reduce the size of the PZT particles, planetary milling was used. Zirconia balls and PZT powder were taken in the ratio of 2:1 and 4:1 by weight and mixed with propanol to form slurry which was enclosed in a pot and milled in the planetary ball mill for 24 hrs. The particle size of the sample removed from the mill after 12 hrs was analysed using a Beckman Coulter Delsa Nano Z particle size analyzer. It was found that the particle size decreased from 3  $\mu$  to 1  $\mu$ . Thereafter, no change in particle size was observed at the end of the milling process.

For the second composition, PZT (1  $\mu$ ) + MWCNT + PDMS were mixed in specific percents by weight. The weight percent of PZT in the composite was taken as 9% and 16% in two different compositions. MWCNT was taken in 0.5 wt% and 1 wt% proportions respectively in the two compositions. Two methods were used to mix these materials. Firstly they were mixed in a bottle with zirconia balls using a roller mill for

about 24 hours. The composite was then removed and mixed manually with curing agent in the ratio 10:1. It was then cast in a square Teflon mould and allowed to set at room temperature for 24 hrs. The composition mentioned above was again formulated but this time the mixing was done manually. The compositions were cured at room temperature as well as under heat treatment. The cured rubber-films ranged in the thickness of 1 mm to 2 mm. They were cut into square pieces of an inch square in size and silvered on one side with silver paste. They were kept aside for 24 hrs at room temperature for the silver paste to cure completely. Then these samples were subjected to corona poling with the silvered surface acting as the ground. The conditions maintained in the corona poling setup were – temperature 70°C and electric field 50–80 kV. The poling was carried out for about 30 min with the hot plate in the setup switched off after about 20 min and the electric field kept on. The samples were removed and kept aside for a few minutes. The second sides of the samples were then silvered and they were kept aside for another 24 hrs at room temperature. The next day, the samples were tested for piezoelectric constant values using a Piezotest PM300 d33 meter. No significant values were observed. Electrically conductive copper tapes (by Klim Enterprises, Vasai, Maharashtra, India) of thickness 50  $\mu\text{m}$  were adhered to both sides of the samples to act as leads. The samples were also tested with a DSO to check for any voltage generated. But no significant signals were observed. However, upon testing with a digital multimeter, a peak AC voltage of around 300 mV was observed indicating that the material had some piezoelectric property. Figure 2.8 shows the samples fabricated.

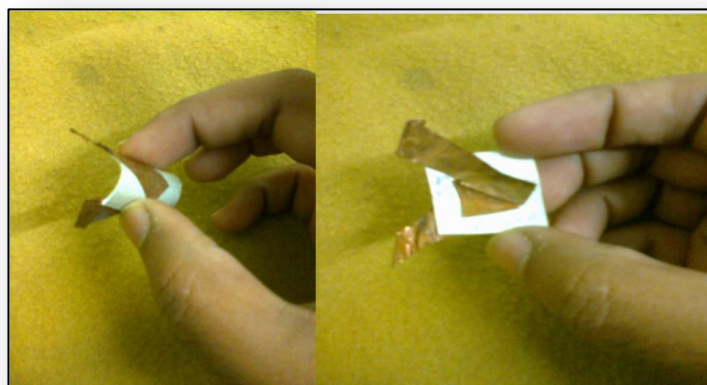


**Figure 2.8 The PZT flexible composite**

As the next step, commercially available piezocomposite diaphragms were analyzed for their ability to generate sufficient voltage in response to deformation. Piezoelectric buzzer elements were chosen for this purpose due to their ready availability and suitable dimensions.

A stack of four piezo discs (two discs were of diameter 32 mm and two were of 40 mm) shown in Figure 2.9 was constructed with the discs connected electrically in parallel. The maximum output current measured across a 100 k resistor was 380  $\mu\text{A}$  while maximum voltage was about 20 volts (AC) when the arrangement was bent using the fingers. However, the structure was not mechanically durable and hence was discarded.



**Figure 2.9 Stack of four Piezo Discs connected in parallel**

## **2.5 CONCLUSION**

Piezocomposite materials have shown potential as sources of alternative electrical power capable of generating enough energy to power ultra low power microelectronic. Although our initial endeavour into fabrication of flexible piezocomposites did not yield significant results, we intend to further refine the fabrication procedure of flexible piezo harvesters to get better outputs as we believe the problem is in the fabrication process. Also, the focus in the succeeding chapters will be on energy harvesting using piezocomposite diaphragms.

# DEVELOPMENT OF PIEZOELECTRIC ENERGY GENERATORS

---

A circular piezocomposite diaphragm consists of a thin piezoceramic disc adhered to a metal substrate (generally brass, steel or aluminium) (figure 3.1) [78]. The circular structure is one that is commonly used for sensors. Generally, an external force applied on the pressure sensor persists for a long time [60]. It is a well established theory in engineering mechanics that the highest stresses occur in the plane of a bent composite structure [61]. The composite structure can undergo large deformations as compared to a monolithic PZT disc which is brittle in nature. Due to their thin form factor and size, they can be incorporated into various structures. Owing to these reasons, circularly shaped piezocomposite elements are suitable as energy harvesters for high as well as low stress applications in a wide frequency range. The present work explores the performance of these elements in different excitation profiles.

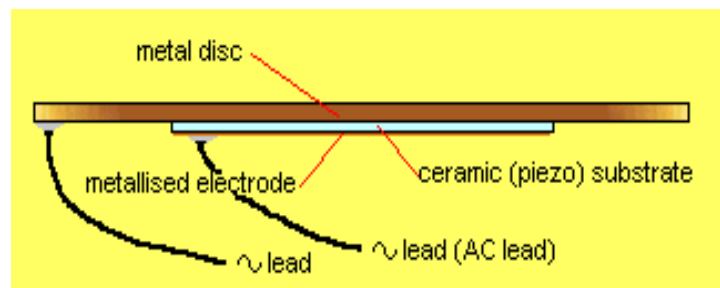


**Figure 3.1 Structure of a piezocomposite diaphragm [78]**

Piezoelectric diaphragms are commercially available and employed as buzzer elements in acoustic systems such as alarms, ringers, guitar pickups, etc. They are available in various sizes (figure 3.2) and the size which suits a particular application can be easily selected. Their dimensions are optimum for incorporation into structures like shoes, vibrating surfaces, etc.





**Figure 3.2 Piezoelectric buzzer elements**

The present work studies the energy harvesting performance of piezocomposite diaphragm harvesters in low frequency high amplitude as well as high frequency low amplitude profiles. The piezoelectric material used in the piezocomposite elements is PZT-5H.

The criteria that determine the output power of a piezoelectric diaphragm are:

1. Ratio of thickness of piezo disc to that of metal substrate [ $h_p/h_m$ ]
2. Ratio of radii of piezo disc and metal substrate [ $R_1/R_2$ ]

Maximum energy is obtained for  $h_p/h_m = 1.5$  and  $R_1/R_2 = 0.72$ . However, increasing the thickness of the piezo disc is equivalent to increasing the amount of piezo material in the element. This does increase the energy output but at the cost of increased bending resistance leading to reduced deflection and hence less energy gain [79]. Also, the gain in energy is not significant. Hence, for the present work, a thickness ratio of 1 was chosen. Table 3.1 gives the dimensions of the diaphragm harvesters used in the present work.

Flexural composite discs or diaphragms have been studied extensively by researchers for their energy harvesting capabilities as already described. In the present work, the energy harvesting ability of drum harvesters under low stress has been studied. Two different sizes of buzzer elements were used for the present work viz. 35 mm and 27 mm (standard sizes available commercially). From table 3.1 it is clear that the two sizes

selected have optimum values of  $h_p/h_m$  and  $R_1/R_2$ . The 40 mm buzzer was rejected due to its inability to withstand large impact forces (of the order of 100 N or more) without being permanently deformed.

Generally, an energy harvester extracts the maximum amount of power when operating at resonance. However, in many cases, it becomes impractical to match the resonance frequency of the piezoelectric elements with the input frequency.

**Table 3.1 Dimensions of piezoelectric diaphragms used in the present work**

| Diameter of metal substrate (mm) | Diameter of piezo disc (mm) | Thickness of metal substrate (mm) | Thickness of piezo disc (mm) | $h_p/h_m$ | $R_1/R_2$ |
|----------------------------------|-----------------------------|-----------------------------------|------------------------------|-----------|-----------|
| 27                               | 20                          | 0.20                              | 0.20                         | 1         | 0.74      |
| 35                               | 25                          | 0.25                              | 0.25                         | 1         | 0.71      |
| 40                               | 25                          | 0.19                              | 0.19                         | 1         | 0.63      |

### 3.1 EXPERIMENTAL TESTING OF PIEZO BUZZERS (HIGHER FREQUENCY LOW AMPLITUDE)

A piezoelectric element can be modeled mechanically as a spring-mass-damper system represented mathematically by a linear, time-invariant second order differential equation [80] as

$$m \frac{d^2 z(t)}{dt^2} + b \frac{dz(t)}{dt} + k z(t) = m \frac{d^2 y(t)}{dt^2} \quad (1)$$

where  $m$  is the effective mass,  $b$  is the damping coefficient and  $k$  is the structure stiffness.

Under an applied force, the open circuit output voltage ( $V$ ) of the ceramic is given as

$$V = E \cdot t = -g \cdot x \cdot t = -g \cdot F \cdot \frac{t}{A} \quad (2)$$

where  $E$  is the electric field,  $t$  is the thickness of the piezoceramic,  $x$  is the stress,  $A$  is the area and  $g$  is the piezoelectric voltage coefficient.

The power available under cyclic excitation is given by

$$P = \frac{1}{2} \cdot CV^2f \quad (3)$$

where  $f$  is the frequency of excitation [65]. Previous reports [62, 65, 81-84] have suggested that application of suitable pre-stress reduces the resonant frequency and, at the same time, increases the power output. Table 3.2 describes the ambient sources of vibrations [42].

**Table 3.2 Ambient vibration sources**

| <b>Vibration Source</b>             | <b>Acceleration<br/>(m/s<sup>2</sup>)</b> | <b>Frequency<br/>(Hz)</b> |
|-------------------------------------|---|---------------------------|
| Car engine compartment              | 12  | 200                       |
| Base of 3-axis machine tool         | 10  | 70                        |
| Blender casing                      | 6.4                                       | 121                       |
| Clothes dryer                       | 3.5                                       | 121                       |
| Person nervously tapping their heel | 3   | 1                         |
| Car instrument panel                | 3   | 13                        |
| Door frame just after door closes   | 3   | 125                       |
| Small microwave oven                | 2.5                                       | 121                       |
| HVAC vents in office building       | 0.2 – 1.5                                 | 60                        |

|                                   |     |     |
|-----------------------------------|-----|-----|
| Windows next to a busy road       | 0.7 | 100 |
| CD on notebook computer           | 0.6 | 75  |
| Second story floor of busy office | 0.2 | 100 |

Impedance analysis of the piezoelectric buzzers was carried out using a Agilent 4294A impedance analyzer and  $d_{33}$  measurement was done using a PiezoTest PM300  $d_{33}$  meter. The results of the analysis are shown in Appendix A. An electrodynamic shaker (Type SP2 by Spranktronics Bangalore) was used as the excitation mechanism. Customized holders were fabricated for each buzzer element so that it could be screwed on to the central shaft of the shaker and allow transmission of vibrations vertically to the elements. The experimental setup is shown in figure 3.3. The holders were circular in shape and the buzzers were adhered to them by means of an adhesive (Fevibond). Care was taken to properly insulate the holders electrically as they were metallic and could electrically short the buzzer elements. As shown in figure 3.3, the holders were screwed onto the shaft of the shaker. A function generator was used together with a power amplifier to provide sinusoidal excitation input to the shaker. Mechanical weights from a standard weight box were attached on top of the buzzer elements to apply pre-stress.

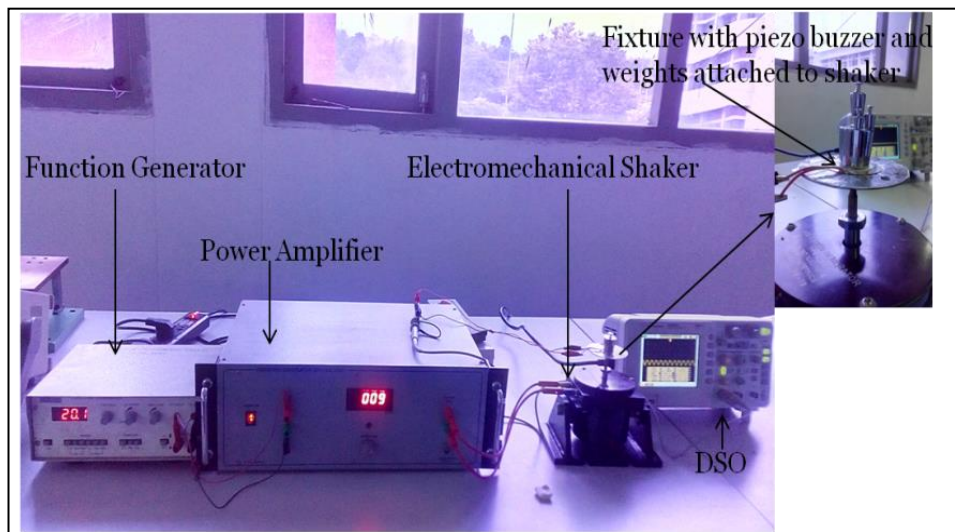


**Figure 3.3 Experimental setup for vibration analysis of piezo buzzers**

The weights (pre-stress) and excitation frequency were varied to get the peak AC voltage output at resonance for both the buzzers. The AC output of the buzzers was fed to a standard interface circuit consisting of a schottky bridge rectifier and capacitor. A resistive load was connected across the capacitor. Peak DC output voltage was achieved and subsequently measured, by varying the resistance. The resistance and electrolytic capacitor were replaced by a 5 V zener diode (used to limit the charging voltage across the supercapacitor) and a supercapacitor (Cornell Dubilier 5.5 V/ 0.1 F) and the charging of the supercapacitor was studied. The charging of the supercapacitor was recorded using a digital multimeter (Rishabh 16S) and compatible data logger (SI 232). The acceleration of the arrangement (shaker+holder) was measured using a 3-axis accelerometer (ADXL335). Real time values from the accelerometer were recorded on a laptop using Data Acquisition Card (NI-9174 by National Instruments) and LabVIEW.

## 3.2 RESULTS AND DISCUSSIONS

### 3.2.1 Effect of mechanical pre-stress on output voltage

The output voltages of the piezo buzzer elements with and without mechanical pre-stress were studied. Figures 3.4 & 3.5 give plots of AC voltage output ( $V$ ) vs. frequency ( $F$ ) for the buzzer elements without mechanical pre-stress for 35mm and 27mm buzzer respectively.

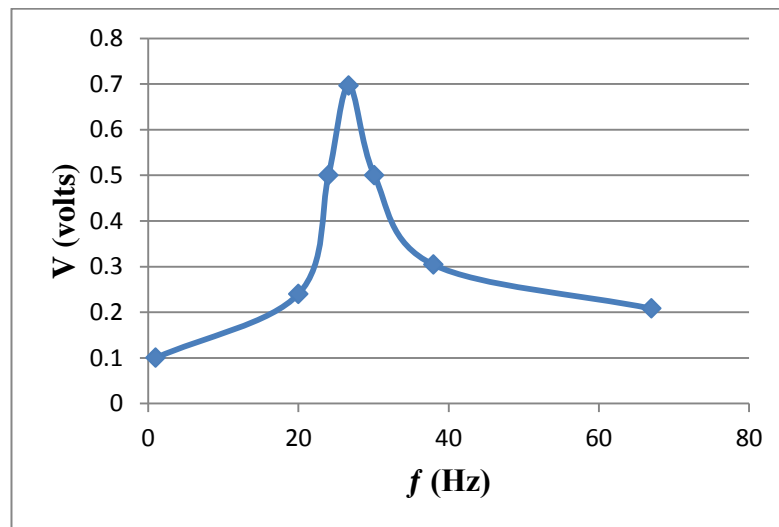


Figure 3.4 Voltage output without mechanical pre-stress for 35 mm buzzer

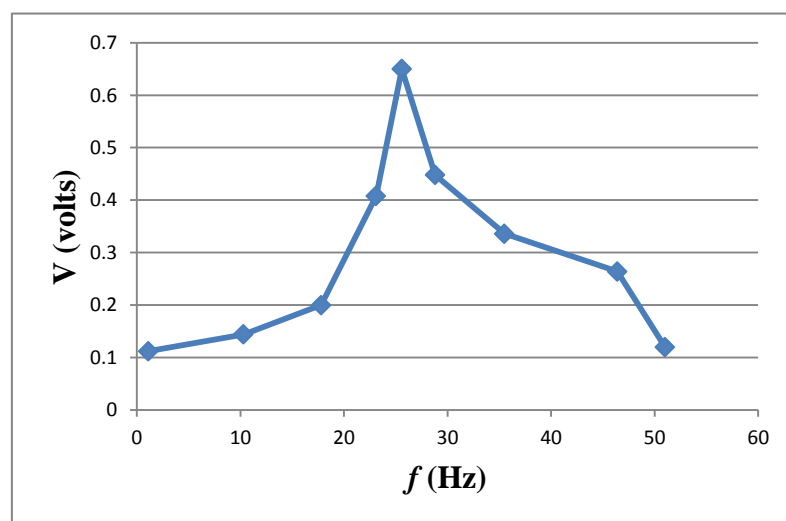
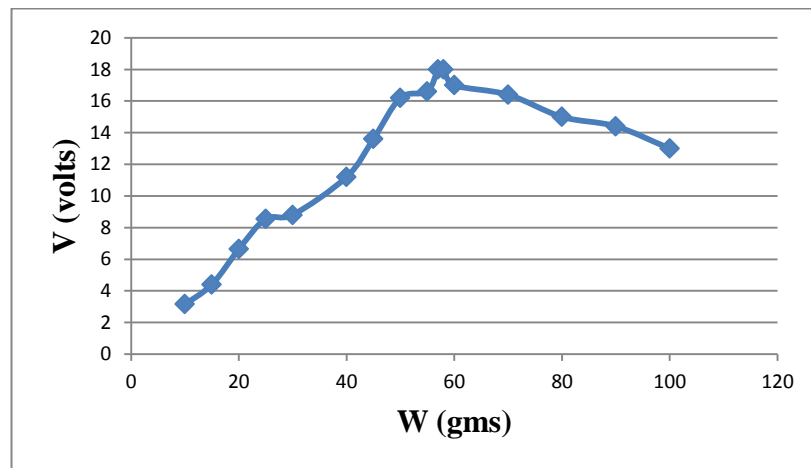


Figure 3.5 Voltage output without mechanical pre-stress for 27 mm

As can be seen from the figures, the output voltage without pre-stress is very low. The highest voltages obtained at resonance were 0.7 and 0.65 volts for the 35 mm and 27 mm buzzers respectively.

The buzzer elements were then subjected to pre-stress by attaching weights to the top surface. The pre-stress was increased in steps of 5 gms and the corresponding output voltages were measured. Figures 3.6 & 3.7 give plots of output voltage ( $V$ ) vs. pre-stress ( $W$ ).



**Figure 3.6 Voltage output with mechanical pre-stress for 35 mm buzzer**

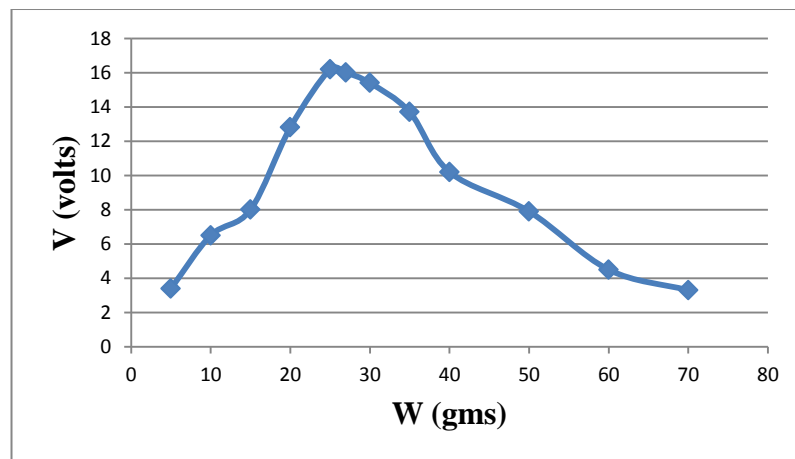


**Figure 3.7 Voltage output with mechanical pre-stress for 27 mm buzzer**

### 3.2.2 Effect of mechanical pre-stress on resonance frequency

Increasing the pre-stress had the effect of reducing the resonance frequency of the piezo buzzer elements. Without the pre-stress, the resonance frequencies were 26.7 Hz and 25.6 Hz for the 35 mm and 27 mm buzzer elements respectively. After application of pre-stress, the resonance frequencies reduced to 22.6 Hz and 24.2 Hz for the 35 mm and 27 mm buzzer elements respectively. Figures 3.8 & 3.9 give a plot of frequency ( $F$ ) vs. pre-stress ( $W$ ) for the two buzzer elements.

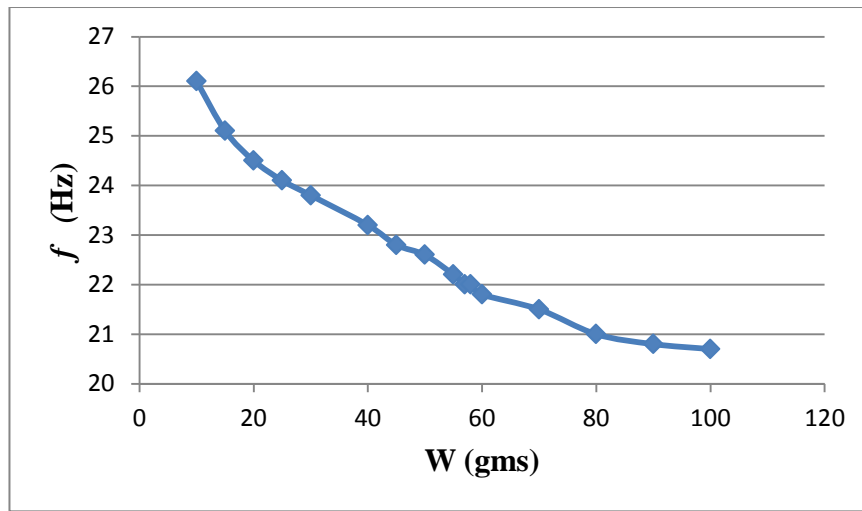


Figure 3.8 Frequency v/s weight (pre-stress) for 35 mm buzzer

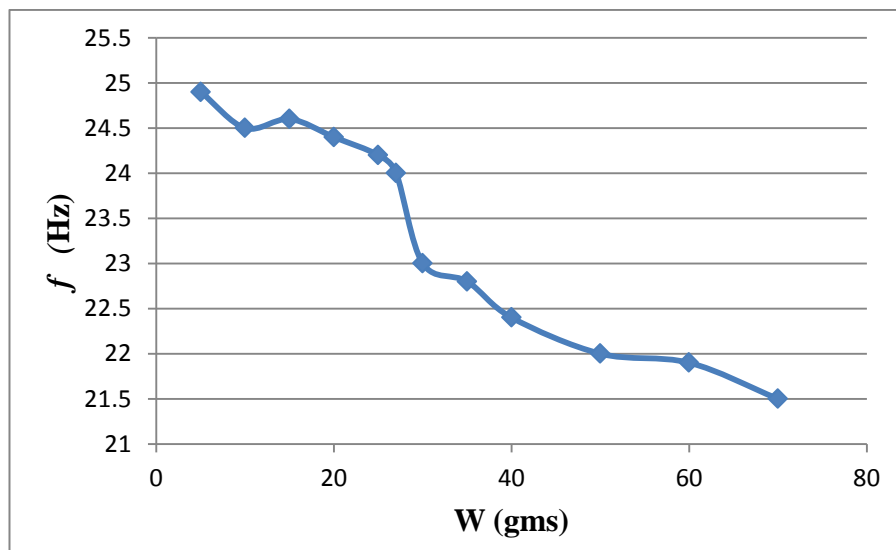


Figure 3.9 Frequency v/s weight (pre-stress) for 27 mm buzzer



### 3.2.3 Power delivered to a resistive load

Figures 3.10 and 3.11 depict plots of power ( $P$ ) vs.resistive load ( $R$ ) for the two buzzer elements. Peak powers obtained were - 223  $\mu\text{W}$  across a 126  $\text{k}\Omega$  resistive load for the 35 mm buzzer and 86  $\mu\text{W}$  across a 133  $\text{k}\Omega$  resistive load for the 27 mm buzzer respectively, at resonant frequencies mentioned earlier.

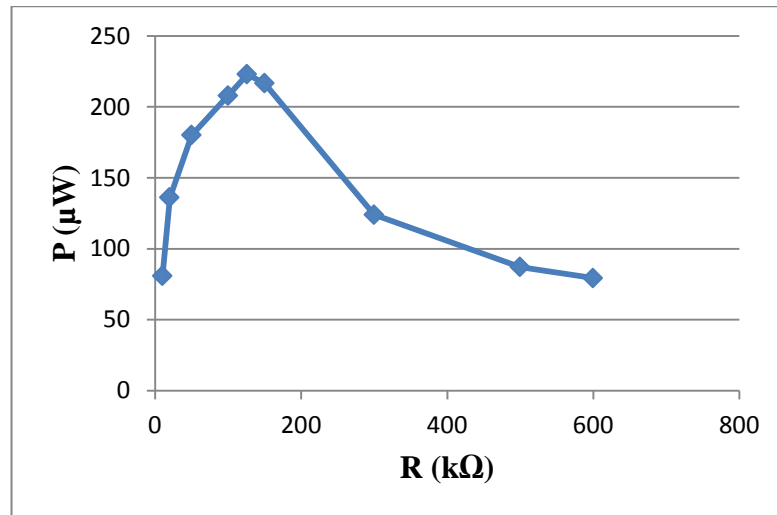


Figure 3.10 Power v/s load plot of 35 mm buzzer

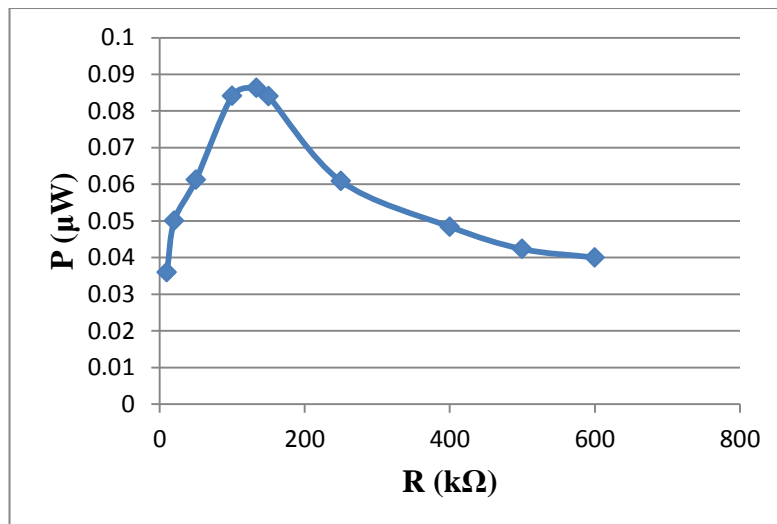


Figure 3.11 Power v/s load plot of 27 mm buzzer

### **3.3 ASSEMBLY AND TESTING OF PIEZOCOMPOSITE DRUM HARVESTERS (HIGHER FREQUENCY LOW AMPLITUDE)**

Piezoelectric materials can be used to harvest energy in high stress as well as high vibration environments [33, 77]. Examples of high stress scenarios are tyre pressure in vehicles, heel strikes in human ambulation, etc. Vibrations are mostly encountered in and around machinery like heavy rotary machines, HVACs, air conditioners, refrigerators, etc. Most of the research carried out on piezoelectric energy harvesters has been with cantilever type harvesters [13-19]. For high stress applications, circular composite structures have been developed. Examples are Moonie [77], cymbal [65] and drum transducers [66]. Moonie harvesters have been used in shoes where an energy output of 81 uJ or 81 uW per step and a power density of 56 uW/cm<sup>3</sup> were reported. Drum transducers and actuators were studied by Wang et al and Sun et al respectively. They reported a maximum output power of 11 mW at 590 Hz from a drum transducer having dimensions (20 x 1) mm<sup>2</sup>. It was also found that deformation of the structure could be increased by changing the steel ring internal diameter.

Drum harvesters work in the d<sub>31</sub> mode. The electrical/mechanical coupling for the 31 mode is lower than that for 33 mode. But the main advantage of operating piezo harvesters in the 31 mode is that the system is much more compliant, hence larger strains can be produced with smaller input forces. Also, the resonant frequency is much lower [48].

Various ambient vibration sources can be used to harvest energy and act as a power source for low power microelectronic devices like ultra-low power sensors and microcontrollers available today. These can be used for environmental monitoring, structural health monitoring, emergency backup power supply, emergency signalling and message transmission, among a myriad of other applications.

A comparison of various energy harvesting structures studied by researchers is given in Table 3.3. This is to compare the cantilevers with piezocomposite diaphragms as well as other circular piezo harvesters as regards the frequency range of excitation, the power generated and the magnitude of the resistive load.

**Table 3.3 Comparison of resonant and impulse driven energy harvesting structures.**

| <b>Reference</b> | <b>Device type</b>        | <b>Peak Power (mW)</b> | <b>Frequency (Hz)</b> | <b>Load at resonance (k<math>\Omega</math>) [as applicable]</b> |
|------------------|---------------------------|------------------------|-----------------------|---|
| Roundy [28]      | Resonant cantilever       | 0.375                  | 120                   | -   |
| Sodano [49]      | Resonant cantilever       | 1.5 - 2                | 0 - 250               | 1   |
| Zheng [50]       | Resonant cantilever       | 0.0325                 | 150                   | 98  |
| Glynn-Jones [51] | Resonant cantilever       | 0.003                  | 80                    | 333   |
| Chen [58]        | Circular diaphragm        | 12                     | 113                   | 33  |
| Minazara [59]    | Circular diaphragm        | 1.7                    | 1710                  | 5.6   |
| Kim [65]         | Cymbal                    | 39                     | 100                   | 400   |
| Wang [66]        | Drum transducer           | 1.1                    | 590                   | 18  |
| Leinonen [77]    | Moonie                    | 0.082                  | 1                     | -   |
| Marinkovich [86] | Resonant – Impulse driven | 0.025                  | 60                    | 9200  |
| Renaud [87]      | Impulse driven            | 0.040                  | 1                     | 385   |

### 3.4 EXPERIMENTAL PROCEDURE

Commercially available piezo buzzers of two different dimensions (35 mm and 27 mm) were chosen for this study as already described earlier. Steel rings (Figure 3.12) of 3 different internal diameters (IDs) for each piezo element were fabricated using SS 304 grade stainless steel.



**Figure 3.12** The piezoelectric buzzer elements with steel rings

The components were adhered using a commercially available synthetic rubber-based adhesive (Fevibond). The adhesive was applied to both surfaces to be adhered and they were kept aside for about 10 minutes before joining them. The bonding achieved was excellent and at no time during the experiments was any structural disintegration noticed. Wires were soldered on the central piezo disc and on the metal substrate at the periphery to act as leads. Figure 3.13 shows the drum harvesters fabricated. Figure 3.14 shows the experimental setup. Table 3.4 gives the dimensions of the components used to make the drums.



**Figure 3.13 The drum harvesters**

**Table 3.4 Dimensions of the piezo buzzer elements used to make drum harvesters**

| <b>Diameter of metal substrate (mm)</b> | <b>Diameter of piezo disc (mm)</b> | <b>Thickness of metal substrate (mm)</b> | <b>Thickness of piezo disc (mm)</b> | <b>Steel ring ID (mm)</b> |
|---|------------------------------------|--|-------------------------------------|---------------------------|
| 27                                      | 20                                 | 0.20                                     | 0.20                                | 23, 24, 25                |
| 35                                      | 25                                 | 0.25                                     | 0.25                                | 33, 34, 35                |

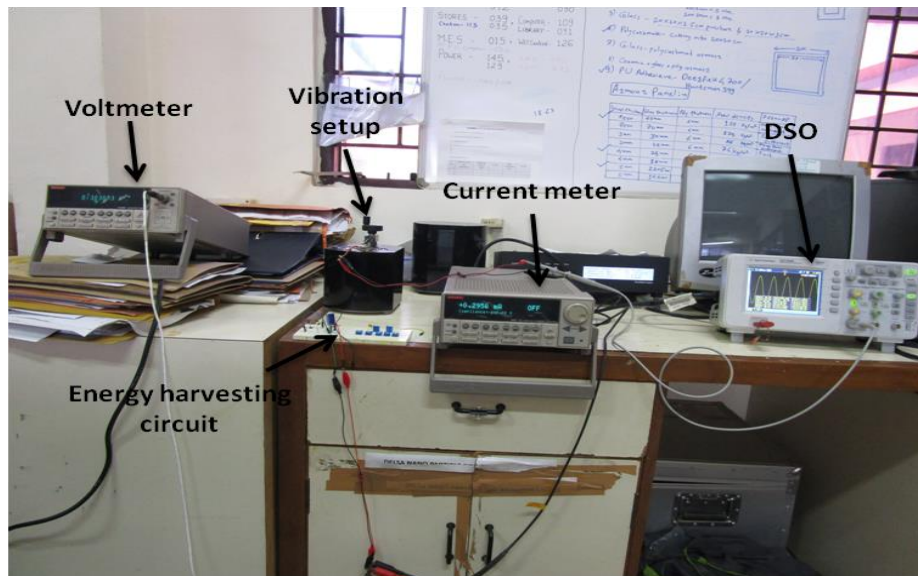


**Figure 3.14** Experimental setup for vibration analysis of drum harvesters

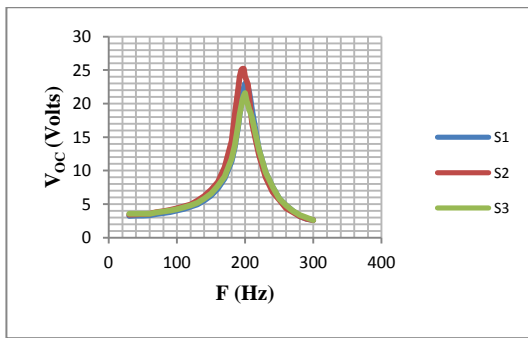
Impedance analysis of the piezoelectric buzzers was carried out using an Agilent 4294A impedance analyzer and  $d_{33}$  measurement was done using a PiezoTest PM300  $d_{33}$  meter. The results of the analysis are shown in Appendix A. The  $d_{33}$  meter was also used as the excitation mechanism for the drum harvesters. A maximum sinusoidal dynamic force of 0.5N could be applied using this setup. The excitation frequency range was 30 – 300 Hz. The drum was fixed to the holder of the  $d_{33}$  meter using insulated circular clamps provided with the device. The diameter of the clamps was 10 mm.

The AC voltage output of the drum harvester was monitored and recorded using a digital storage oscilloscope (Agilent DSO 1052B). The AC voltage was converted into DC using a conventional bridge rectifier circuit employing 1N5819 schottky diodes across which a capacitor of 470  $\mu$ F was added. The power deliverability of the drum was measured by connecting a current source (Keithley 6221 DC and AC current source) working in sink mode acting as a resistive load in parallel with the output capacitor. The current sinking capacity of the current source acting as a load was varied and the corresponding output voltage was recorded. Short circuit current and open circuit voltage delivered by the drum harvesters were measured.

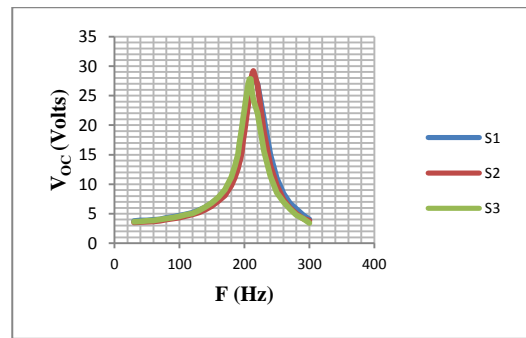
The voltage developed across the output capacitor was measured using a voltmeter (Keithley 2182A). The load resistance value was calculated by dividing the voltage across the output capacitor by the current.

### 3.5 RESULTS AND DISCUSSIONS

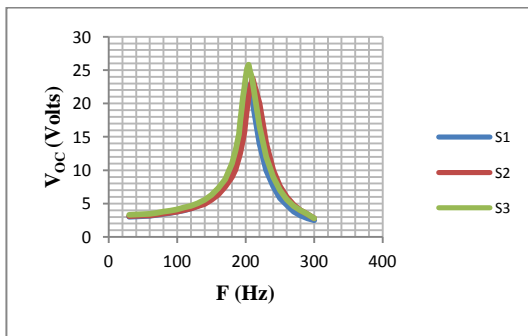
The analysis was done with samples in triplicate that is 3 samples for each configuration. Figures 3.15 (a to f) shows a plot of the AC output voltage ( $V_{OC}$ ) as a function of the frequency ( $f$ ) for different steel ring IDs.



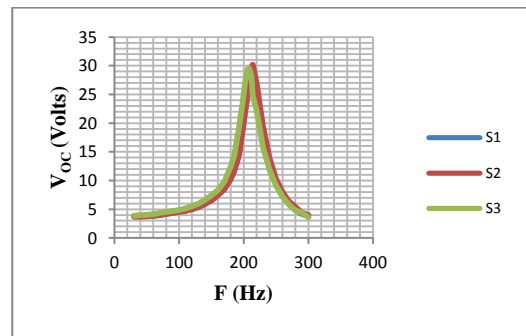
a) Steel ring ID 31 mm



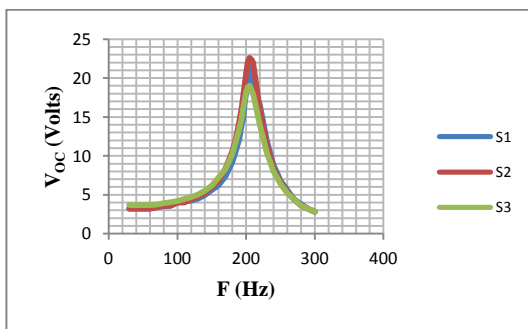
d) Steel ring ID 23 mm



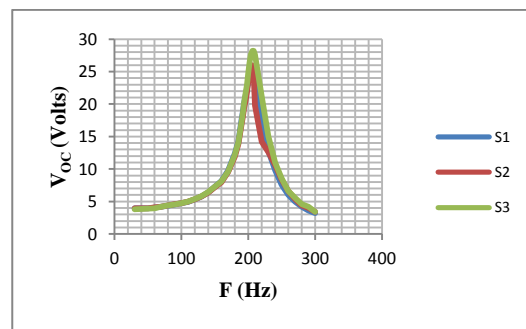
b) Steel ring ID 32mm



e) Steel ring ID 24 mm



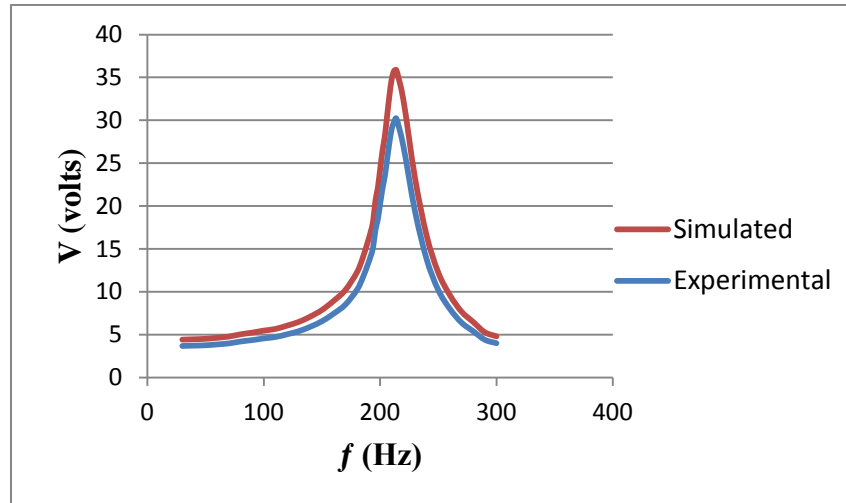
c) Steel ring ID 33 mm



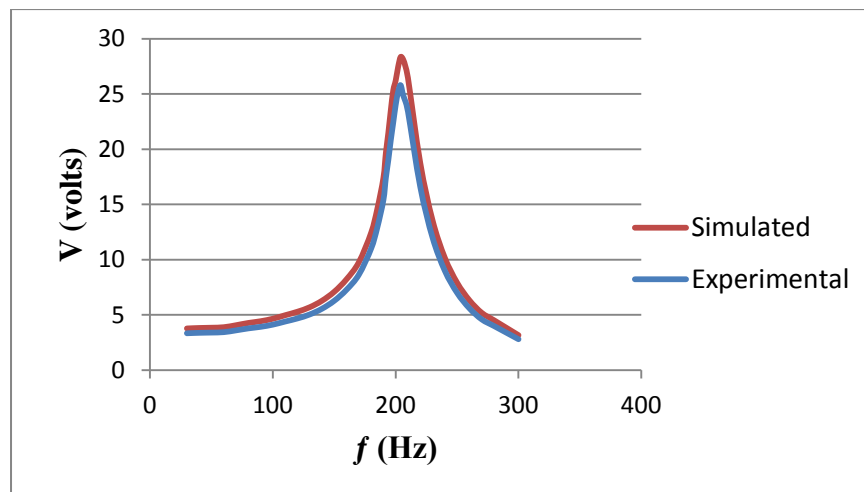
f) Steel ring ID 25 mm

**Figure 3.15 Open circuit voltage of drum harvesters under excitation for different steel ring IDs (a), (b), (c) – 35 mm and (d), (e), (f) - 27 mm**

A comparison of the experimental results with simulations carried out in ANSYS is shown in figures 3.16 (a & b) Experimental and simulated values are in excellent agreement.



(a)



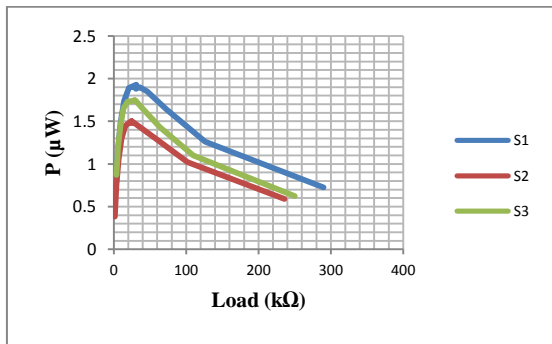
(b)

**Figure 3.16 Peak open circuit voltage comparison of experimental and simulated results for (a) 27 mm drum with steel ring ID 24 mm and (b) 35 mm drum with steel ring ID 32 mm**

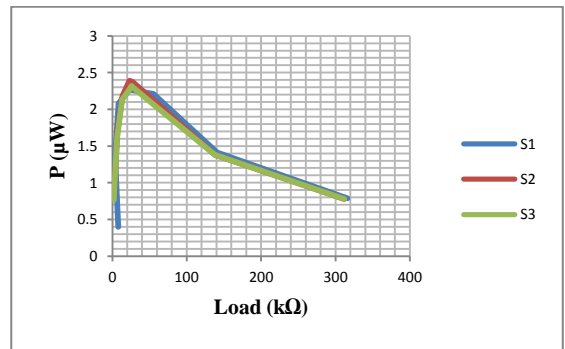
As it is evident from the plots in Fig. 3.15, the output voltage increases with frequency, reaches a peak at resonance (for the given excitation profile) and then decreases. Also, the peak voltage values were highest for the 35 mm drum with steel ring ID 32 and in the case of the 27 mm drum peak voltage was observed for the steel



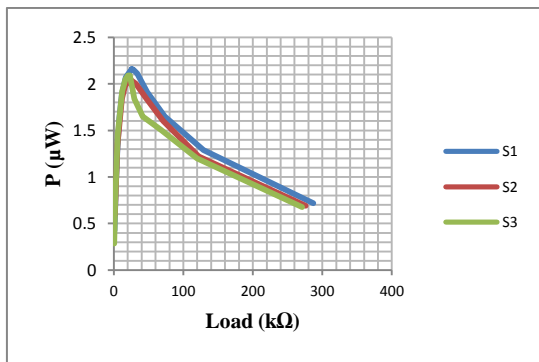
ring ID of 24 mm. The DC power ( $P$ ) vs. resistive load plots for different steel ring IDs are shown in Fig. 3.17 (a to f).



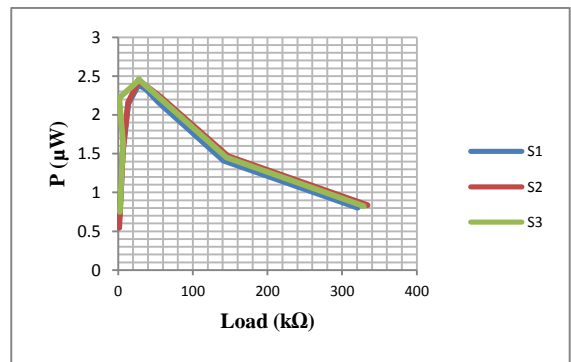
a) Steel ring ID 31 mm



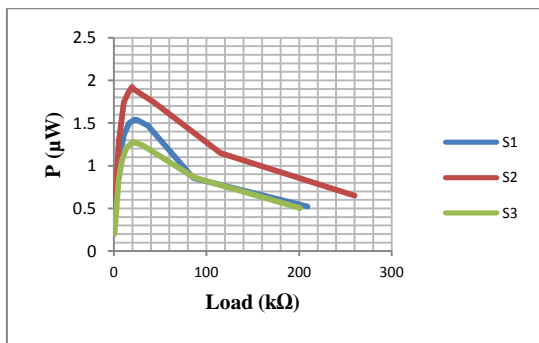
d) Steel ring ID 23 mm



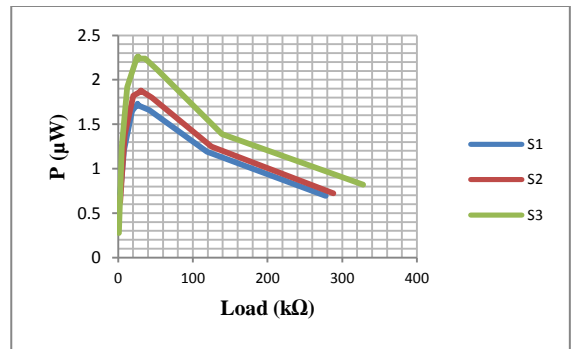
b) Steel ring ID 32 mm



e) Steel ring ID 24 mm



c) Steel ring ID 33 mm



f) Steel ring ID 25 mm

**Figure 3.17 Power output of drums vs. load resistance with different steel ring IDs (a), (b), (c) – 35 mm drum and (d), (e), (f) – 27 mm drum.**

**Table 3.5 Power output of drum harvesters at resonance.**

| <b>Drum OD<br/>(mm)</b> | <b>Steel ring<br/>ID (mm)</b> | <b>Sample<br/>No.</b> | <b>Resonance<br/>Frequency<br/>(Hz)</b> | <b>V<sub>AC</sub><br/>(volts)</b> | <b>V<sub>DC</sub><br/>(volts)</b> | <b>Peak<br/>Power<br/>(mW)</b> | <b>Load<br/>(kΩ)</b> |
|-------------------------|-------------------------------|-----------------------|---|-----------------------------------|-----------------------------------|--------------------------------|----------------------|
| 35                      | 33                            | S1                    | 205                                     | 29                                | 14.5                              | 1.932                          | 30.93                |
| 35                      | 33                            | S2                    | 205                                     | 33.2                              | 16.49                             | 1.504                          | 24.29                |
| 35                      | 33                            | S3                    | 203                                     | 27.6                              | 13.77                             | 1.752                          | 28.26                |
|                         |                               |                       |   |                                   |                                   |                                |                      |
| 35                      | 32                            | S1                    | 206                                     | 33                                | 16.64                             | 2.142                          | 23.80                |
| 35                      | 32                            | S2                    | 211                                     | 30.2                              | 15.23                             | 2.037                          | 22.63                |
| 35                      | 32                            | S3                    | 209                                     | 30.4                              | 15.2                              | 2.092                          | 21.10                |
|                         |                               |                       |   |                                   |                                   |                                |                      |
| 35                      | 31                            | S1                    | 206                                     | 26.2                              | 13.1                              | 1.537                          | 21.72                |
| 35                      | 31                            | S2                    | 210                                     | 29                                | 14.67                             | 1.918                          | 19.33                |
| 35                      | 31                            | S3                    | 204                                     | 23.2                              | 11.62                             | 1.273                          | 22.14                |
|                         |                               |                       |   |                                   |                                   |                                |                      |
| 27                      | 25                            | S1                    | 207                                     | 32                                | 16.19                             | 1.725                          | 25.62                |
| 27                      | 25                            | S2                    | 213                                     | 33.2                              | 16.75                             | 1.870                          | 29.92                |
| 27                      | 25                            | S3                    | 210                                     | 36.2                              | 18.5                              | 2.259                          | 26.88                |
|                         |                               |                       |   |                                   |                                   |                                |                      |
| 27                      | 24                            | S1                    | 216                                     | 37.4                              | 18.68                             | 2.379                          | 28.31                |
| 27                      | 24                            | S2                    | 214                                     | 37                                | 18.76                             | 2.447                          | 27.08                |
| 27                      | 24                            | S3                    | 213                                     | 37.4                              | 19.02                             | 2.463                          | 27.40                |

|    |    |    |     |      |       |       |       |
|----|----|----|-----|------|-------|-------|-------|
|    |    |    |     |      |       |       |       |
| 27 | 23 | S1 | 215 | 38   | 19.03 | 2.332 | 25.50 |
| 27 | 23 | S2 | 219 | 35.8 | 17.95 | 2.384 | 23.00 |
| 27 | 23 | S3 | 215 | 35.4 | 17.76 | 2.321 | 25.82 |

Table 3.5 gives a summary of the analysis for all the samples tested. As can be seen, for the 35 mm drum, a steel ring ID of 32 mm gave maximum peak power indicating that the optimum ring ID is around 32 mm. For the 27 mm drum, the maximum peak power was obtained at a ring ID of 24 mm similarly indicating that the optimum ID is around 24 mm.

The resonance frequencies of the drum harvester samples ranged between 200 and 220 Hz. A maximum dynamic force of 0.5 N could be applied with the setup used.

The load resistance at resonance is in the range of 20-30 k $\Omega$ , which means that low impedance devices can be powered using these energy harvesters. Previous research (as clear from Table 3.3) has reported high matching loads with power output mostly in the microwatt range.

Further, the 27 mm drums were able to generate more power compared to the 35 mm drums. This may be attributed to the fact that the contact area of the clamps used to apply the force was greater for the smaller drum harvesters. Hence an analysis also needs to be done on the effect of contact area on power output.

Pre-stress has been shown in previous literature to increase the power output and at the same time lower the resonance frequency of drum harvesters. Due to unavailability of suitable instruments, pre-stress analysis could not be conducted. Future work will incorporate effect of pre-stress on the power output and resonance frequency.

### 3.6 CONFIGURATION OF DRUM STACKS

Drum harvesters were fabricated using the piezo buzzer elements as already described earlier with slight modification to make them suitable for embedding in shoes as shown in figure 3.18 and 3.19. Use of the steel ring enables utilization of the 31 mode.

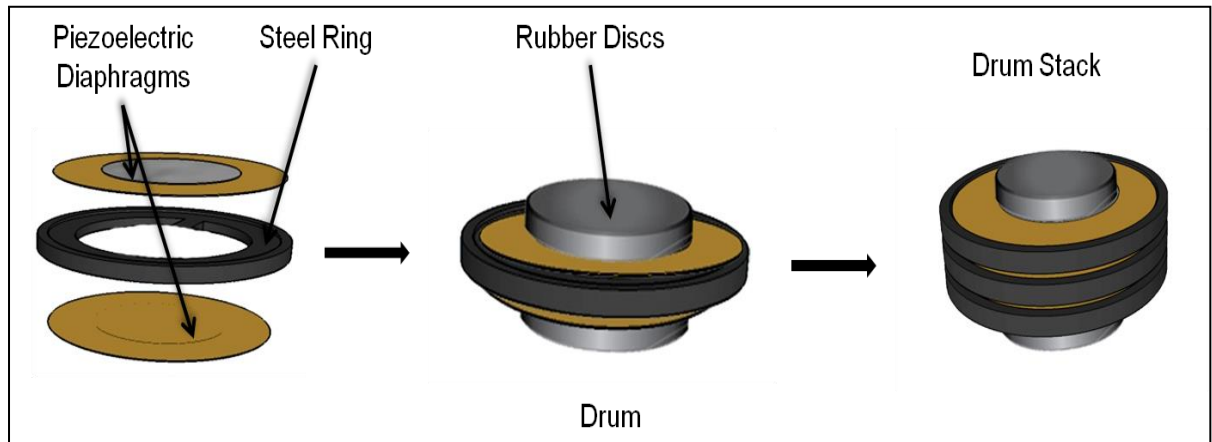


**Figure 3.18 Drum harvesters and (b) Drum stack**



(a)



(b)

**Figure 3.19 (a) Drum harvesters with rubber discs adhered to them. (b) Stacks made using drum harvesters.**

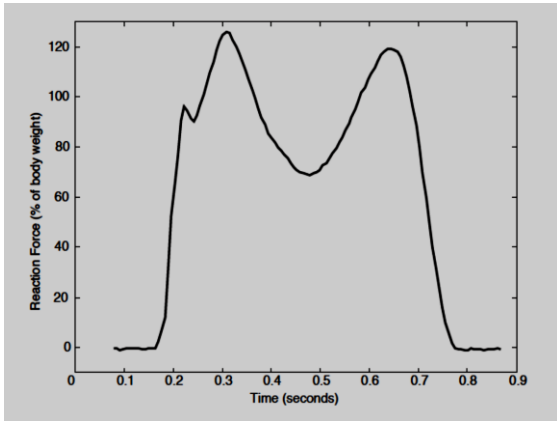
Wires were soldered to each drum harvester to act as positive and negative leads. All types of wires used are multistrand copper wires. To couple the force generated from the heel strike and forefoot strike to the stacks, each drum harvester has a rubber disc centrally adhered to the piezo elements (using the same adhesive) on both sides. This acts to couple the force to the active material as well as preventing damage to the discs from the high impacts. The rubber discs also act as damping elements and together

with the air gap in each drum harvester, act as a spring mechanism providing the restoring force during the toe-off phase.

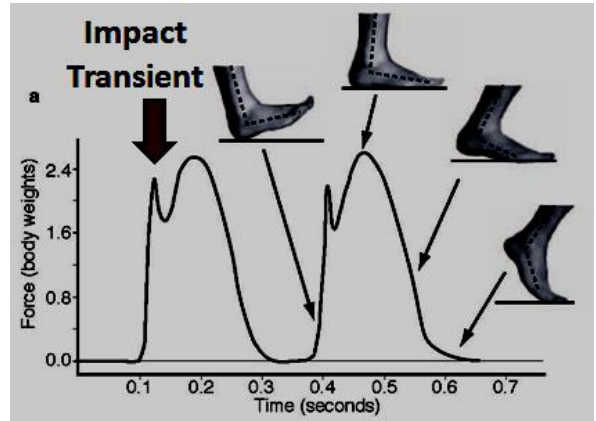
Stacks were made using the aforementioned drum harvesters, their diameters being 35 mm and 27 mm respectively. Three drum harvesters were used in the 35 mm stack (embedded in the heel) and two in the 27 mm stack (embedded under the ball of the foot). A total of 6 diaphragms were used in the larger stack and 4 in the smaller one. The number of drums in each stack was fixed by taking into consideration, two factors – the space available in the heel and forefoot and the enhancement in the current output upon addition of extra drums in the stack. Three different steel ring IDs were used in the drums. The stacks weigh approximately 30 g and 10 g respectively.

### **3.6.1 Testing of the drum stacks with a custom footfall simulator**

Before their incorporation in shoes, there was a need for initial testing of the piezo generators using a low frequency high impact setup that could simulate conditions of footfalls. However, no standard bench-testing instrument was available for simulating footfalls. A custom footfall simulator was designed for testing of the piezo generators (figure 3.21). The simulator consisted of a solenoid driven mechanism with a hammer, a variac, a proximity sensor and displacement sensor. The variac was used to control the current through the solenoid which in turn controlled the amplitude of the impact. A proximity sensor was used to return the hammer back to its original position after every impact. The displacement sensor served to control the distance through which the hammer fell in each impact, that is, the impact distance. The arrangement was operated using a pre-programmed Arduino microcontroller board which enabled varying the impact frequency in the range of 1 to 10 Hz. The mechanism was designed to provide impact force equivalent to that encountered under the foot of a 60 kg person. For an average person, while walking, approximately 130% of the body weight is the force of impact under the foot [2] whereas for running; it is about 250% of body weight [88] as shown in figure 3.20.



(a)



(b)

**Figure 3.20 Force under the foot while (a) walking and (b) running [2] [88]**

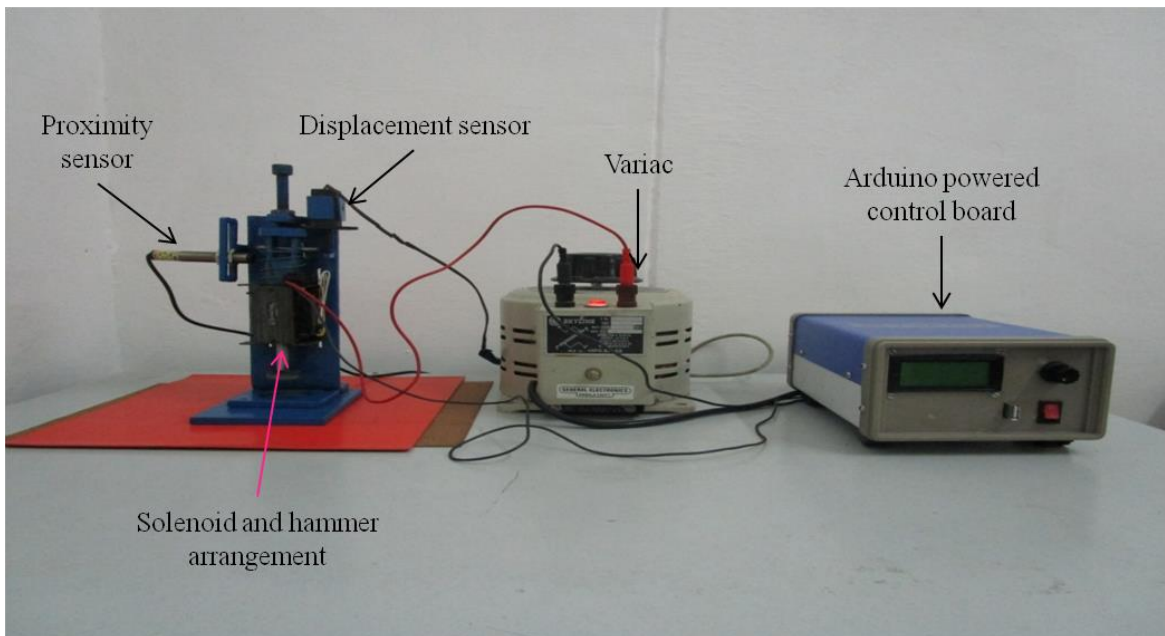


**Figure 3.21 Footfall simulator**

### 3.6.2 Results and discussions

Figures 3.22 and 3.23 give plots of the power output vs. increasing number of drums in the stack for the 35 mm and 27 mm drums. The experiments were carried out using the footfall simulator.

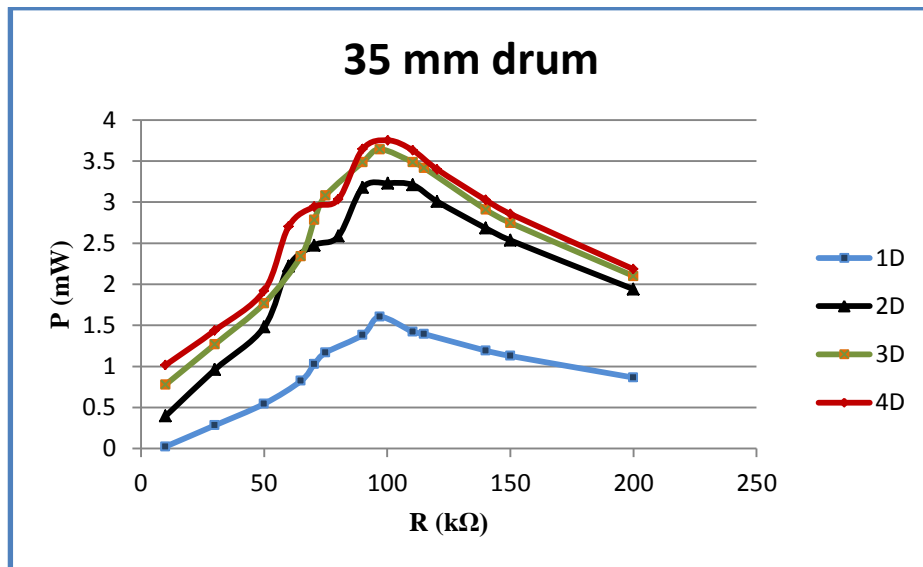


Figure 3.22 Power output vs. increasing number of drums (D) (35 mm)

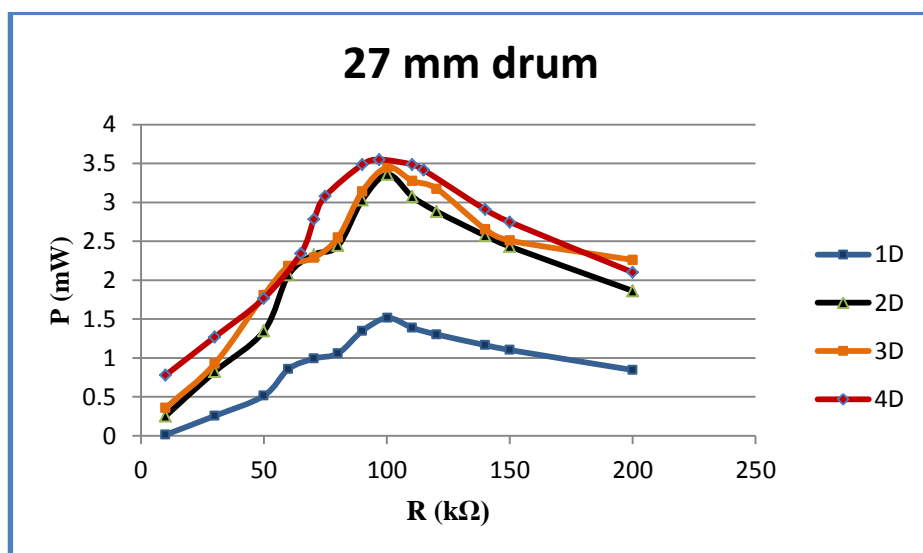


Figure 3.23 Power output vs. increasing number of drums (D) (27 mm)

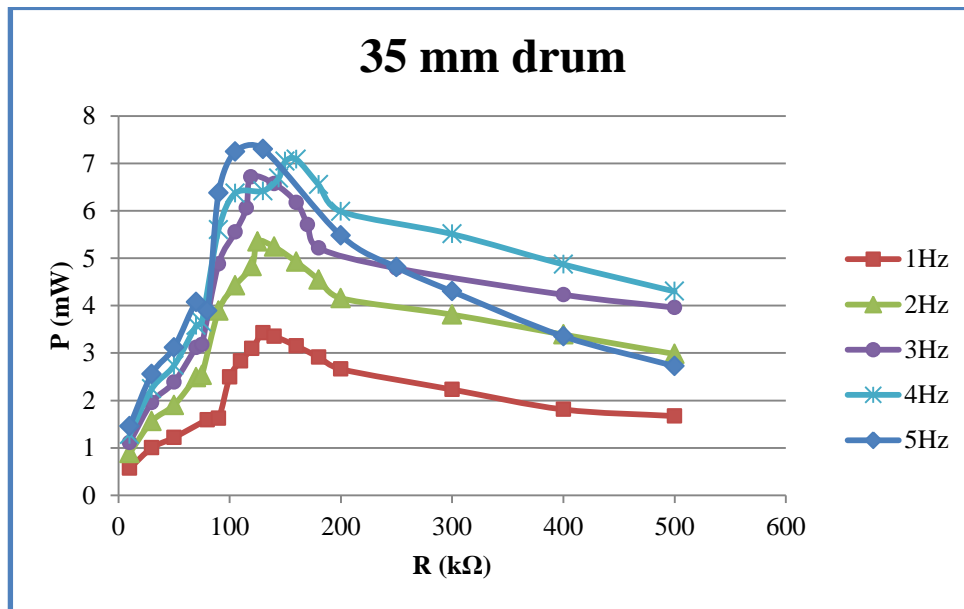
\*D in the legend of the power curves stands for Drum

Table 3.6 summarizes the results of output power with increasing number of drums as per the above plots.

**Table 3.6 Power output v/s increasing number of drums**

| No. of drums | Peak Power output (mW) |       |
|--------------|------------------------|-------|
|              | 27 mm                  | 35 mm |
| 1            | 1.51                   | 1.60  |
| 2            | 3.27                   | 3.23  |
| 3            | 3.45                   | 3.64  |
| 4            | 3.55                   | 3.75  |

From Table 3.6 it can be inferred that as the number of drums increases, the power increases. But after adding 3 drum in the stack, there is very little increase in the power output. This may be due to the increased rigidity of the stack as more drums are added. Figures 3.24 and 3.25 depict the power vs. impact frequency curves.



**Figure 3.24 Power output vs. increasing impact frequency for 35 mm drum stack**



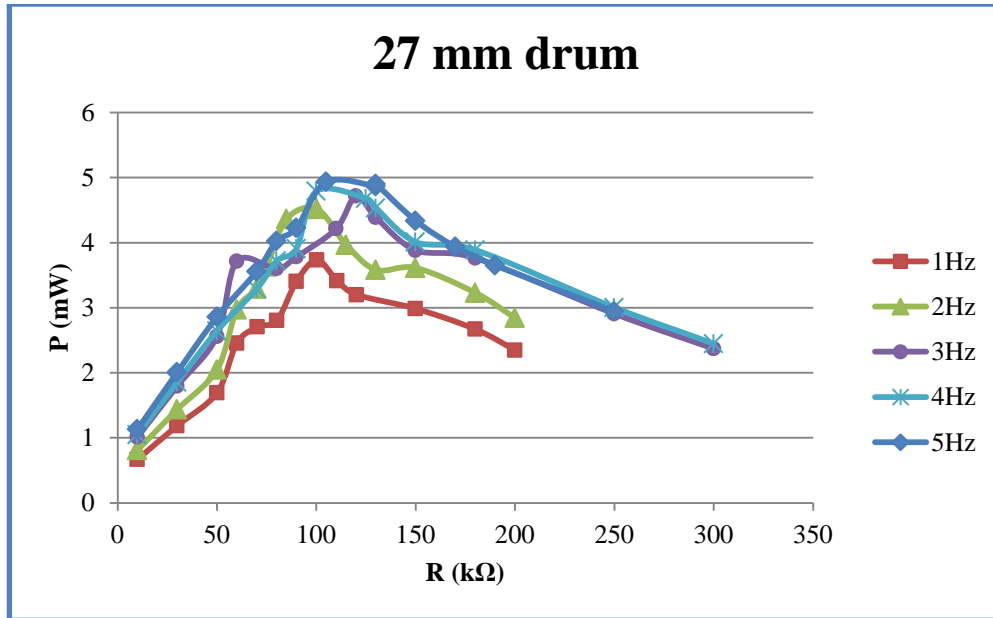


**Figure 3.25 Power output vs. increasing impact frequency for 27 mm drum stack**

Table 3.7 summarizes the results of output power with increasing impact frequency as per the above plots. It indicates that increasing the impact frequency increases the power output for both the stacks. But the power saturates at about 5 Hz.

**Table 3.7 Power output v/s impact frequency**

| Impact Frequency | Peak Power output (mW) |       |
|------------------|------------------------|-------|
|                  | 27 mm                  | 35 mm |
| 1                | 3.73                   | 3.42  |
| 2                | 4.51                   | 5.35  |
| 3                | 4.68                   | 6.71  |
| 4                | 4.79                   | 7.08  |
| 5                | 4.93                   | 7.30  |

### 3.7 SHOE-BASED ENERGY HARVESTERS

As a real world application of impact energy harvesting, two shoe-based harvester models were constructed using the drum harvesters. In Model 1 (M1), the energy harvesting

stacks were embedded in the heel and forefoot of standard army DMS shoes as shown in figure 3.26. The positions of maximum pressure under the feet were identified using pedobarography images of the feet shown in Figure 3.27 [89].



**Figure 3.26 DMS shoes with energy harvesting stacks embedded in the heel and forefoot sections (M1).**

Another configuration employed an arrangement of individual drum harvesters (only 27 mm drums, [Model 2 (M2)] in the heel and forefoot sections of commercially available sneakers. It consisted of a shoe insole made of flexible polycarbonate sheet of thickness 2 mm. The polycarbonate sheet was shaped in the form of a shoe insole. Drum transducers were placed accordingly on the polycarbonate insole in a sandwich structure as shown in figure 3.28.

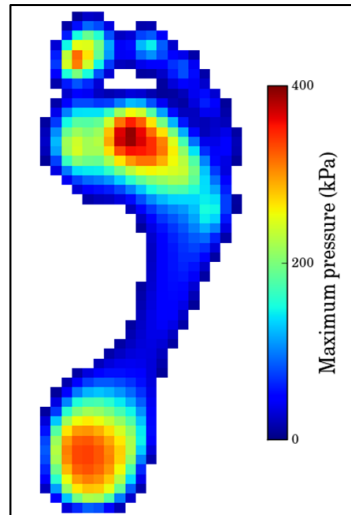


**Figure 3.27** Areas of maximum pressure under the foot [100].

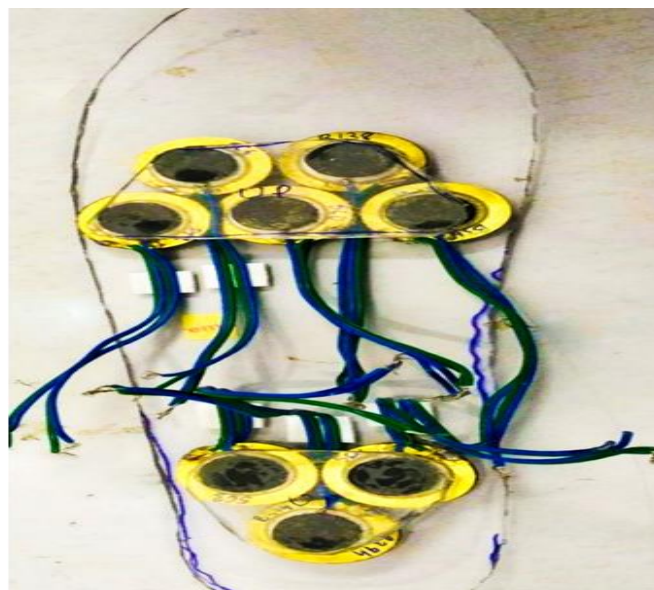


**Figure 3.28** Insole made of polycarbonate sheet and drum harvesters (M2).

The piezoelectric drums were checked for polarity and the connecting leads were marked and paired accordingly. Depending on the shape of the foot, three drums were placed in the heel section of the insole and 5 drums were placed in the forefoot section. Only the 27 mm drums were used in this model due to space constraints.

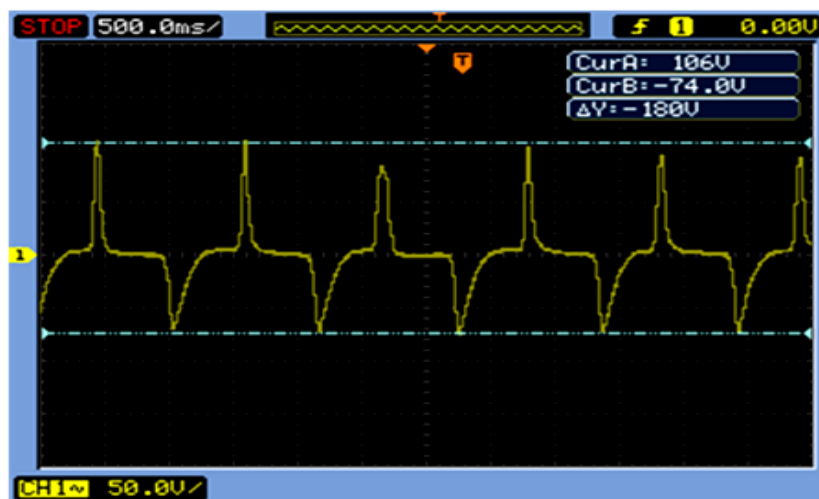
### 3.7.1 Experimental Procedure

Starting first with model 1 (M1) walking simulations were performed using a treadmill with a 60 kg subject wearing the shoes and walking at normal pace (2 steps per second). The left shoe was used to gather the data. The output leads of all stacks/ drums in each shoe model were combined (electrically parallel configuration) and fed to different energy harvesting circuits. The stacks as well as the individual drum harvesters in each stack were connected electrically in parallel to maximize the current and hence the power produced.

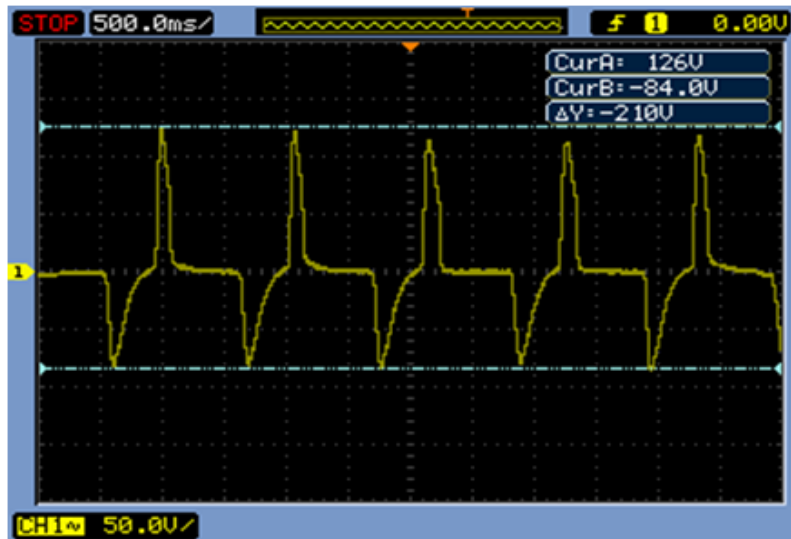
The open circuit voltage waveforms were recorded on a digital storage oscilloscope (Agilent DSO 1052B).

### 3.7.2 Results and Discussions

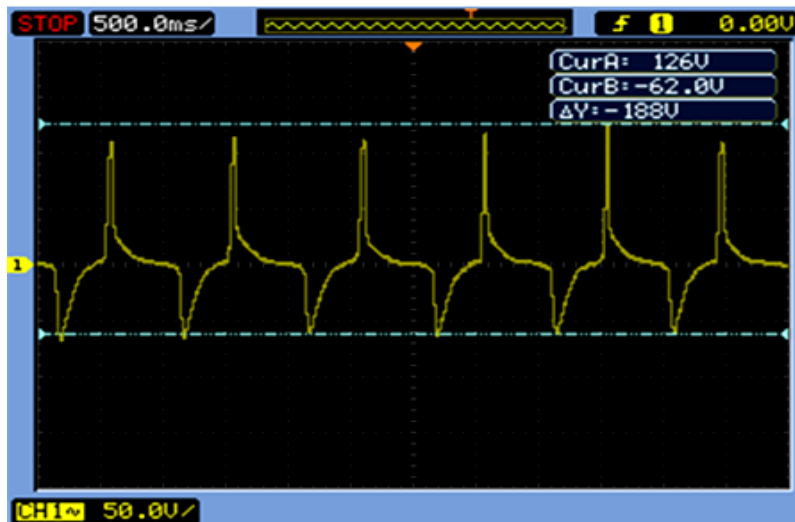
The steel ring IDs were varied to find out the effect on the output power of the drum harvesters. As is clear from the open circuit waveforms in figures 3.29 & 3.30 below, reducing the steel ring ID had the effect of increasing the output voltage.



(a)

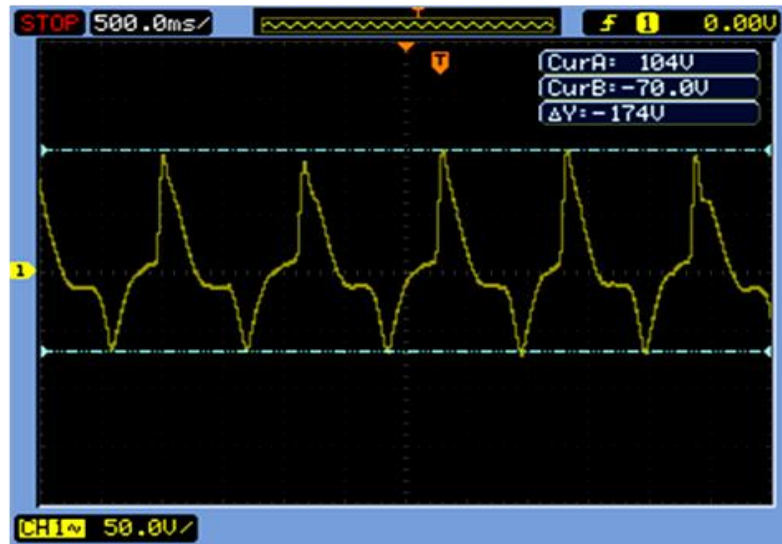


(b)

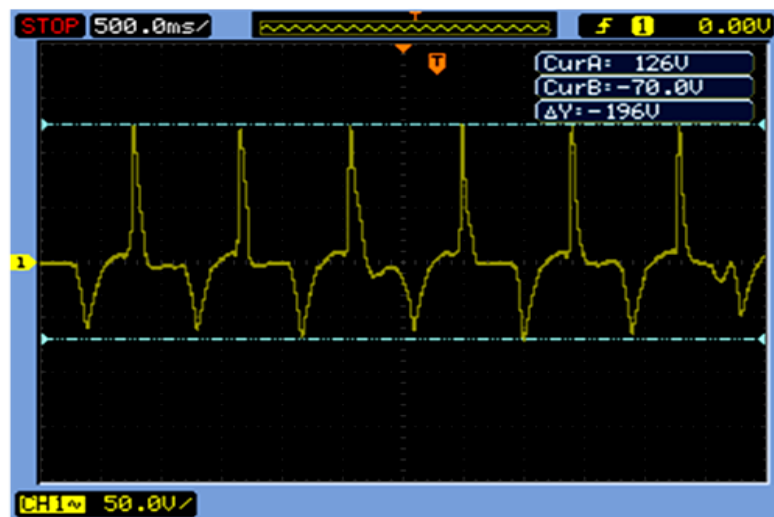


(c)

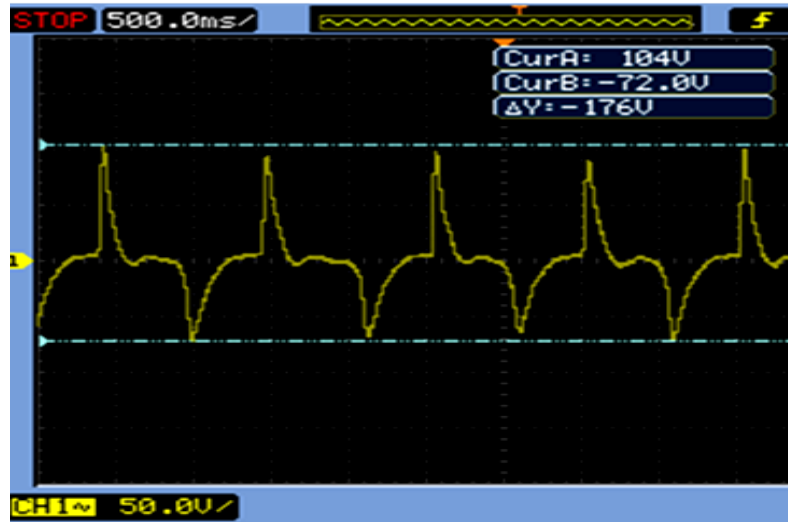
Figure 3. 29 Model 1 open circuit voltage waveforms for 35 mm stack embedded in the heel (a) ID 31 mm (b) ID 32 mm and (c) ID 33 mm ( time = x axis & voltage =y axis)



(a)



(b)



(c)

**Figure 3. 30 Model 1 open circuit voltage waveforms for 27 mm stack embedded in the heel (a) ID 23 mm (b) ID 24 mm and (c) ID 25 mm ( time = x axis & voltage =y axis)**

Figures 3.31 to 3.34 give the power output of the drum stacks embedded in M1 in the heel and forefoot. The 35 mm drum stacks were embedded in the heel section while the 27 mm drum stacks were embedded in the forefoot section of the soles of the shoes. The experiments were carried out with a 60 kg test subject walking and running on a treadmill. The walking and running speeds were approximately 6 kmph and 10 kmph respectively.

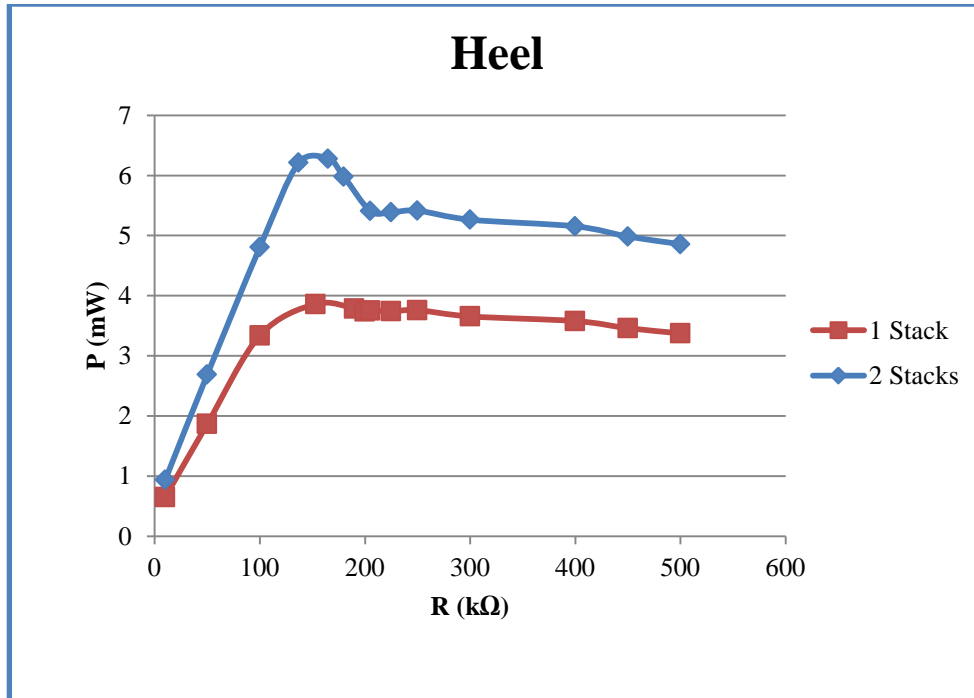


**Figure 3.31 Power curve at the heel for a walk**

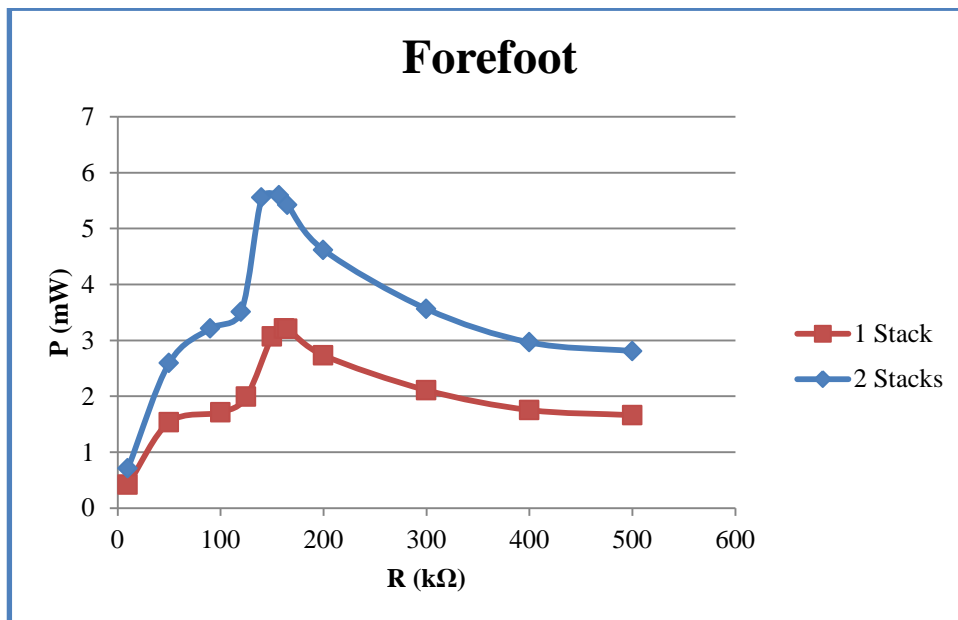


**Figure 3.32 Power curve at the forefoot for a walk**



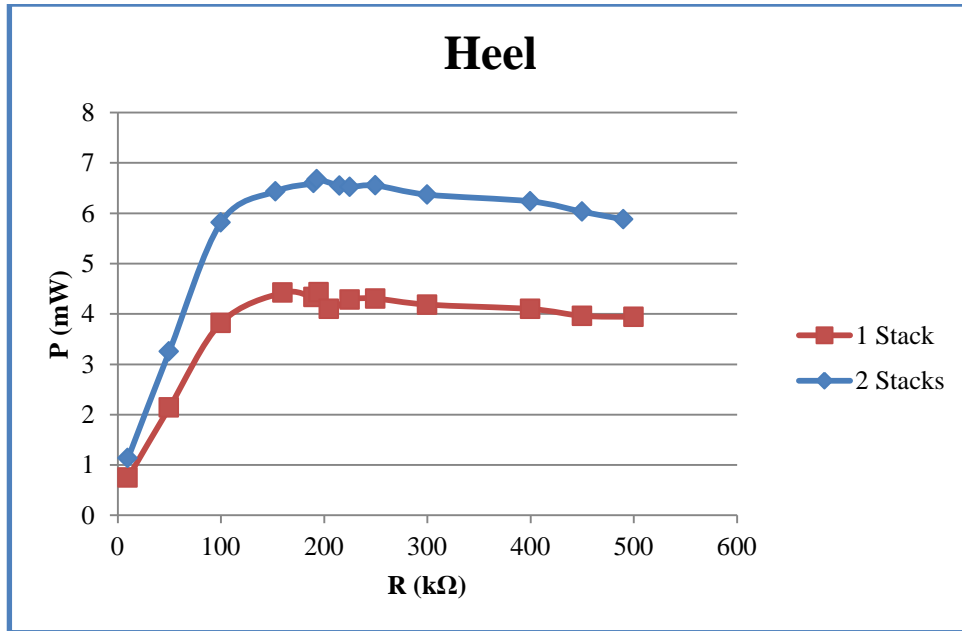


**Figure 3.33 Power curve at the heel for a run**

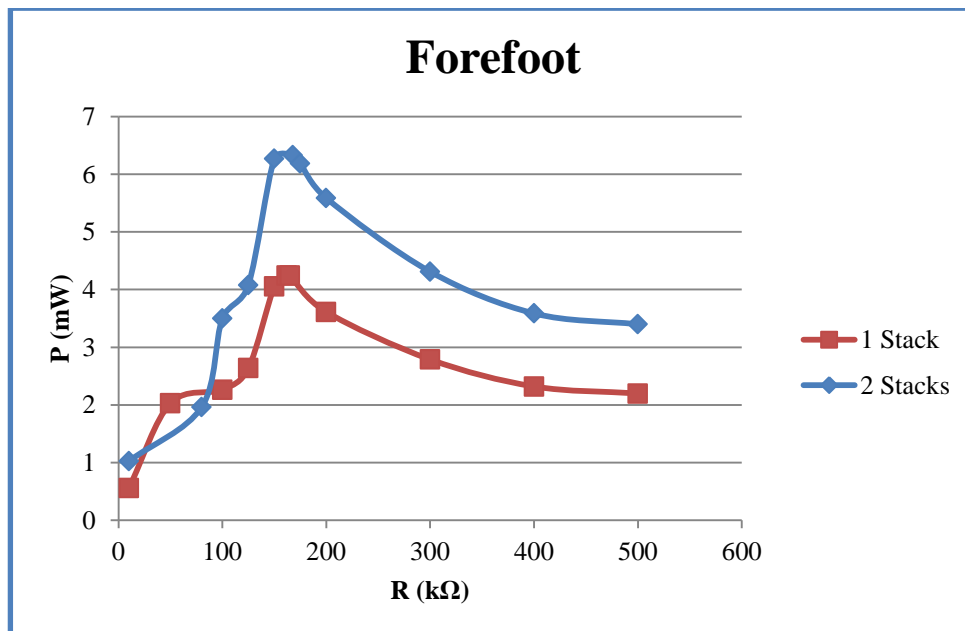


**Figure 3.34 Power curve at the forefoot for a run**

Table 3.8 gives the results of the power output in walking and running experiments with the stacks embedded in shoes. It is clear that the output power is greater for 2 stacks than for one stack embedded in the shoe. Also running produces more power as compared to

walking. As expected, the voltage output and consequently the power at the heel are greater than that at the forefoot as the ground reaction force during heel strike is greater than that at the forefoot strike. Hence, more power is generated during heel strike.

**Table 3.8 Power output vs. number of stacks in shoe**

| Profile | Heel                   |          | Forefoot               |          |
|---------|------------------------|----------|------------------------|----------|
|         | Peak Power output (mW) |          | Peak Power output (mW) |          |
|         | 1 Stack                | 2 Stacks | 1 Stack                | 2 Stacks |
| Walk    | 3.86                   | 6.27     | 3.20                   | 5.59     |
| Run     | 4.43                   | 6.59     | 4.24                   | 6.32     |

### 3.7.3 Comparison of M1 and M2

By varying the resistive load and measuring the peak output voltage developed across it, the power was calculated using the formula  $P = \frac{V^2}{R}$ . Figure 3.35 shows a graph comparing the output power generated by Model 1 (M1) and Model 2 (M2) with a walk profile.

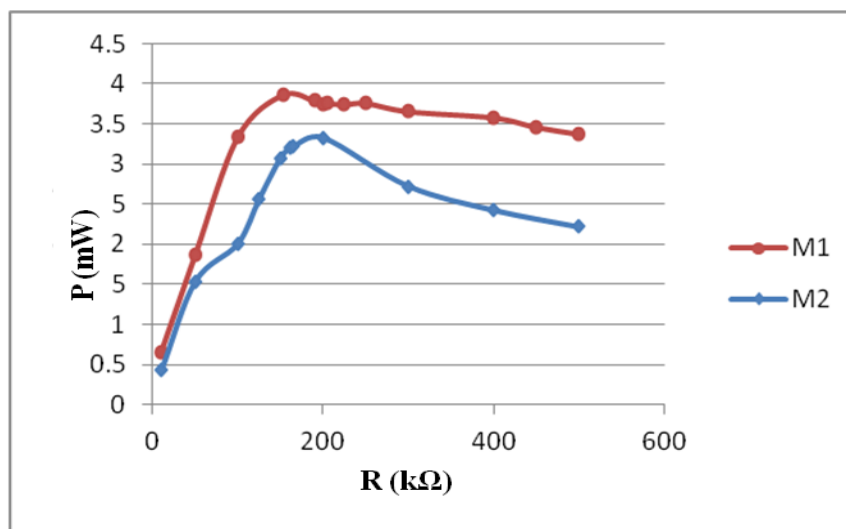


**Figure 3.35 Output power vs. load resistance for Model 1 and Model 2.**

### 3.8 CONCLUSION

Piezocomposite diaphragm elements were analyzed as energy harvesters in an experimental vibration setup with mechanical pre-stress. Optimum pre-stress in the form of an equivalent mechanical weight was found to be 57 gm and 25 gm for the 35 mm and 27 mm buzzer respectively. Peak powers of 220  $\mu\text{W}$  across an optimum resistive load of 126 k $\Omega$  for the 35 mm buzzer and 86  $\mu\text{W}$  across an optimum resistive load of 133 k $\Omega$  for the 27 mm buzzer were observed. Resonance frequencies under optimum mechanical pre-stress were found to be 22.6 Hz and 24.2 Hz for the 35 mm and 27 mm buzzers respectively. The acceleration was 2  $\text{m/s}^2$ . These piezocomposite elements are cheap, robust, commercially available and due to their thin form factor, are easily integrable into a variety of vibrating structures which facilitates the scavenging of vibration energy to generate useful electrical energy which can be used to power microelectronic devices like Bluetooth, GPS modules, microcontrollers and low power sensors, wireless sensor nodes, etc. Results also indicate that these piezo elements are capable of generating sufficient power even at very low vibration frequencies (hitherto unreported) and accelerations.

Drum harvesters were fabricated using the piezocomposite elements. The IDs of the steel rings used to make the drum harvesters were varied and an optimum ring ID was found which generated the highest power. A maximum power of 2.463 mW was obtained with the 27 mm drum with steel ring ID of 24 mm whereas a maximum power of 2.142 mW was obtained with the 35 mm drum with steel ring ID of 32 mm. Compared to the 35 mm drum harvesters, the 27 mm drums were able to generate more power. This may be due to the contact area of the clamps used to apply the force. The effect of contact area on output power will be studied in the future. These drum harvesters are also suitable for high stress applications. Therefore, future work will incorporate a study on effect of pre-stress on power output and performance under high cyclic stress conditions.

The drum harvesters were suitably modified for embedding in shoes. A custom footfall simulator was designed and fabricated to test the drum stacks under different excitation conditions. Increasing the number of drums in the stack was found to increase the power output of the stack. But the power output saturated after adding 3 drums to the stack for both the drum sizes. Increasing the impact frequency was

found to increase the power output of the drum stack. However, the power output saturated at impact frequency of 5 Hz. Maximum powers of 4.97 mW for the 27 mm stack and 7.30 mW for the 35 mm stack were obtained with an impact frequency of 5 Hz.

Different alignments of the drum harvesters were incorporated in shoes and real time testing with different ambulation profiles was carried out. Peak powers of 6.27 mW and 5.59 mW were generated with walking in the heel and forefoot respectively whereas 6.59 mW and 6.32 mW were generated with running in the heel and the forefoot respectively.

The fabrication process of drum harvesters is cheap, easy and fast. They are quite robust and as such may be embedded in a variety of structures like shoes, under floors, roads, etc. to generate useful electrical energy which can be used to power microelectronic devices like Bluetooth, GPS modules, microcontrollers and low power sensors. Future work would include studying power output of these energy harvesters under higher force profiles, designing and fabricating arrays of these energy harvesters and using the energy harvested to charge rechargeable batteries and power low-power microelectronic devices. The steel ring ID can also be further optimized to improve the power output.

## DEVELOPMENT OF ENERGY HARVESTING AND POWER CONDITIONING CIRCUITS

A piezoelectric element can be represented by a series resistor and capacitor [figure 4.1] in an equivalent circuit representation. The values of both these components change with frequency. The series values may be transformed to an exactly equivalent parallel resistor and capacitor combination [90].

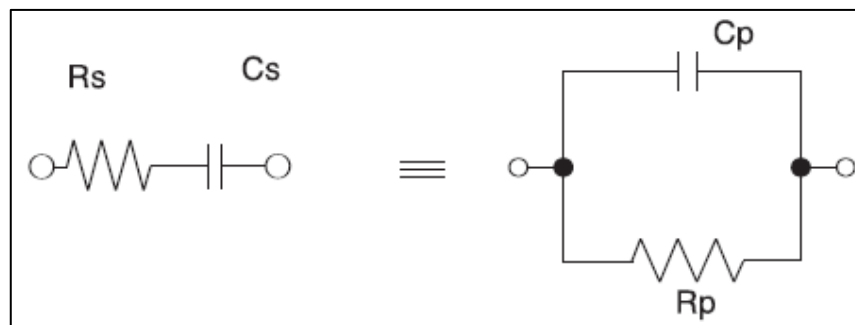


**Figure 4.1 Electrical equivalent of a piezoelectric element.**

When compared with mechanical vibration sources, human induced motions are challenging for energy harvesting design because of the following reasons [91]:

1. Low frequency (1 -10 Hz), aperiodic, and time-varying characteristics. The commonly used high-Q resonant-type energy harvesters, which are based on an under-damped, single-degree-of-freedom, mass-spring-damper system are generally not suitable for human movement energy harvesting since that these resonant systems are optimized to accomplish maximum output power within a small frequency range under oscillatory accelerations.
2. It is very difficult to tune the resonant frequency to the low frequencies of human motions and simultaneously maintain high quality factor, especially all while keeping the device dimensions compact.

3. They are typically designed for only one rectilinear degree of freedom, while normal human movements occur in three dimensions and involve a high degree of rotational, rather than oscillatory, motions.
4. The use of piezo harvesters in applications such as walking which have very low frequency (few Hz) makes them essentially purely capacitive sources, and during walking they produce high-voltage, low-energy, low-duty cycle current pulses at approximately one cycle per second. This excitation profile results in very high source impedance giving voltage output in the range of hundreds of volts and currents of the order of  $10^{-7}$  A. Linear regulation schemes are, therefore, not well suited to the electrical characteristics of a piezoelectric element excited by a brisk walk. Table 4.1 summarizes the various shoe-powered energy harvesting systems.

A suitable low frequency equivalent circuit model for a piezoelectric energy harvester is a capacitance in series with a resistor which represents the dielectric leakage [92]. At frequencies far below resonance, piezoelectric transducers are essentially capacitors so that the capacitance value at 1 Hz can be taken as the static capacitance value [93]. The static capacitance values of the drum harvesters measured using a capacitance meter (Kusam Meco 207-MK-1T) are given in table 4.1. The equivalent circuit in this case can be given as shown in figure 4.2.

**Table 4.1 Static capacitance of 27 mm and 35 mm drum harvesters**

| Sample no | Capacitance (nF) |            |
|-----------|------------------|------------|
|           | 27 mm drum       | 35 mm drum |
| 1         | 44.4             | 51.1       |
| 2         | 44               | 54.2       |
| 3         | 44.2             | 52.6       |

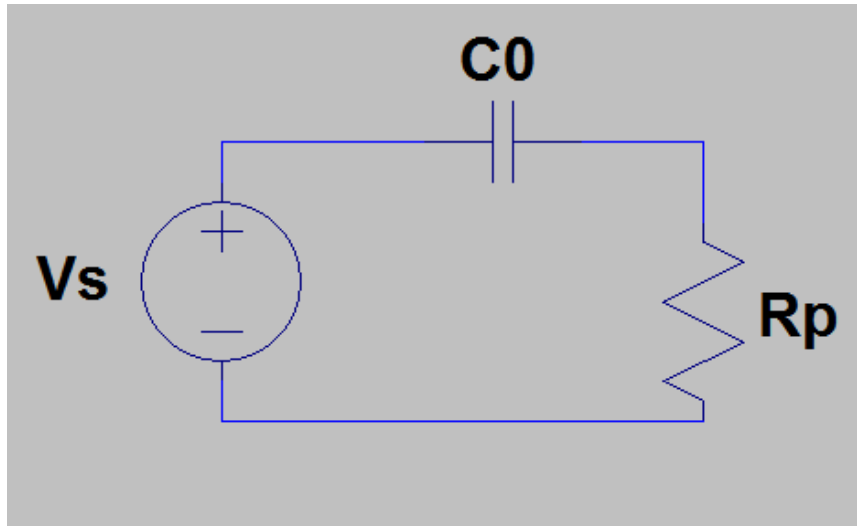


**Figure 4.2 Equivalent circuit model of a piezoelectric element at very low frequencies**

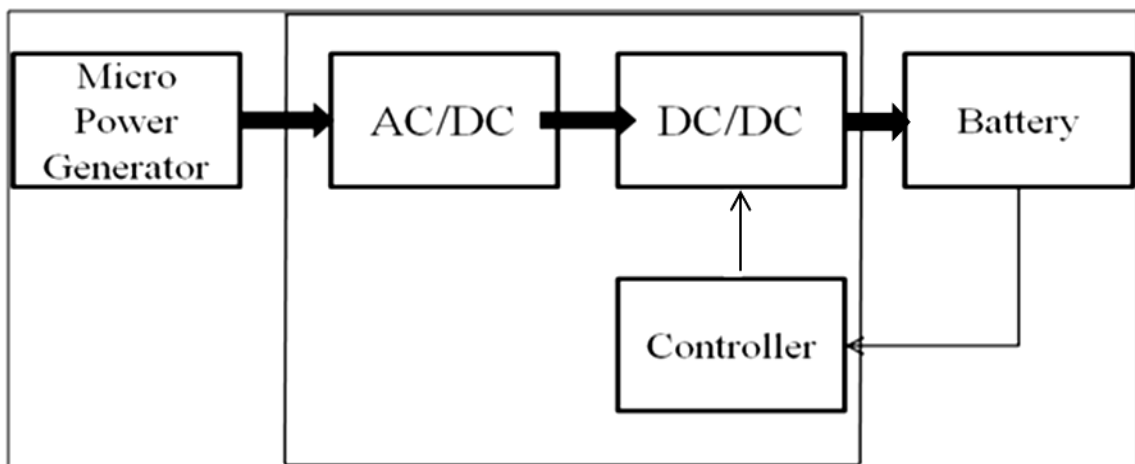


**Figure 4.3 Block diagram for a typical energy harvesting circuit interface for a piezoelectric vibration energy harvester**

Figure 4.3 above gives the block diagram of an inclusive energy harvesting system. The leftmost block is the piezoelectric generator the development of which has already been discussed in chapter 3. Since piezoelectric energy harvesters are AC sources and microelectronic devices work on DC power, the first step in utilizing the energy is to convert the AC to DC which is shown in the second block. Section 4.1 discussed this. The DC-DC down conversion (block 3) is also necessary since the DC voltage obtained is still too high to be used directly with most microelectronic devices. Also, a regulated DC

output (controller block) is desirable for proper operation of these devices. These objectives are discussed in section 4.2.

## 4.1 AC TO DC CONVERSION

### 4.1.1 Standard Interface Analysis

A piezoelectric element under vibrational excitation generates an ac voltage whereas the powering of electronic devices and charging of batteries need a dc voltage, hence the first stage needed in an energy harvesting circuit is an ac–dc rectifier connected to the output of the piezoelectric device. Figure 4.3 depicts the standard interface circuit consisting of a bridge rectifier and a filter capacitor connected to an external load. It is assumed that the dc filter capacitor is large enough so that the output voltage is effectively constant; the load is modeled as a constant current source and the diodes are assumed to exhibit ideal behavior [94, 95].

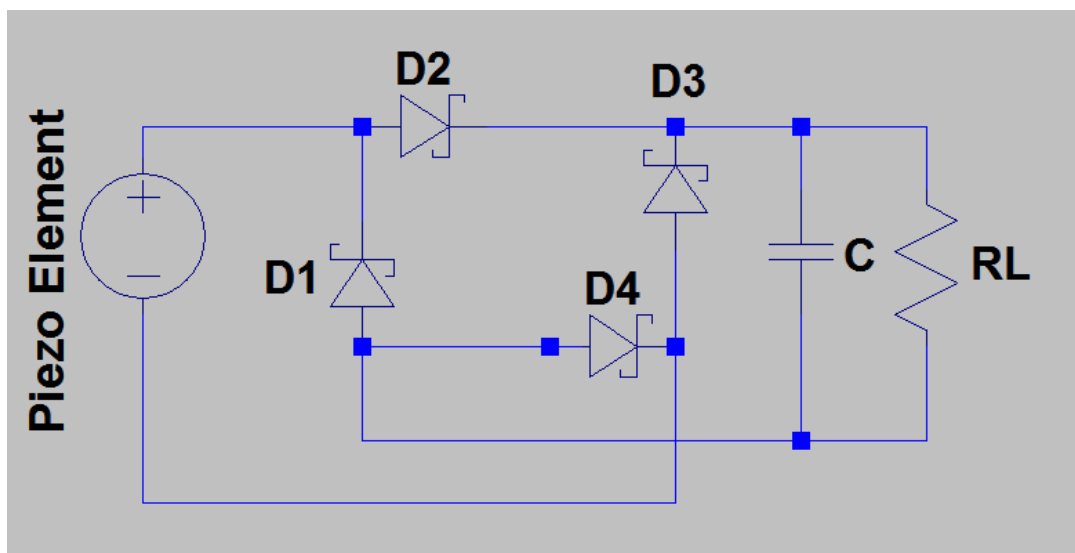


**Figure 4.4 The standard energy-harvesting interface for a piezo energy harvester**

Initial power analysis of the drum harvesters as vibration energy harvesting elements and shoe based energy harvesters was done using a standard interface which consists of a bridge rectifier and a filter capacitor as already described earlier. Schottky diodes (SR



110) were used as they have minimum voltage drop resulting in minimal power loss. The details of the schottky diode are given in appendix B.

Figures 4.5 and 4.6 depict the DC open circuit voltage across the bridge rectifier as measured using a DSO.

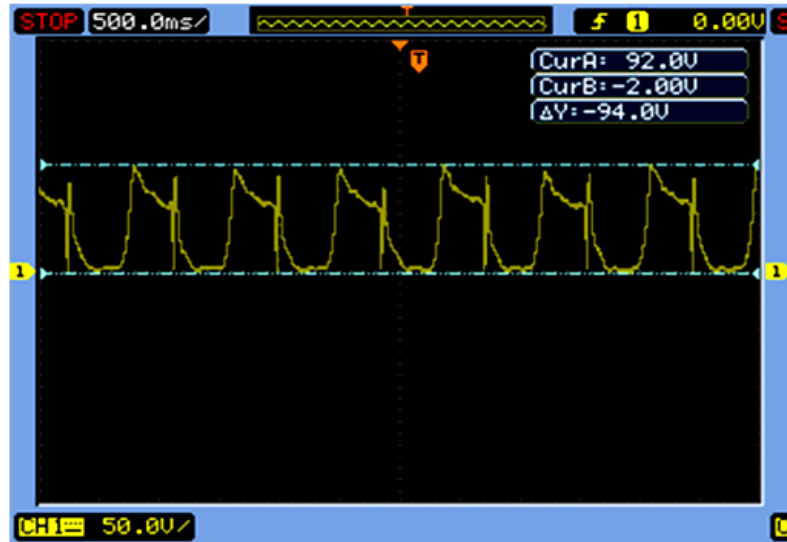


Figure 4.5 DC open circuit waveforms of 27 mm drum with diode bridge rectifier

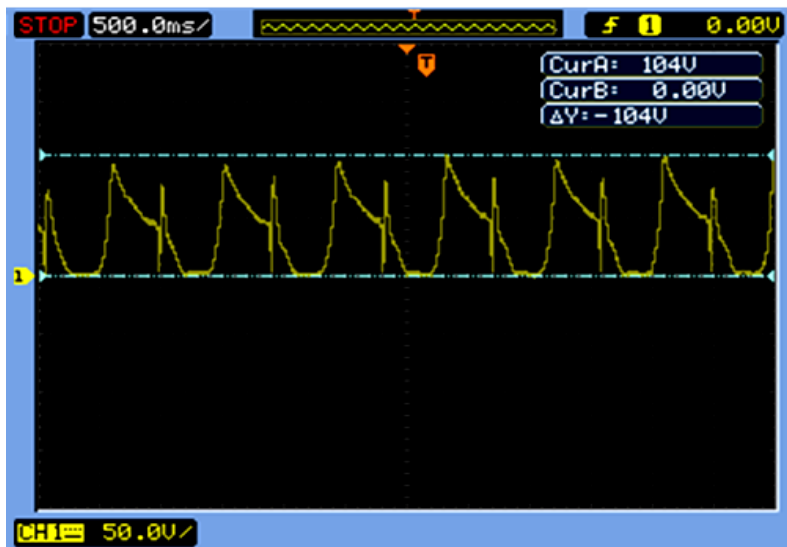


Figure 4.6 DC open circuit waveforms of 35 mm drum with diode bridge rectifier

\*( time = x axis & voltage = y axis)

### 4.1.2 MOSFET Bridge

A disadvantage of the standard four-diode rectifier bridge is the inevitable forward voltage drop ( $V_f$ ) of two diodes when current is flowing. With conventional silicon diodes, this could, in general, amount to 1.5 volts or more. This results in wasted power and reduction in efficiency in power supply applications, or loss of working voltage in telephony or battery-powered applications.

As most integrated circuits malfunction under power supply reversals, it is common practice for the line-powered electronics to be coupled with a full-wave rectifier bridge in order to guarantee power supply polarity. But where only a small voltage of the order of a few volts is available, a drop in the rectifier would leave very little voltage for the electronics. Similarly, in battery powered circuits, usually the loss of efficiency caused by series diodes to protect against unintended battery reversal is undesirable [96].

The circuit shown in figure 4.7 eliminates this drawback by replacing the diodes with MOSFETs. The four MOSFETs are connected in such a way as to conduct in opposing pairs. Which pair conducts is a function of the polarity of the applied voltage. The conducting pair is such as to steer the applied voltage to the correct output terminals so that the same polarity is always maintained at the output. Simply put, rectification is achieved.

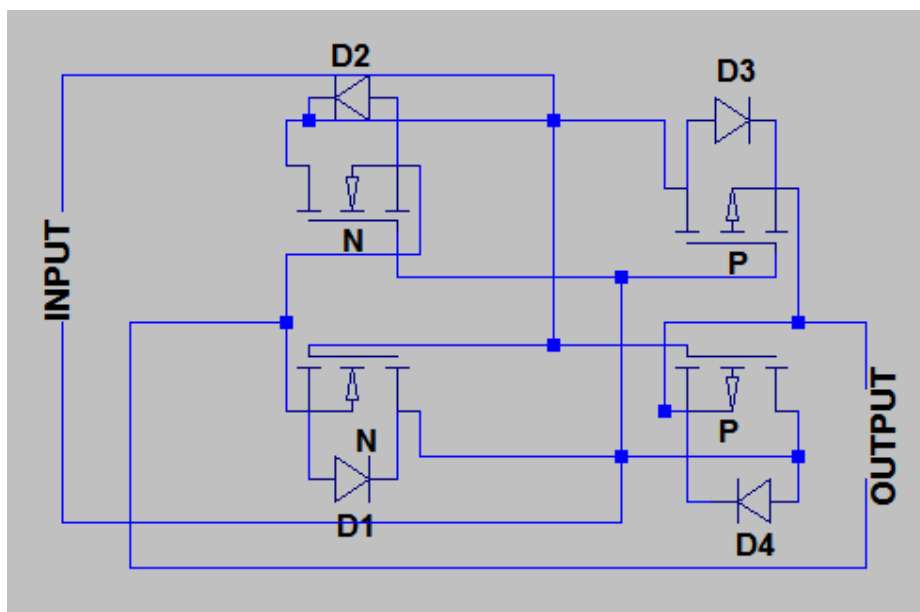
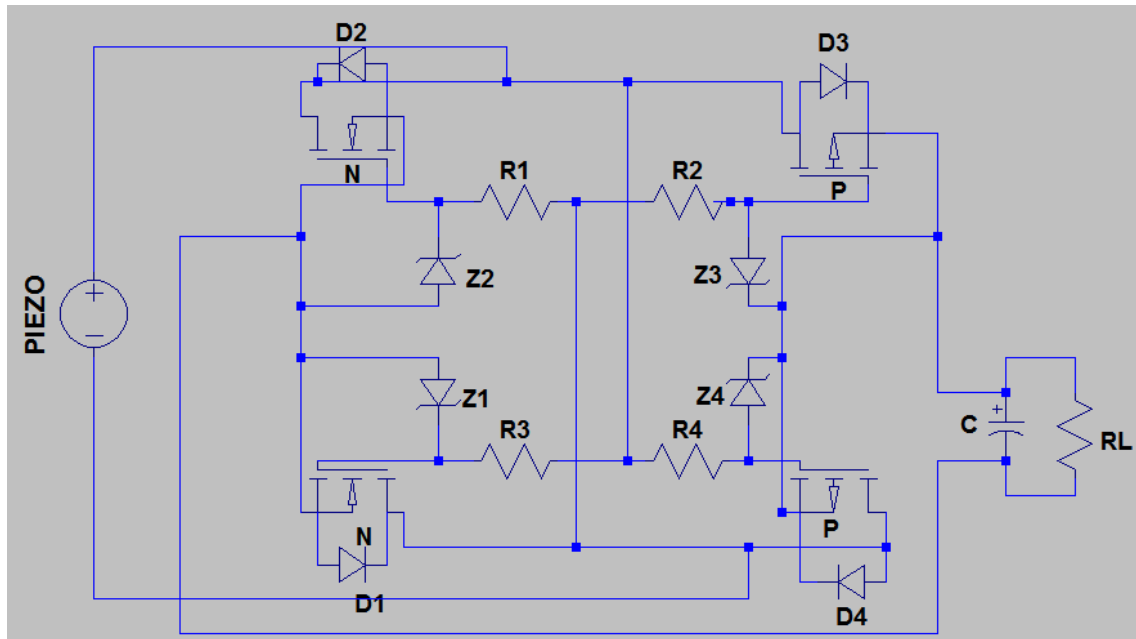
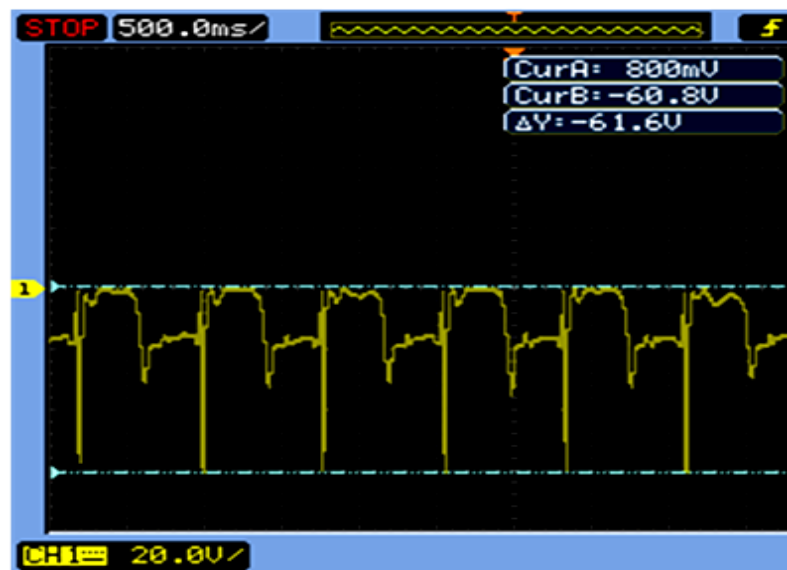


Figure 4.7 MOSFET Bridge rectifier

The MOSFET bridge rectifier circuit used for the present analysis is as shown in figure 4.8. Two n-channel (IRF Z44N) and two p-channel (IRF 9640N) MOSFETs were used to make the bridge rectifier. Figures 4.9 and 4.10 depict the DC open circuit waveforms with shoe harvesters.



**Figure 4.8 MOSFET Bridge rectifier circuit for piezo drum harvesters**



**Figure 4.9 DC open circuit waveform of 27 mm drum with MOSFET bridge rectifier**

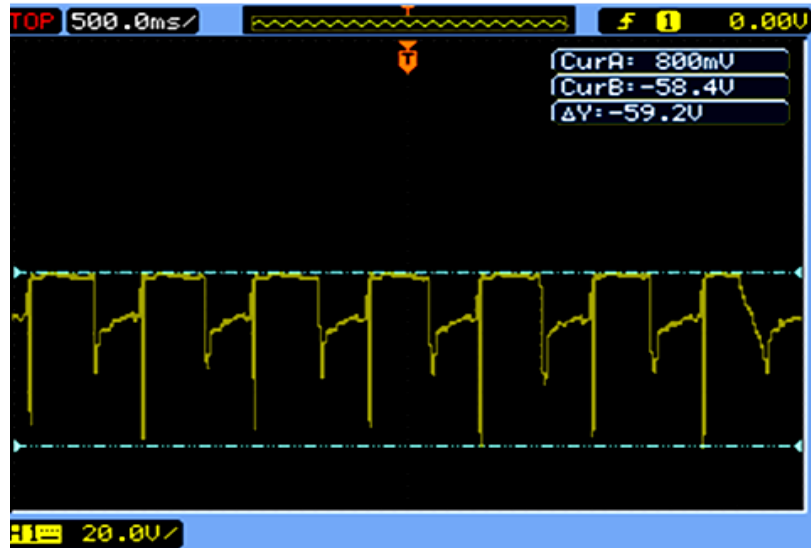


**Figure 4.10 DC open circuit waveform of 35 mm drum with MOSFET bridge rectifier**

\*( time = x axis & voltage = y axis)

A commercially available MOSFET IC FDS4559 was also used as it contains both p-channel and n-channel MOSFETs in a single SMD package. Details of FDS4559 are given in Appendix B. Figure 4.11 gives a plot of output power vs. load resistance for shoe models M1 and M2 with a MOSFET bridge rectifier.

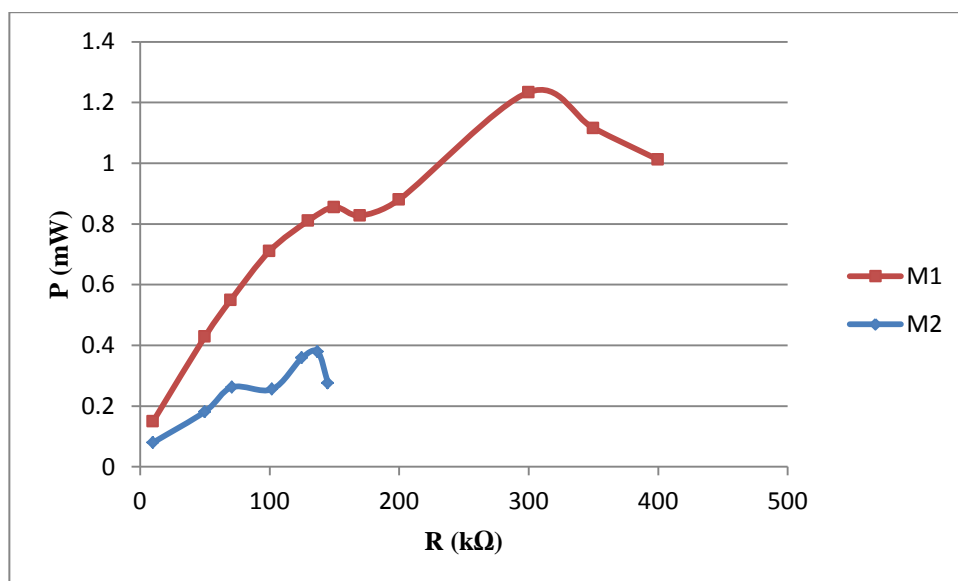


**Figure 4.11 Output power vs. load resistance for Model 1 and Model 2.**

As can be seen from figures 4.11 and 3.35, the maximum power generated by Model 1 is greater than that generated by Model 2 for both the circuits. In addition, the power obtained using the standard interface is greater than that obtained using the MOSFET rectifier.

Linear regulation schemes are not suitable as an excitation profile like walking results in extremely high source impedance generating a high voltage and low energy, low duty cycle current pulses. Researchers have proposed various non-linear techniques to harvest optimum electrical energy from piezo harvesters. A discussion of these techniques is what follows. Non linear operation is also independent of the physical phenomenon which makes it useful for other conversion effects as well.

## **4.2 NON-LINEAR PIEZOELECTRIC ENERGY HARVESTING CIRCUITS**

The first approach to switching is when the piezoelectric element is directly connected to the storage stage. If a switching element consisting of an inductor and a switch is connected in parallel or series to the piezo harvester, the technique is called *Synchronized Switch Harvesting on Inductor* (SSHI). In the parallel mode (figure 4.12), voltage inversion occurs after energy extraction while in the series mode (figure 4.13) both occur simultaneously. The inductor can also be replaced by a transformer in which case the technique is referred to as SSHI-MR. SSHI-MR allows electrical decoupling of the storage stage from the extraction stage which makes it possible to have a hybrid SSHI configuration (figure 4.14) consisting of the parallel and transformer modes in combination which enables harvesting four times per period; during inversion as well as conduction of the rectifier when rectified voltage is less than maximum piezo voltage, as against two in the earlier cases.

SSHI can give a gain of up to 10 over the classical method under constant displacement magnitude. It also allows an increase in bandwidth. However, the damping, which is characteristic of vibration energy harvesting, limits the power output which is the same as the standard case but with the added advantage of reduced volume of the piezoelectric element with power limit being reached for a lower global coupling coefficient.

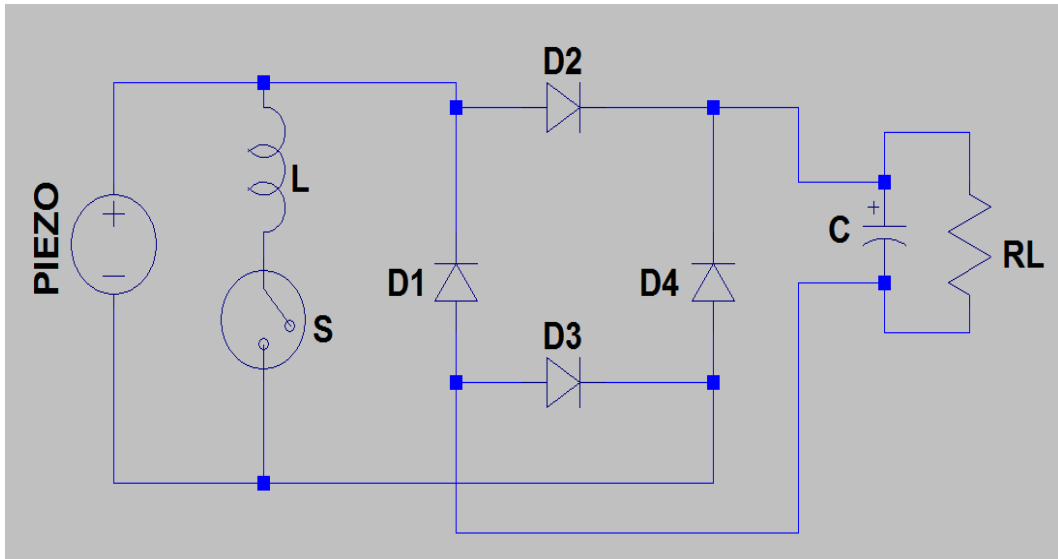


**Figure 4.12 Parallel SSHI**

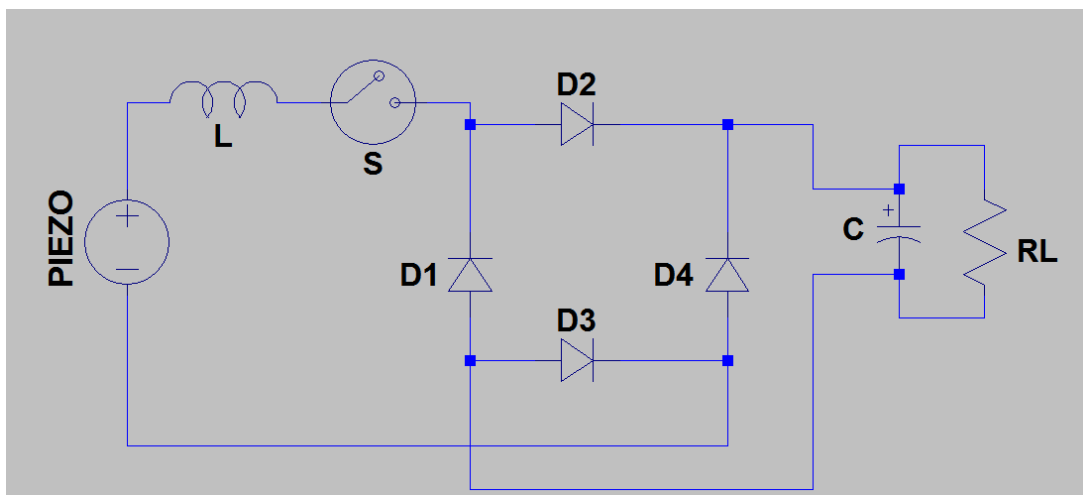


**Figure 4.13 Series SSHI**

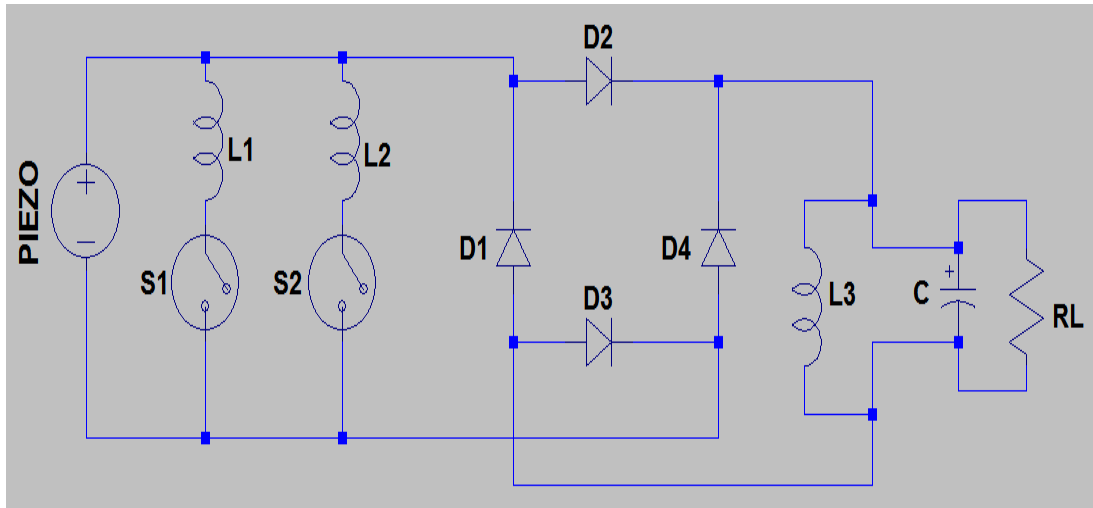


**Figure 4.14 Hybrid SSHI**

The SSDCI (synchronized switching and Discharging to a storage Capacitor through an Inductor) is similar to the series SSHI but with a tailored switch control. In this method, the electrostatic energy available on the piezo element is transferred to a storage capacitor through an inductor (figure 4.15). The switching is naturally stopped by the rectifier when the piezo voltage equals zero during which time there is still energy in the inductor which is transferred to the storage capacitor. For high load values, the piezo voltage doesn't reach zero and the circuit acts as a series SSHI. This approach reportedly permits four times more energy than the standard case over a wider load range [97].

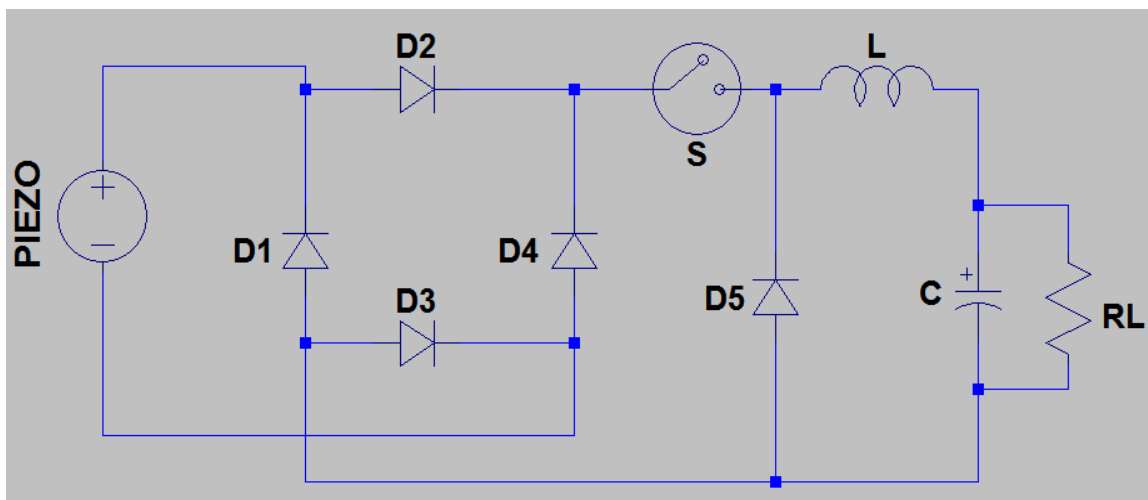


**Figure 4.15 SSDCI**

The switching process for voltage inversion can also be carried out using an inverter through PWM. This method is called active energy harvesting scheme. It permits an almost perfect voltage inversion [98, 99] yielding an outstanding harvested energy level. The only drawback is the external energy requirement to drive the PWM.

A two step switching technique can also be adopted to enhance the voltage inversion and hence the power output. This approach has been found to increase the energy output of the SSHI techniques by 40% under constant displacement magnitude [100].

In practical applications, the load may not be fixed in advance and can possibly change with time according to the state of the connected system. For example, sleep mode, RF communications, etc. The second approach to switching is modelled around this particular factor. Here, an inductor is used as an energy storage element. The direct interface of the piezo element to the load is circumvented by transferring the energy in two stages –

1. From the piezo element to the inductor (after which the piezo element is disconnected from the circuit).
2. From the inductor to the storage capacitor.

This technique (figure 4.16), known as the Synchronous Electric Charge Extraction (SECE), harvests energy independent of the connected system.

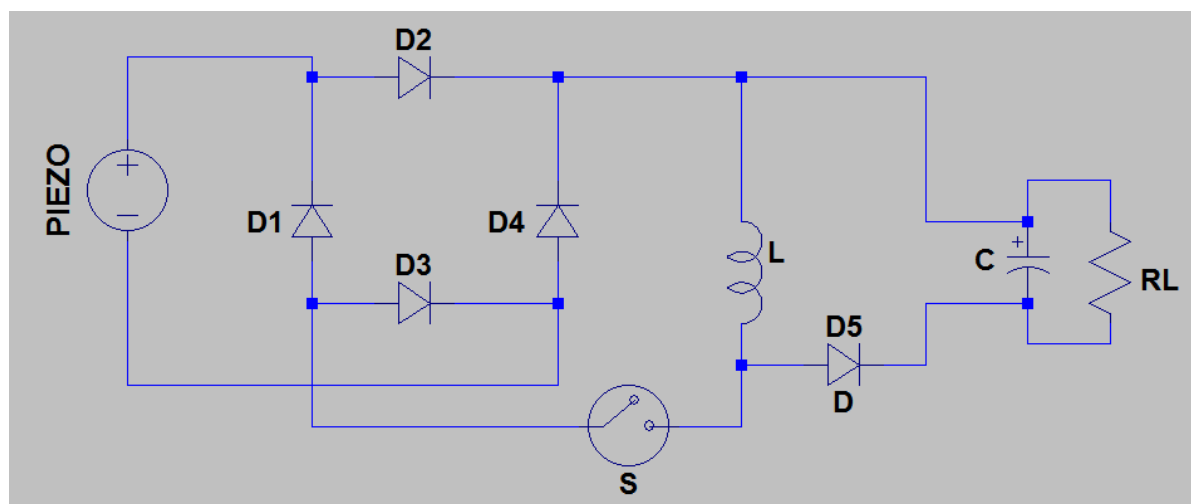


**Figure 4.16 SECE**



It permits a gain of 4 in terms of energy harvested as compared to the standard technique. But when damping is considered, this technique has a critical value of the figure of merit given by the product of the quality factor  $Q_M$  (effective available energy) and the square of the coupling coefficient  $k$  (amount of energy that can be converted into electrical energy). The harvested energy decreases above this threshold as  $k^2 Q_M$  increases.

To circumvent the above problem, the series SSHI and SECE can be combined to give a technique known as *Double Synchronized Switch Harvesting* (DSSH) [101]. Here (figure 4.17) a part of the energy from the harvester is transferred to an intermediate capacitor  $C_{int}$  and the remaining energy is then used for the inversion. Finally the energy on  $C_{int}$  is transferred to an inductor and then to the storage. By properly tuning the ratio of the intermediate capacitance to the piezo capacitance, the amount of energy extracted can be controlled. This tuning can give six times as much power as the classical energy harvesting interface.

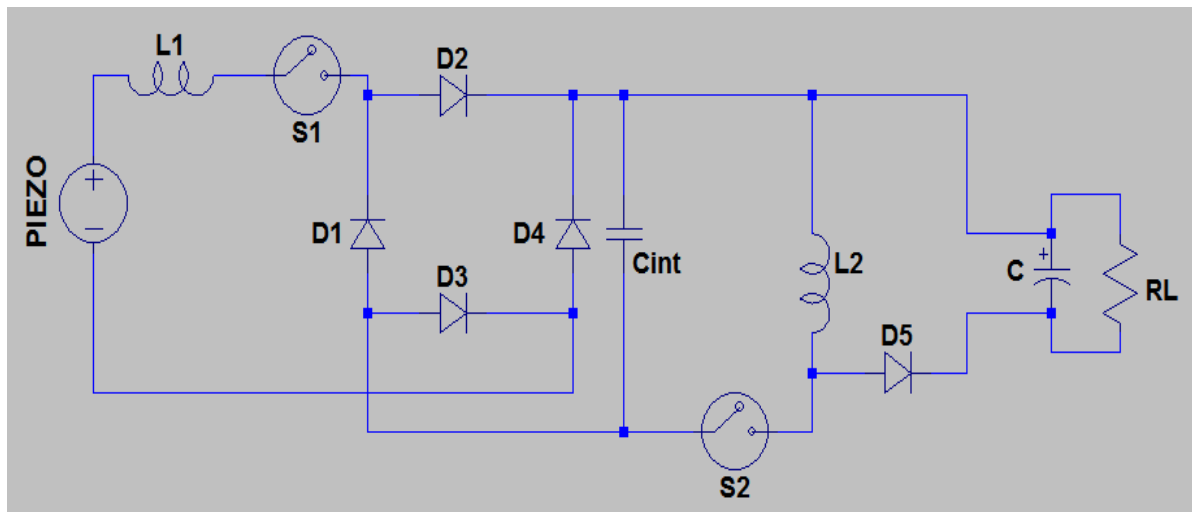


**Figure 4.17 DSSH**

**\*All circuits above, barring figure 4.1, were made using LTSpice (by Linear Technology)**

The above technique can be further enhanced by leaving a small amount of energy i.e. non- zero voltage on the intermediate capacitance. This improvement is called *Enhanced Synchronized Switch Harvesting* (ESSH). It allows a finer control of the trade-offs between energy extraction and voltage increase and between harvested energy and the damping effect. It also permits greater tolerance to a mismatch in the capacitance ratio mentioned earlier [102].

The SSHI technique can be improved by adding an energy feedback loop between the storage and the piezo element. In this technique, a part of the energy from the storage stage is fed to the piezo element. The voltage is then allowed to increase by leaving the active (piezo) material in open circuit condition. This technique overcomes the unidirectional limitations of the techniques discussed so far (except the active technique). A theoretical maximum gain of 40 is possible with this technique when compared to a classical system with constant displacement magnitude [103].

The above methods are, however, not suitable for very low frequencies like those encountered during walking. At a walking pace of 1 Hz, resonant shunting requires an inductance of the order of  $10^5$  H which is impractical if one expects the device to fit in a shoe [92]. The natural alternative will be switching converters. They have two advantages over linear systems: 1) They are true power converters and not just voltage regulators which makes them much more efficient in cases where the difference between input and output voltages is big and 2) They are effectively impedance converters in that the average DC output current can be greater than the average DC input current.

## **Non-linear Energy Harvesting IC**

LTC 3588 energy harvesting IC by Linear technology is a commercially available energy harvesting solution which can be interfaced with a variety of piezoelectric energy harvesters in a wide frequency range. It employs a non-linear interface for energy harvesting. It comes in two variants viz. the LTC 3588 – 1 and LTC 3588 – 2 which are capable of giving maximum regulated output voltages of 3.6 V and 5 V respectively, although there is also the option of tuning the output voltage using certain input pins [104, 105].

The LTC 3588 has an integrated low-loss full-wave bridge rectifier together a high efficiency buck converter forming an inclusive energy harvesting solution that is optimized for piezoelectric, solar, or magnetic transducers which have high output impedance. An ultralow quiescent current under voltage lockout (UVLO) mode with a wide hysteresis window allows accumulation of charge on an input capacitor until the buck converter is enabled to efficiently transfer a part of the accumulated charge to the output. The input and output quiescent currents are minimal during regulation when the LTC 3588 enters a sleep state. The buck converter turns on and off as necessary to sustain

the regulation of output voltage. Four different output voltage levels viz. 1.8 V, 2.5 V, 3.3 V and 3.6 V, are configurable with up to 100 mA of continuous output current. The output capacitor may however be selected suitably to provide a higher output current burst. A 20 V input protective shunt allows greater energy storage for a given amount of input capacitance [104, 105]. The internal block diagram and pin configuration of LTC 3588 are given in Appendix C.

### **Internal Bridge Rectifier**

Both the LTC 3588 ICs have an internal full-wave bridge rectifier which can be accessed through the PZ1 and PZ2 inputs that rectifies AC input. The rectified output which is stored on a capacitor at the VIN pin can be used as an energy reservoir for the buck converter. The low-loss bridge rectifier has an overall drop of about 400 mV with typical currents ( $\sim 10 \mu\text{A}$ ) generated by piezoelectric sources. The bridge can carry a maximum current of 50 mA. One side of the bridge can be operated as a single-ended DC input. When the bridge is employed, care must be taken to never short PZ1 and PZ2 together [104, 105].

### **Undervoltage Lockout (UVLO)**

As the voltage on VIN crosses the UVLO rising threshold, the buck converter is enabled and charge is transferred from the input capacitor to the output capacitor. For LTC 3588 – 1, a wide ( $\sim 1\text{ V}$ ) UVLO hysteresis window is employed with a lower threshold of around 300 mV above the selected regulated output voltage to avoid short cycling for the duration of buck power-up. Similarly, for LTCC 3588 – 2, a wide ( $\sim 2\text{ V}$ ) UVLO hysteresis window permits a part of the energy stored on the input capacitor to be transferred to the output capacitor by the buck. Once the input capacitor voltage goes below the UVLO falling threshold the buck converter is disabled. Very low quiescent current (450 nA typical for LTC 3588 – 1, 830 nA typical, VIN = 12 V for LTC 3588 – 2) in UVLO allows energy to accrue on the input capacitor where low power sources are used for energy harvesting [104, 105].

## **Internal Rail Generation**

The high side PMOS and low side NMOS of the buck converter are driven by two internal rails viz. CAP and VIN2 generated from VIN, respectively. The VIN2 rail also acts as logic high for output voltage select bits D0 and D1. The VIN2 rail is regulated at 4.8 V above GND whereas the CAP rail is regulated at 4.8 V below VIN. These are not to be used as external rails. CAP and VIN2 pins have bypass capacitors connected to them that act as energy reservoirs which can drive the buck switches. VIN2 is equal to VIN and CAP is held at GND when VIN is below 4.8 V, [104, 105].

## **Buck Operation**

Using the internal feedback from the VOUT sense pin together with a hysteretic voltage algorithm the buck regulator controls the output. Through an inductor, an output capacitor is charged by the buck converter to a value slightly higher than the regulation point. This is achieved by ramping the inductor current up to 260 mA through an internal PMOS switch and then ramping it down to 0 mA through an internal NMOS switch. In this way, energy is efficiently delivered to the output capacitor. VIN, VOUT, and the inductor value determine the ramp rate. If the input voltage falls below the UVLO falling threshold before the output voltage reaches regulation, the buck converter switches off and does not turn on until the input voltage again rises above the UVLO threshold. For this period of this time, the output voltage will be loaded by roughly 100 nA.

The converter enters a low quiescent current sleep state that monitors the output voltage with a sleep comparator when the buck brings the output voltage into regulation. For the duration of this operating mode, load current is supplied by the buck output capacitor. When the output voltage falls below the regulation point, the buck regulator wakes up and the cycle is repeated. This hysteretic method of providing a regulated output reduces losses linked with FET switching and maintains an output at light loads. The buck delivers a minimum of 100 mA of average current to the output when it is switching.

Upon indication from the sleep comparator that the output has reached the sleep threshold the buck converter may be in the middle of a cycle with current still flowing through the inductor. Usually both synchronous switches would turn off and the current in the inductor would freewheel to zero through the NMOS body diode. The LTC 3588 (1 and

2) keeps the NMOS switch on for this duration to prevent the conduction loss that would occur in the diode if the NMOS were off. If the PMOS is on when the sleep comparator trips the NMOS will turn on immediately in order to ramp down the current. If the NMOS is on it will be kept on until the current reaches zero.

Despite the quiescent current when the buck is switching being much greater than the sleep quiescent current, it's still a small percentage of the average inductor current which leads to a high efficiency for the majority of load conditions. The buck operates only when adequate energy has been accumulated in the input capacitor and the time taken by the converter to transfer energy to the output is much less than the time it takes to build up energy. As a result, the buck operating quiescent current is averaged over a long period of time so that the total average quiescent current is low. This feature is best suited for sources harvesting minute amounts of ambient energy. Four selectable voltages are available by tying the output select bits, D0 and D1, to GND or VIN2. The pin configuration logic for selectable voltages is shown in Appendix C. Figure 4.18 and 4.20 give the application of LTC 3588 (1 & 2) as energy harvesting solutions for piezoelectric energy harvesting elements.

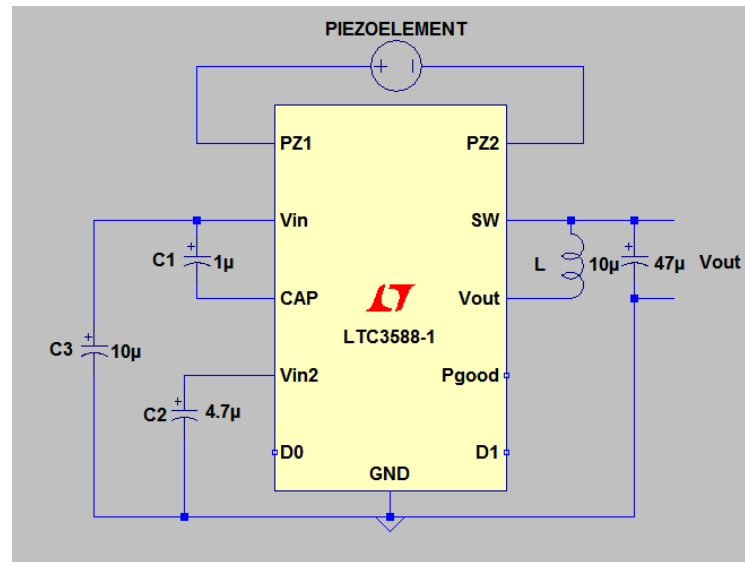
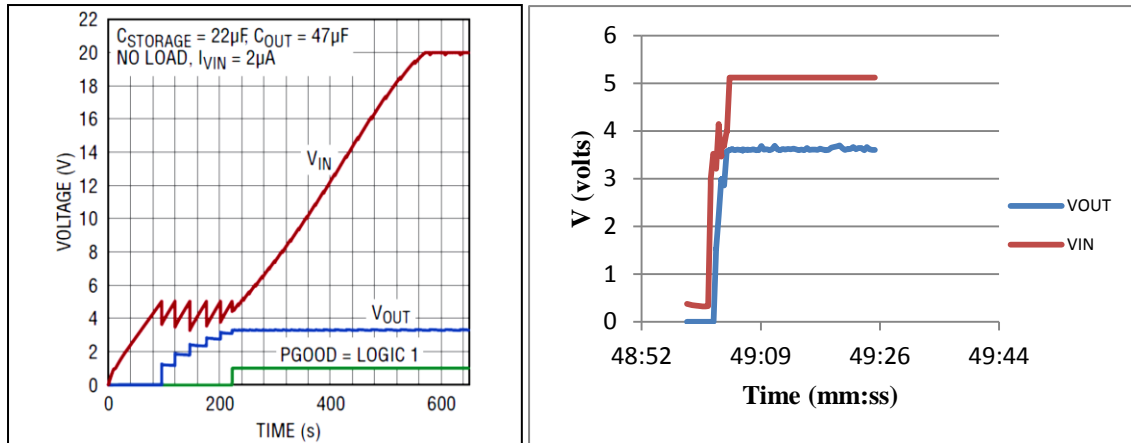


**Figure 4.18 Circuit for piezoelectric energy harvesting with LTC 3588 – 1 with output of 3.6 V**



(a)

(b)

**Figure 4.19 LTC 3588 – 1 (a) Standard input/ output plots from datasheet (b) Results obtained with shoe harvesters**

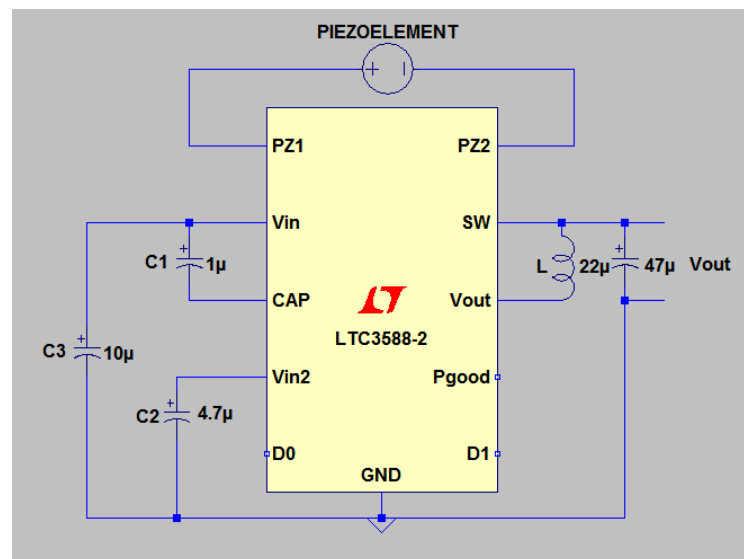


**Figure 4.20 Circuit for piezoelectric energy harvesting with LTC 3588 – 2 with output of 5 V**

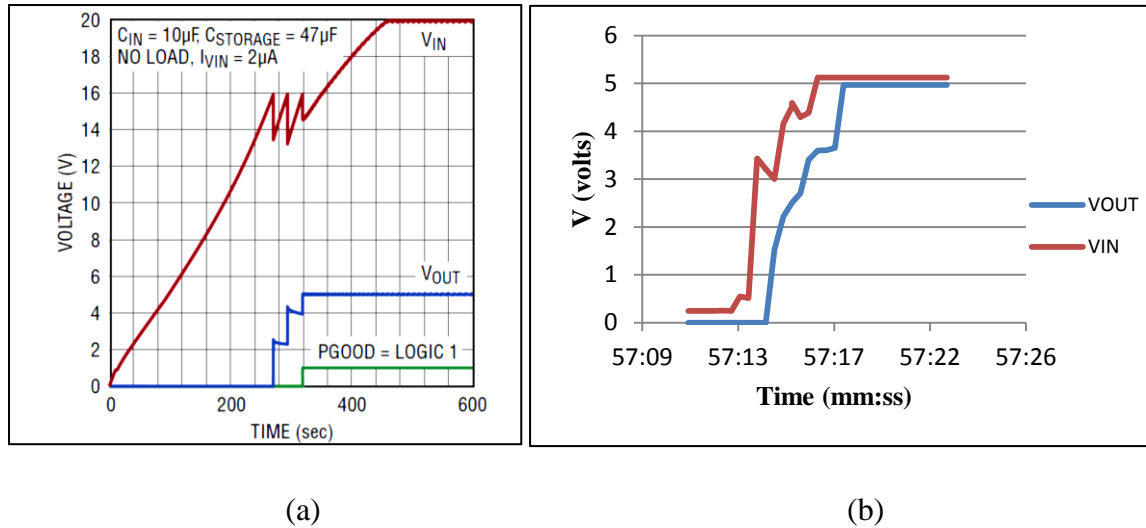


**Figure 4.21 LTC 3588 – 2 (a) Standard input/ output plots from datasheet (b) Results obtained with shoe harvesters**

Figures 4.19 and 4.21 show the input and output waveforms obtained experimentally with the shoe harvesters. The input waveforms shown in figures 5.16 and 5.18 are capped at 5 V as the NI DAQ module used in the experiments could measure a maximum input voltage of only 5 V. Nevertheless, the waveforms obtained experimentally are in excellent agreement with those given in the datasheets for the energy harvesting ICs.

The energy harvesting circuit as depicted in figure 4.2 was configured on a PCB and tested with the drum harvesters excited at their resonance frequencies as the input source. The power delivered was calculated using the same setup as described in section 3.4. It was able to deliver a constant DC output of 5 volts and a maximum current of 0.2 mA which was measured using the current source in sink mode. Thus, the power delivered was found to be 1 mW (using the formula  $P = VI$ ).

### **4.3 CONCLUSION**

LTC 3588 gives the option of designing a piezoelectric energy harvesting circuit with selectable voltage levels along with providing, rectification, step down and regulation. Hence, it is an ideal solution for interfacing with piezoelectric energy harvesting elements in a variety of excitation profiles. In the present study, it was found to be useful for impact energy harvesting as employed in shoe-based piezo energy harvesters (described in chapter 4) as well as higher frequency vibration energy harvesting as applied to drums and piezo diaphragms in different vibration profiles (described in chapter 3). It has high energy conversion efficiency which enables its use in piezoelectric energy harvesting which is characterized by low power output. The output of LTC 3588 interfaced with a piezoelectric energy harvester can be directly used to power microelectronic devices like microcontrollers, RF transmitters, and can also be used to charge energy storage devices like supercapacitors, batteries, etc.



### DEVELOPMENT OF ENERGY STORAGE MECHANISM

---

Before working on the energy storage analysis, a shoe-based energy harvesting mechanism was designed fabricated and analyzed for its power output as discussed in chapter 3. Then, coupled with the circuits discussed in chapter 4, different energy storage elements were tested as suitable storage media.

#### 5.1 ANALYSIS OF ENERGY STORAGE ELEMENTS

##### 5.1.1 Electrolytic capacitors

Electrolytic capacitor is the general term which includes three different types of capacitors viz. Aluminum electrolytic capacitors, Tantalum electrolytic capacitors and Niobium electrolytic capacitors [106]. All electrolytic capacitors are polarized capacitors. The anode is made of a particular metal on which an insulating oxide layer is formed by anodization, acting as the dielectric of the electrolytic capacitor. A solid electrolyte which covers the surface of the oxide layer acts as the cathode of the capacitor. Due to their very thin dielectric oxide layer and enlarged anode surface, electrolytic capacitors have a much higher capacitance-voltage (CV) per unit volume product compared to ceramic capacitors or film capacitors, but a much smaller CV value than supercapacitors. As far as the present study is concerned, electrolytic capacitors suffer from the following drawbacks:

- High leakage
- High voltage rating
- Low charge storage capacity
- Uncontrolled discharge
- Not suitable for directly powering of microelectronic devices

### **5.1.2 Supercapacitors**

A supercapacitor or ultracapacitor, is a high-capacity electrochemical capacitor with capacitance values much greater than other capacitors that bridge the gap between electrolytic capacitors and rechargeable batteries. Their typical storage capacity is 10 to 100 times more (energy per unit volume or mass) than electrolytic capacitors. They can accept and deliver charge much faster than batteries, and tolerate many more charge and discharge cycles than rechargeable batteries. For a given charge, however, they are 10 times bigger in size than conventional batteries [107].

Supercapacitors are used in applications requiring many rapid charge/discharge cycles rather than long term compact energy storage: within cars, buses, trains, cranes and elevators, where they are used for regenerative braking, short-term energy storage or burst-mode power delivery.

### **5.1.3 Lithium ion batteries**

Lithium-ion batteries are ubiquitous in household electronics. They are one of the most popular types of rechargeable batteries for portable electronics, with a high energy density, insignificant memory effect and low self-discharge. Apart from consumer electronics, they are also increasingly being used for military, battery electric vehicle and aerospace applications. Lithium-ion batteries can be dangerous under some conditions and can pose a safety hazard since they, unlike other rechargeable batteries, contain a flammable electrolyte and are kept pressurized. Li rechargeable batteries have a typical self-discharge rate as declared by manufacturers to be 1.5-2% per month [108].

As far as the present study is concerned, Li-ion battery suffers from the following drawbacks:

- Long charging time (300 mV in 1 hr as observed in shoe-charging experiments)
- Need complex circuitry for proper charging
- Cannot be completely discharged as it reduces battery life
- Not efficient at sub-zero temperatures [109]

### 5.1.4 NiMH batteries

A nickel–metal hydride battery, abbreviated NiMH or Ni–MH, is a type of rechargeable battery. NiMH batteries nominally operate at 1.2 V per cell, somewhat lower than conventional 1.5 V cells, but will operate many devices designed for that voltage. Charging voltage is in the range of 1.4–1.6 V per cell. In general, a constant-voltage charging method cannot be used for automatic charging. Self-discharge rate can be as low as 1.25% per month [110]. As far as the present study is concerned, NiMH batteries have the following advantages:

- No voltage regulation needed [111].
- Voltage ratings compatible with those of electronic devices.
- Can be discharged completely without affecting battery life.
- Can work in the sub - zero temperature range (-20 to +65 °C) [112]

## 5.2 CHARGING OF CAPACITORS

Various capacitors were coupled with the shoe-based harvesters using the standard interface circuit described earlier. The charge accumulated after a 5-min walk was measured in each case. For the supercapacitors, additionally, the charge accumulated over a long walk (1 hr) was also measured. Table 5.1 gives the measured values.

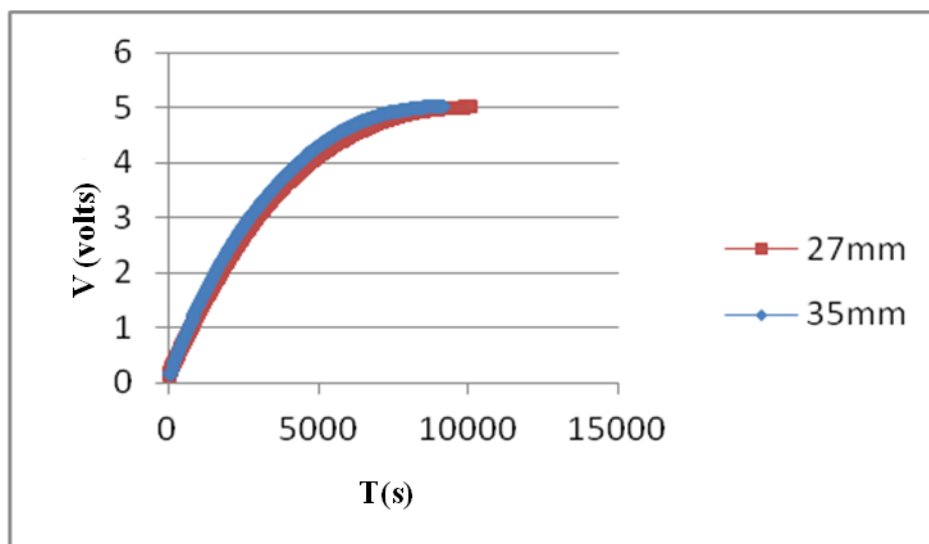
**Table 5.1 Charging of various capacitors with the shoe-based harvesters**

| Sr No | Capacitance    | Value (Farad)/ Rating (volts) | Charging time (min) with walking | Voltage developed (volts) | Energy generated per step ( $\mu$ Joules) |
|-------|----------------|-------------------------------|----------------------------------|---------------------------|---|
| 1     | Electrolytic   | 470 $\mu$ /63                 | 5                                | 20                        | 156                                       |
| 2     | Tantalum       | 100 $\mu$ /15                 | 5                                | 11                        | 10  |
| 3     | Tantalum       | 100 $\mu$ /16                 | 5                                | 11                        | 10  |
| 4     | Supercapacitor | 0.10 $\mu$ /5.5               | 5                                | 0.20                      | 3.3                                       |
|       |                |                               | 60                               | 3.5                       | 170.14                                    |
| 5     | Supercapacitor | 0.33 $\mu$ /5.5               | 5                                | 0.15                      | 6.2                                       |
|       |                |                               | 60                               | 2.5                       | 286.46                                    |

The energy generated per step is calculated as follows:

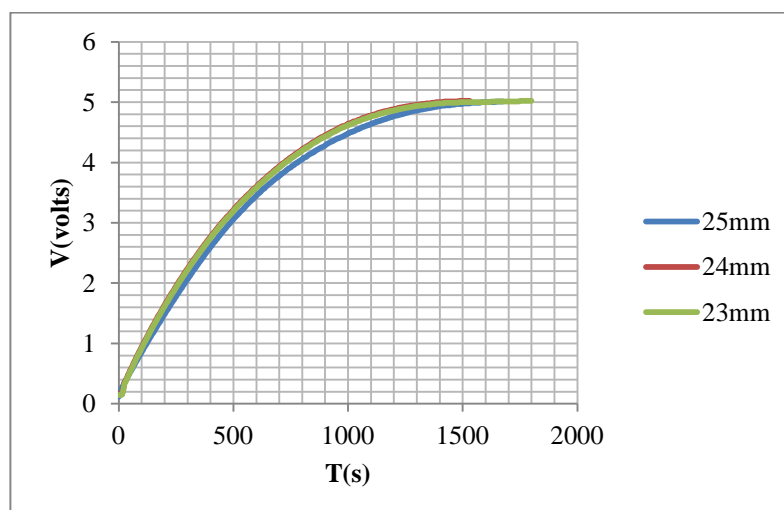
Energy stored in the capacitor is  $E = 1/2CV^2$ . E divided by the number of steps gives the energy generated per step. Here the number of steps per minute is taken as 120 or 2 steps per second.

Figure 5.1 shows the charging curves of a supercapacitor (0.1 F/5.5 V by Cornell-Dubilier) charged using the two piezoelectric diaphragms excited at their respective resonance frequencies. The 27 mm and 35 mm diaphragms took 167 min and 153 min respectively to charge the supercapacitor to 5 V.



**Figure 5.1 Charging curves of supercapacitors charged with piezo diaphragms**

The charging curves of a supercapacitor charged with drum harvesters excited at resonance are as shown in figures 5.2 and 5.3 below. Table 5.2 summarizes the results of the charging experiments with the different drums.



**Figure 5.2 Charging with 27 mm drum and 3 different steel ring IDs**

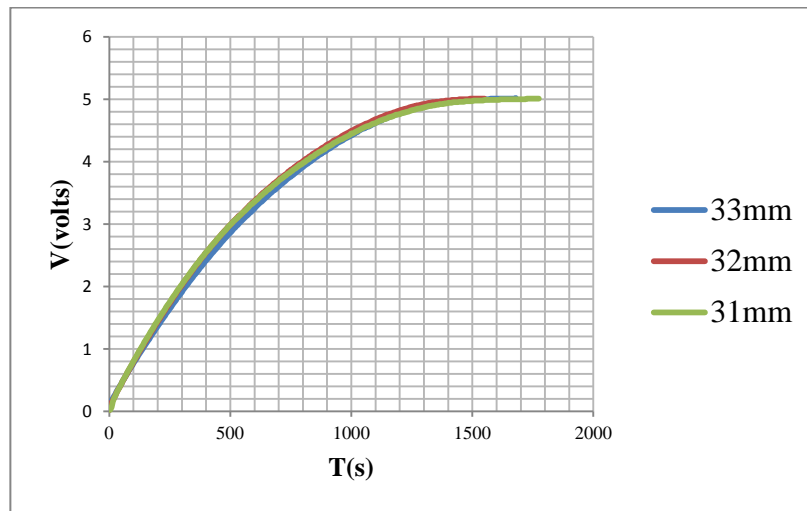


**Figure 5.3 Charging with 35 mm drum and 3 different steel ring IDs**

**Table 5.2 Supercapacitor charging with drum harvesters**

| Drum size (mm) | Steel ring ID (mm) | Charging time (min) |
|----------------|--------------------|---------------------|
| 35             | 33                 | 26                  |
| 35             | 32                 | 24                  |
| 35             | 31                 | 28                  |
| 27             | 25                 | 26                  |
| 27             | 24                 | 23                  |
| 27             | 23                 | 35                  |

Calculating the energy accumulated in half an hour in the supercapacitor by the formula  $E = \frac{1}{2} CV^2 = 0.5 \times 0.1 \times 25$  gives 1.25 J. In comparison, for the charging of a supercapacitor in [113], charging time to reach 5 V was 16 days which amounted to only 33.125 mJ of energy generated in one hour. Hence it can be concluded that a considerable amount of energy can be generated even with very low amplitude vibrations using the drum harvesters fabricated in the present work.

### 5.3 CHARGING OF NiMH BATTERIES

The charging rate of NiMH batteries of 3 different capacities (22 mAh, 70 mAh, 160 mAh/ 4.8 V) using the shoe harvesters was studied. A simple standard interface consisting of a schottky bridge rectifier and a large capacitor (4700uF) was used as the charging interface for this battery. The output of the shoe harvester was fed to this charging interface and the voltage accumulated in the battery over time was recorded using a data acquisition card (NI 9174). Figures 5.4-5.6 illustrate the charging curve of the battery.

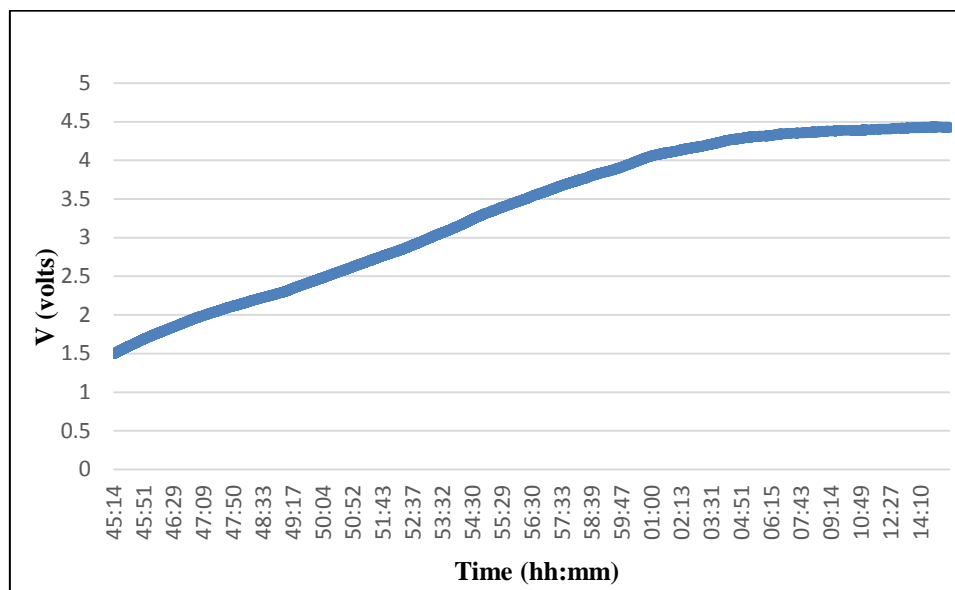


**Figure 5.4 Charging curve of a 22 mAh NiMH battery**

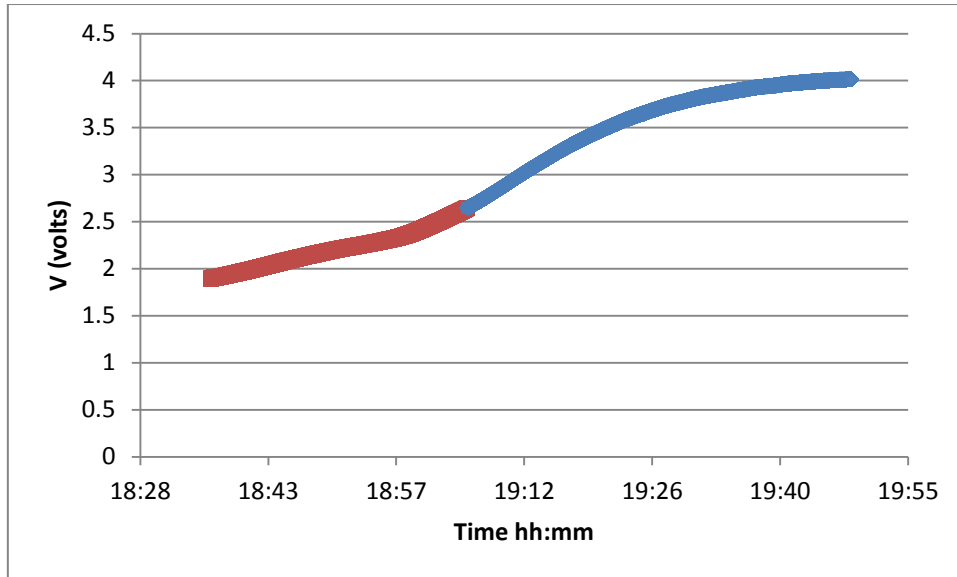


**Figure 5.5 Charging curve of a 70 mAh NiMH battery**

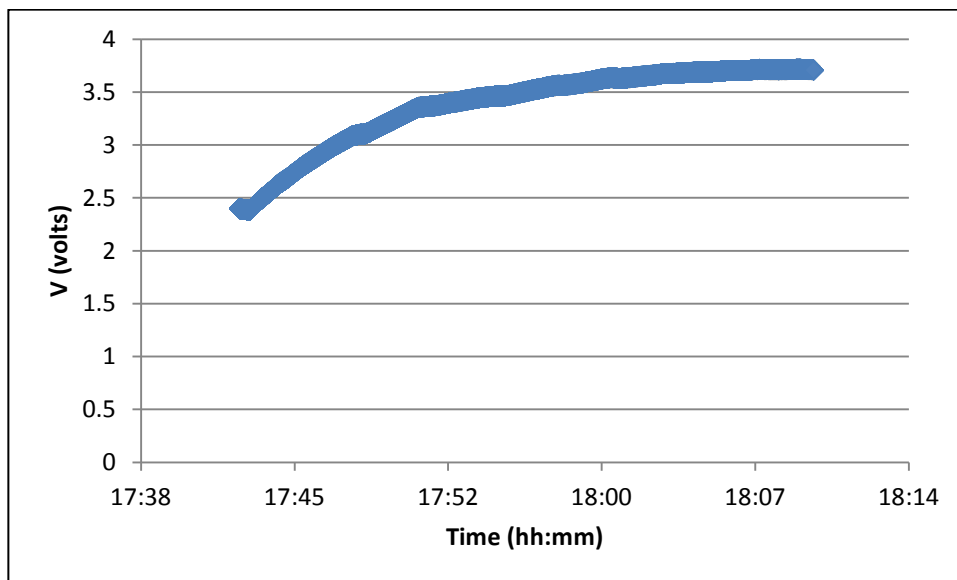


**Figure 5.6 Charging curve of a 160 mAh NiMH battery**

Table 5.3 summarizes the results of the battery charging experiments. It can be seen that the batteries can be charged up to 4 volts in approximately half an hour.

**Table 5.3 NiMH battery charging with shoe-harvesters**

| <b>Battery capacity</b> | <b>Initial voltage<br/>(volts)</b> | <b>Final voltage<br/>(volts)</b> | <b>Charging time @ 120<br/>steps per minute (min)</b> |
|-------------------------|------------------------------------|----------------------------------|---|
| 4.8 V/ 22 mAh           | 1.49                               | 4.42                             | 30  |
| 4.8 V/ 70 mAh           | 1.89                               | 4.01                             | 40  |
| 4.8 V/ 160 mAh          | 2.39                               | 3.70                             | 27  |

## **5.4 CONCLUSION**

Four different types of energy storage elements, viz. electrolytic capacitors, supercapacitors, Li-ion batteries and NiMH batteries, were analyzed for their suitability to store the energy generated by the drum harvesters fabricated in the present work and also with the shoe-based harvesters.

Different capacitors were charged using the shoe harvesters and the energy generated per step was calculated. A maximum energy of 286.46  $\mu\text{J}$  per step could be generated using a supercapacitor charged with shoe harvesters. Also, a maximum energy of 1.25 J could be accumulated in the supercapacitor in approximately half an hour using drums excited with vibrations.

NiMH batteries of three different capacities were charged using the shoe harvesters. The results indicated that the batteries could be charged upto 4 volts in about half an hour of walking.

It can be concluded that supercapacitors and NiMH batteries are suitable energy storage elements for the energy harvesters used in the present work. A useful amount of energy is generated in just half an hour of operation and this energy is enough to power various microelectronic devices like microcontrollers, low power sensors, RF modules, etc.



## INTERFACING INTEGRATED ENERGY HARVESTING MODULE WITH SUITABLE APPLICATION

As discussed in chapter 1, energy harvesting can be employed to power microelectronic devices that are used in a range of devices from consumer electronics to military and aerospace applications. Figure 6.1 gives an outline of the power available from different energy harvesting techniques and the devices that can be powered using them [114].

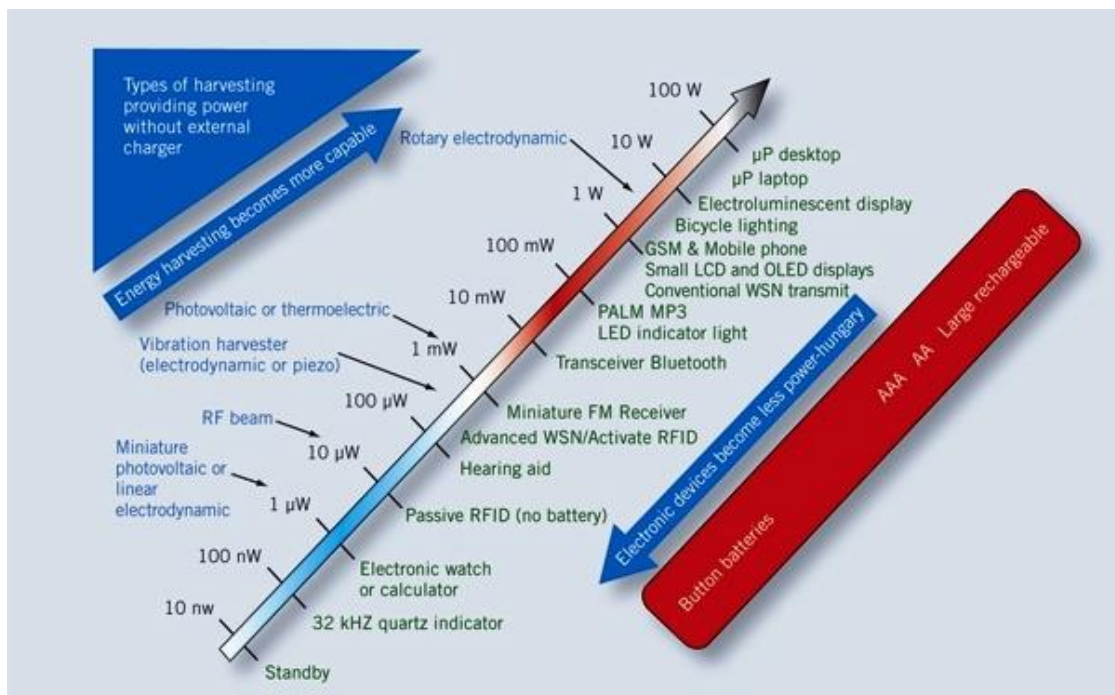


Figure 6.1 Power available from energy harvesting vs. power requirement of electronic devices [114]

## 6.1 POWERING OF A MICROCONTROLLER

The Arduino Uno is a microcontroller board with the ATmega328 microcontroller at its heart. It has 14 digital input/output pins (of which 6 can be used as PWM outputs), 6 analog inputs, a 16 MHz crystal oscillator, a USB connection, a power jack, an ICSP header, and a reset button. It includes everything required to support the microcontroller. It can be directly attached to a computer with a USB cable or powered with a AC-to-DC adapter or battery to get going. The Uno is different from all earlier boards in that it doesn't use the FTDI USB-to-serial driver chip. In its place, it has the Atmega8U2 programmed as a USB-to-serial converter. The Uno is the most recent in a series of USB Arduino boards. The specifications of Atmega328 are as depicted in table 6.1 [115].

**Table 6.1 ATMEGA328 technical specifications**

|                                    |  |
|------------------------------------|--|
| <b>Microcontroller</b>             | ATmega328                                |
| <b>Operating Voltage</b>           | 5V                                       |
| <b>Input Voltage (recommended)</b> | 7-12V                                    |
| <b>Input Voltage (limits)</b>      | 6-20V                                    |
| <b>Digital I/O Pins</b>            | 14 (of which 6 provide PWM output)       |
| <b>Analog Input Pins</b>           | 6  |
| <b>DC Current per I/O Pin</b>      | 40 mA                                    |
| <b>DC Current for 3.3V Pin</b>     | 50 mA                                    |
| <b>Flash Memory</b>                | 32 KB of which 0.5 KB used by bootloader |
| <b>SRAM</b>                        | 2 KB                                     |
| <b>EEPROM</b>                      | 1 KB                                     |
| <b>Clock Speed</b>                 | 16 MHz                                   |

### **6.1.1 Programming the Arduino Board**

The Arduino Uno can be programmed with the Arduino IDE software (download). The ATmega328 on the Arduino Uno comes preburned with a bootloader which allows uploading of new code without the need of an external hardware programmer. It communicates by means of the original STK500 protocol (reference, C header files). The bootloader can also be bypassed and the microcontroller can be programmed using the ICSP (In-Circuit Serial Programming) header. The ATmega8U2 firmware source code is also available. The ATmega8U2 is loaded with a DFU bootloader, that can be activated by connecting the jumper on the back of the board and then resetting the 8U2. Atmel's FLIP software (Windows) or the DFU programmer (Mac OS X and Linux) can then be used to load a new firmware. Alternatively, the ISP header with an external programmer can also be used (overwriting the DFU bootloader) [115].

### **6.1.2 Flashing a LED**

The board was pre-programmed with a program to flash an on-board LED by interfacing it with a PC and using the Arduino IDE. The program is inbuilt into the IDE as one of the practice programs [Appendix D] [116].

Even while the LED is off, the Arduino chip is still active and consumes power. But there are functions on the microcontroller to put it to sleep during the time it is inactive, and reactivate the chip when we need to change the state of an output or to perform some measurements. The JeeLib is one such library which reduces the power consumption of the microcontroller in the inactive state by including the header file in the program as `#include <JeeLib.h>` [117].

A supercapacitor (Cornell Dubilier 0.1 F/5.5 V) was charged to 5 V with the drum harvesters operated at resonance (as already described in section 3.4) . The time taken was approximately 30 minutes. The charged supercapacitor was connected to the power input of the pre-programmed Arduino board (figure 6.2). It was able to flash the LED for 10 seconds before stopping. This may be attributed to the minimum voltage requirement of the board which is 3.3 V. As the voltage fell below 3.3 V, the board was unable to operate. With suitable modifications, this operation can be made autonomous wherein the the Arduino board, coupled with a temperature sensor, can be made to periodically transmit, say for example the ambient temperature, to a receiver station.

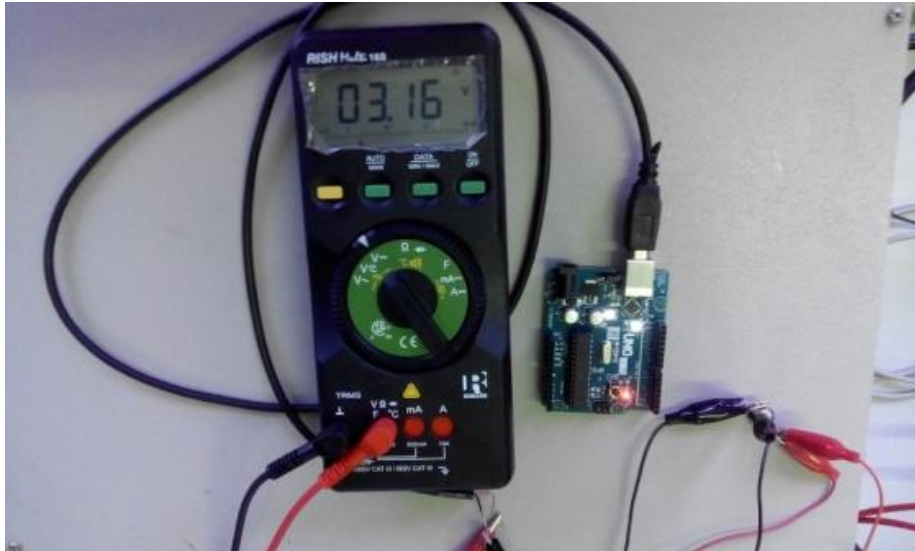


**Figure 6.2** Arduino board powered by the charged supercapacitor

## **6.2 POWERING OF AN RF TRANSMITTER**

### **6.2.1 RF Module**

A radio frequency (RF) module is generally a small electronic device used to transmit and/or receive radio signals between two devices. In an embedded system, wireless communication with another device is often desirable. This wireless communication may be achieved via optical communication or radio frequency (RF) communication. For many applications, the medium of choice is RF since it does not necessitate line of sight. RF communications integrate a transmitter and/or receiver.

RF modules are extensively used in electronic design due to the difficulty of designing radio circuitry. Good electronic radio design is infamously complex because of the sensitivity of radio circuits and the accuracy of components and layouts necessary to achieve operation on a particular frequency. Additionally, reliable RF communication circuit requires careful monitoring of the manufacturing process to make sure that the RF performance is not unfavorably affected. Finally, radio circuits are, more often than not, subject to limits on radiated emissions, and require Conformance testing and certification by a standardization organization like ETSI or the U.S. Federal Communications Commission (FCC). For these reasons, design engineers often design a circuit for an application that requires radio communication and then "drop in" a pre-made radio module rather than endeavor on a discrete design, saving time and money on development [118].

RF modules are frequently used in medium and low volume products for consumer applications such as garage door openers, wireless alarm systems, industrial remote controls, smart sensor applications, and wireless home automation systems. They are occasionally used to replace older infrared communication designs as they have the benefit of not needing line-of-sight operation.

Several carrier frequencies are universally used in commercially available RF modules, including those in the industrial, scientific and medical (ISM) radio bands such as 433.92 MHz, 915 MHz, and 2400 MHz. These frequencies are used as national and international regulations governing the use of radio for communication permit their utilization without any restrictions. Short Range Devices may also use frequencies accessible for unlicensed bands such as 315 MHz and 868 MHz. RF modules may conform to a defined protocol for RF communications such as Zigbee, Bluetooth low energy, or Wi-Fi, or they may implement a proprietary protocol [118].

### **6.2.2 RF transmitter**

A wireless radio frequency (RF) transmitter and receiver can be simply made using HT12D Decoder, HT12E Encoder and ASK RF Module. Wireless transmission can be achieved by using 433 MHz or 315MHz ASK RF Transmitter and Receiver modules. In these modules digital Amplitude Shift Keying (ASK) is used as the modulation technique. Radio Frequency (RF) transmission is stronger and reliable than Infrared (IR) transmission owing to following reasons [119]:

- RF signals can travel longer distances than Infrared.
- Only line of sight communication is possible with IR while RF signals can be transmitted even through obstacles such as walls.
- Infrared signals will fall prey to interference from other IR sources but signals on one frequency band in RF will not interfere with other bands.

A typical RF transmitter module is shown in Appendix D. HT12E Encoder IC converts 4 bit parallel data given to pins D0 – D3 to serial data available at DOUT. This output serial data is given to ASK RF Transmitter. Address inputs A0 – A7 can be used to provide data security. Status of these Address pins should match with status of address pins in the

receiver for the transmission of the data. An 8-bit code can be set on both the transmitter and receiver side so that one pair communicates only within themselves and erroneous transmission to some other receiver can be avoided. Data is transmitted only when the Transmit Enable pin (TE) is held LOW. 1.1 M $\Omega$  resistor provides the necessary external resistance for the operation of the internal oscillator of HT12E. In the transmitter used for the present work, a 433.92 MHz crystal oscillator was used.

A typical RF receiver module is shown in Appendix D. ASK RF Receiver receives the data transmitted by the ASK RF Transmitter. HT12D decoder converts the received serial data to 4 bit parallel data D0 – D3. The status of address pins A0-A7 must match with status of address pin in the HT12E at the transmitter for the transmission of data. The VT pin goes high every time a signal is received. The LED connected to the pin gives a visual indication of valid data transmission whenever a signal is received. The 51 K $\Omega$  resistor provides the necessary resistance required for the internal oscillator of the HT12D [119].

The shoe-based drum stack harvesters were interfaced with LTC 3588 energy harvesting circuit as already described in chapter 5. The output of the energy harvesting circuit was fed to the transmitter module as well as to a 70 mAh NiMH battery. The circuit was modified such that through a switch, the transmitter could be powered solely with the shoe or with the battery. The battery could be charged with the shoe harvesters. As the need arises, the arrangement can be self-powered or battery-powered. The entire unit is a self-contained energy harvesting source needing no external power supply. After walking every 4-5 steps, enough energy was generated to power the transmitter module which was able to transmit a signal. Pressing of a switch enabled discharging the energy accumulated in the storage element of the energy harvesting circuit. This process can be made autonomous wherein a signal will be transmitted every 4-5 steps as the storage element discharges automatically into the transmitter. When transmission is not needed, the output of the energy harvesting shoes could be switched to the battery so that it charges. And when continuous transmission is required, the battery could be switched to the transmitter. The circuits are as shown in figure 6.3.

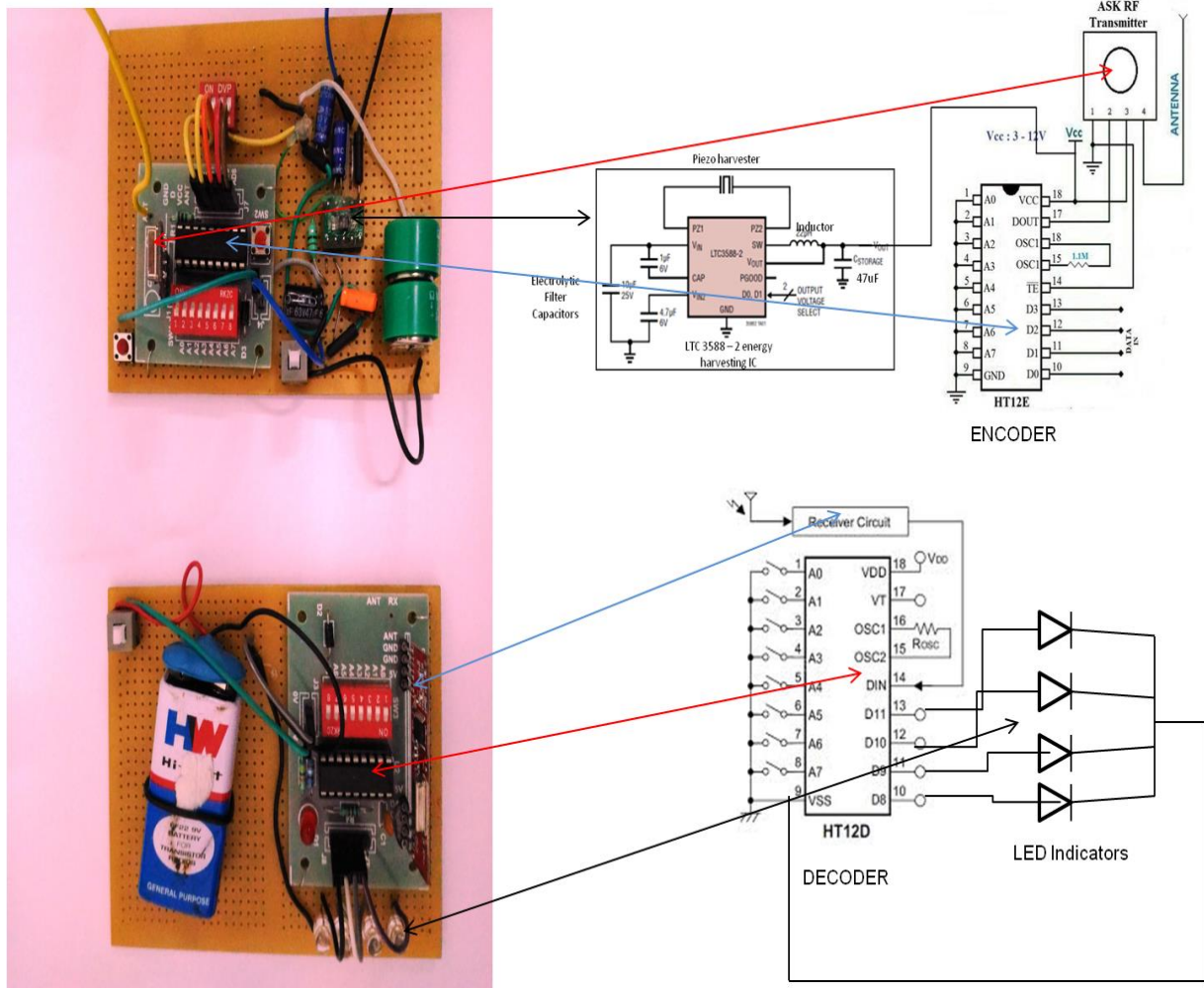


Figure 6.3 Shoe-powered transmitter module and battery powered receiver module

### **6.3 CONCLUSION**

Application of energy harvested with shoe-based piezoelectric energy harvesters and with vibrations was demonstrated through the powering of microelectronic devices with the energy accumulated. Two devices viz. Arduino microcontroller and a 433.92 MHz RF transmitter module were successfully powered using the energy accumulated. The Arduino board could run a program to flash a LED for 10 seconds when powered with a supercapacitor charged using drum harvesters. A dual power mode self-powered RF transmission module was also fabricated that can be operated battery-less or with a battery that can be recharged using the shoe-based energy harvesters. Future work may incorporate designing a self-powered wireless sensor node like an ambient temperature sensing module which could transmit ambient temperature periodically.



### CONCLUSION AND FUTURE SCOPE

---

In the present work, a novel method of fabricating flexible piezocomposites was attempted. Also, a very simplified method of developing piezoelectric drum harvesters using generic piezocomposite diaphragms has been described. The procedure for fabrication of these drum harvesters is simple, cheap and time efficient. The piezocomposite diaphragms and the drum harvesters made using them can be potentially incorporated in various structures and vibration profiles to generate useful amounts of energy. They are suitable as ambient energy harvesters over a wide range of frequency and stress. In the present case, energy harvesting from low amplitude vibrations as well as high amplitude impact were analyzed.

In the case of low amplitude vibration energy harvesting using piezocomposite diaphragms, the effect of pre-stress on the power output and resonance frequency was studied. Application of pre-stress was found to greatly increase the power output as well as reduce the resonance frequency. Energy generated was in the range of a few hundred microwatts. The energy generated was used to charge supercapacitors, which were successfully used to power a microcontroller board.

Drum harvesters were fabricated using the piezocomposite diaphragms. The power output of these energy harvesters was optimized by varying the steel ring IDs. Optimal values of the steel ring IDs were found through experiment. A comparison with simulated values using ANSYS was also carried out. The energy harvesting ability of these drum harvesters under a low amplitude profile was studied. It was found that useful amounts of energy (2 – 3 mW) can be generated for a low stress (0.5 N) excitation. The energy generated was accumulated in supercapacitors, which were then used to power a microcontroller.

The drum harvesters were modified to make them suitable for impact energy harvesting. A stack was configured using the drums. A novel impact simulator was designed and

fabricated for bench testing of the drums and stacks. Thorough analysis was carried out on the effect of increasing the number of drums in the stacks and the impact frequency on the power output. It was found that increasing the number of drums in the stack increases the power output but beyond a certain number of drums, the power output saturates. Similarly, increasing the impact frequency increases the power output but the output saturates after an impact frequency of 4 Hz. Subsequently, the drum stacks were embedded in shoes and their power generation capabilities as shoe-based harvesters was studied under different ambulation profiles such as walking and running. The shoe-harvesters were found to generate between 3 and 8 mW, with running generating more power compared to walking.

Various energy-harvesting circuits were analyzed as suitable energy harvesting interfaces for the energy harvesters designed in the present work. A comparison of the standard interface with a MOSFET bridge rectifier was carried out. It was concluded that the standard interface was a better option compared to the MOSFET bridge for the present case. Additionally, as a complete energy harvesting circuit solution, circuits employing LTC 3588 energy harvesting ICs were used, which were able to provide regulated outputs of 3.6 V as well as 5 V as per requirement.

To select a suitable energy storage device for the energy harvesters, various energy storage elements were analyzed. Different capacitors were charged with the shoe-harvesters. The energy accumulated in supercapacitors over a long period of walking (2 hours) was experimentally deduced. Battery charging was also studied. Li-ion batteries were found to be unsuitable for the harvesters used in the present work. NiMH batteries of different capacities were successfully charged with the shoe-harvesters.

As an application of the utilization of power generated from the shoe harvesters, a RF transmitter module was successfully powered.

Future work will incorporate analysis of performance of the piezoelectric diaphragms and drum harvesters under a high amplitude vibration profile. Also, effect of pre-stress and contact area of the clamping on the power output of the drum harvesters will be studied. Optimizing the internal diameter of the steel ring may further enhance the power output of the drums. Substituting steel with some other light and durable material like polycarbonate can also be conceptualized. This can potentially enhance the flexibility of the drum structure and make it lighter. A wireless sensor node that can relay ambient

parameters like temperature in real time utilizing the power generated by the harvesters is also a potential application.

Regarding shoe-based energy harvesting, the arrangement of the stacks /drums/diaphragms inside the shoes can be optimized further to prolong the operational life of the harvesters and increase the power output. Ultra low power GPS and wireless communication modules can also be potentially powered using energy generated with the shoes. Design and fabrication of an indigenous and affordable energy harvesting circuit is also possible to circumvent the need for importing foreign parts and reduce the cost and time in product development.

# PUBLICATIONS

---

## Journal Publications

1. **R. Mishra**, S. Jain, C. Durgaprasad, “A Review On Piezoelectric Material As A Source Of Generating Electricity And Its Possibility To Fabricate Devices For Daily Uses Of Army Personnel” , International Journal of Systems, Control and Communications (IJSCC) 6(3), pp 212-221, 2015. doi>[10.1504/IJSCC.2015.068908](http://www.inderscience.com/info/inarticle.php?artid=68908).<http://www.inderscience.com/info/inarticle.php?artid=68908>
2. **R. Mishra** , S. Jain , C. Durgaprasad , S. Sahu, “ Vibration Energy Harvesting Using Drum Harvesters”, International Journal of Applied Engineering Research, 10(14), pp 34995-35001, 2015. [https://www.google.co.in/webhp?sourceid=chrome-instant&ion=1&espv=2&ie=UTF8#q=%E2%80%9C+Vibration+Energy+Harvesting+Using+Drum+Harvesters%E2%80%9D+%2C+International+Journal+of+Applied+Engineering+Research%2C+10\(14\)%2C+pp+34995-35001:+2015](https://www.google.co.in/webhp?sourceid=chrome-instant&ion=1&espv=2&ie=UTF8#q=%E2%80%9C+Vibration+Energy+Harvesting+Using+Drum+Harvesters%E2%80%9D+%2C+International+Journal+of+Applied+Engineering+Research%2C+10(14)%2C+pp+34995-35001:+2015).
3. **R. Mishra**, S. Jain, B. Thakur, Y. P. Verma, C. Durgaprasad “Analysis of piezoelectric drum transducers as shoe-based energy harvesters”, International Journal of Electronics Letters. <http://dx.doi.org/10.1080/21681724.2016.1253777>.

## Conference Publications

4. **R. Mishra**, S. Jain, C. Durgaprasad, “Analysis of Piezoelectric Buzzers as Vibration Energy Harvesters”, March 16th- 18th, 2016, pp 2476-2480, 10th INDIACom: 3rd 2016 International Conference on Computing for Sustainable Global Development, BVICAM, New Delhi.

## Patents

5. “Energy Harvesting Footwear”, **Ritendra Mishra**, Dr. Sunil Kumar Hota, Dr. C. Durgaprasad, Dr Shruti Jain, Col. Vasant Ballewar, Dr R B Srivastava, Patent (Filed with the Indian Patent Office) Application number 325/DEL/2015.

## REFERENCES

---

- [1] [http://en.wikipedia.org/wiki/Energy\\_harvesting](http://en.wikipedia.org/wiki/Energy_harvesting)
- [2] Starner T, Paradiso J, “Human generated power for mobile electronics”, Low Power Electronic Design, CRC Press, Pages 45-1-45-35, 2004.
- [3] <http://www.icsense.com/business-cases-categories/low-power>
- [4] [http://www.digitimes.com.tw/tw/B2B/Seminar/Service/download/053A110160/053A110160\\_4VHPYLU9HLIYQW19DQMB.pdf](http://www.digitimes.com.tw/tw/B2B/Seminar/Service/download/053A110160/053A110160_4VHPYLU9HLIYQW19DQMB.pdf)
- [5] <http://www.ti.com/lit/ds/symlink/cc2640.pdf>
- [6] <http://www.holuxdevice.com/gps-module/holux-mn-31540sh.html>
- [7] Zarlink Semi., “ZL70250 Ultra Low Power RF Transceiver”, Shortform Data Sheet, January 2008.
- [8] [www.rnp.org/node/wave-tidal-energy-technology](http://www.rnp.org/node/wave-tidal-energy-technology)
- [9] [http://en.wikipedia.org/wiki/Geothermal\\_electricity](http://en.wikipedia.org/wiki/Geothermal_electricity)
- [10] <http://www.windenergyfoundation.org/about-wind-energy/faqs>
- [11] [http://en.wikipedia.org/wiki/Solar\\_energy](http://en.wikipedia.org/wiki/Solar_energy)
- [12] <http://alabamaquake.com/energy.html#>
- [13] Starner T, “Human Powered Wearable Computing”, IBM Systems Journal, vol 35, nos 3&4, 1996.
- [14] <http://en.wikipedia.org/wiki/Piezoelectricity>
- [15] Priya S, Inman D, “Energy Harvesting Technologies”, Springer 2009.
- [16] <http://energy.gov/energysaver/small-wind-electric-systems>.
- [17] Military Embedded Systems, Publisher – Open Systems Media, ISSN 1557-3222.

- [18] [http://in.mouser.com/applications/benefits\\_energy\\_harvesting](http://in.mouser.com/applications/benefits_energy_harvesting)
- [19] <https://en.wikipedia.org/wiki/Socket>
- [20] [http://www.sustainabledanceclub.com/products/sustainable\\_dance\\_floor/](http://www.sustainabledanceclub.com/products/sustainable_dance_floor/)
- [21] <http://www.gizmag.com/npower-peg-charger-for-hand-held-electronics/14957/>
- [22] <http://www.bbc.co.uk/news/business-12137680>
- [23] <http://www.businesstoday.in/magazine/cover-story/coolest-start-ups-in-india-lumos-design-technology/story/204514.html>
- [24] Paradiso J, Starner T, “Energy Scavenging for Mobile and Wireless Electronics” IEEE Pervasive Computing, vol 4 issue 1, March 2005.
- [25] <http://sroeco.com/solar/most-efficient-solar-panels>.
- [26] [en.wikipedia.org/wiki/Energy\\_harvesting](http://en.wikipedia.org/wiki/Energy_harvesting).
- [27] Flynn A M and Sanders S R (2002) ‘Fundamental limits on energy transfer and circuit considerations for piezoelectric transformers, IEEE Transactions on Power Electronics, vol. 17 no. 1, pp 8-14, January 2002.
- [28] Roundy S and Wright P K, “A piezoelectric vibration based generator for wireless Electronics”, Smart Materials and Structures, Vol. 13, No. 5, pp.1131–1142, 2004.
- [29] Worthington E. L., “Piezoelectric Energy Harvesting: Enhancing Power Output by Device Optimization and Circuit Techniques, PhD Thesis, Ac. Yr. 2006-10, Cranfield University.
- [30] <http://www.engineerlive.com/content/power-and-potential-piezoelectric-energy-harvesting>
- [31] <http://dev.nsta.org/evwebs/2014102/news/default.html>
- [32] Cook-Chennault K.A, Thambi N, Sastry A M, “Powering MEMS Portable, Devices – a Review of Non-Regenerative and Regenerative Power Supply

Systems with Emphasis on Piezoelectric Energy Harvesting Systems,” *Smart Materials and Structures*, vol. 17, 043001 (33pp), 2008.

- [33] Beeby S P, Torah R N, Tudor M J, “Kinetic Energy Harvesting”, ACT Workshop on Innovative Concepts. ESA-ESTEC, 28-29 January 2008.
- [34] Beeby S P, Tudor M J, White N M, “Energy harvesting vibration sources for microsystems applications”, *Measurement Science and Technology*, Volume 17, Number 12, October 2006, R175 – R195.
- [35] [www.piceramic.com/download/PI\\_Piezoelectric\\_Ceramic\\_Products\\_CAT125E.pdf](http://www.piceramic.com/download/PI_Piezoelectric_Ceramic_Products_CAT125E.pdf)
- [36] Safari A, “Development of piezoelectric composites for transducers”, *Journal de Physique III*, EDP Sciences, vol. 4 no. 7, pp.1129-1149, 1994.
- [37] <http://www.designinsite.dk/htmsider/k1307.htm>
- [38] <https://en.wikipedia.org/wiki/Unimorph>
- [39] Jain A, Prashanth K J, Sharma A Kr, Jain A and P N Rashmi. (2015), “Dielectric and piezoelectric properties of PVDF/PZT composites: A review”, *Polymer Engineering & Science*, vol. 55, pp 1589–1616, 2<sup>nd</sup> May 2015.
- [40] Kim S, Clark W W, Wang Q-M, “Piezoelectric energy harvesting with a clamped circular plate : Analysis”, *Journal of Intelligent Material Systems and Structures*, Special Issue on energy harvesting, Vol 16, No 10, pp 847-54, Oct 2005.
- [41] Shu, Y C and Lien, I C ‘Efficiency of energy conversion for a piezoelectric power harvesting system’, *Journal of Micromechanics and Microengineering*, Vol. 16, No. 11, pp.24–29, 2006.
- [42] Sodano H A, Inman D J, Park G, “A review of power harvesting from vibrations using piezoelectric materials”, *The Shock and Vibration Digest*, Vol. 36, No. 3, pp. 197–205, May 2004.
- [43] Anton S. R., Sodano H. A., “A review of power harvesting using piezoelectric materials”, *Smart Materials and Structures*, Volume 16 2007, R1-R21.

- [44] Mitcheson P. D., Yeatman E. M., Rao G. K., Holmes A. S., Green T. C., “Energy harvesting from human and machine motion for wireless electronic devices”, Volume 96 No 9, September 2008, Proceedings of the IEEE.
- [45] Goldfarb M., Jones L. D., “On the efficiency of electric power generation with piezoelectric ceramic”, Transactions of the ASME, Volume 121, pp 566-571 September 1999.
- [46] Gambier P, Anton S R, Kong N, Erturk A, Inman D J, “Piezoelectric, thermal and solar energy harvesting for hybrid low power generator systems with thin film batteries”, Volume 23 No 1, pp 1-11, 2012.
- [47] Hehn T, Manoli Y, “CMOS circuits for Piezoelectric Energy Harvesting – Efficient Power Extraction, Interface Modelling and Loss Analysis”, Springer Series in Advanced Microelectronics, Volume 38, 2015.
- [48] Roundy S, Wright P K, Rabaey J, “A study of low level vibrations as a power source for wireless sensor nodes”, Computer Communications Vol 26, pp 1131–1144, 2003.
- [49] Sodano, H A, Magliula, E A, Park, G and Inman D J, “Electric power generation using piezoelectric materials”, Proceedings of the Thirteenth International Conference on Adaptive Structures and Technologies, Potsdam, Germany, pp 153 -161, 7-9 October, 2002.
- [50] Zheng, Q and Xu Y, “Asymmetric air-spaced cantilevers for vibration energy harvesting”, Smart Materials and Structures, vol. 17, no. 5, pp. 055009, 2008.
- [51] Glynne-Jones P, Beeby S. P. and White N. M., “Towards a piezoelectric vibration powered microgenerator”, IEEE Science Measurement and Technology, vol. 148, no. 2, pp. 68-72, March 2001.
- [52] Eichhorn C, Goldschmidtboeing F, Porro Y, Woais P, “A piezoelectric harvester with an integrated frequency tuning mechanism”, PowerMEMS 2009, Washington DC, USA, December 1-4, 2009.



- [53] Leon R A, Pina C A, Yenilmez A, Tansel I N, Pereira C M, Roth L E, “Development of a small energy scavenger”, Florida conference on recent advances in robotics, May 25-26 2006.
- [54] Song H C, Kang C Y, Jeong D Y, Kim H J, Yoon S J, “Piezoelectric thick films on metal substrate for energy harvesting.” Source – Researchgate. [https://www.researchgate.net/profile/SeokJin\\_Yoon/publication/228437965\\_Piezoelectric\\_Thick\\_Films\\_on\\_Metal\\_Substrate\\_for\\_Energy\\_Harvesting/links/02bfe5109f438207b9000000.pdf](https://www.researchgate.net/profile/SeokJin_Yoon/publication/228437965_Piezoelectric_Thick_Films_on_Metal_Substrate_for_Energy_Harvesting/links/02bfe5109f438207b9000000.pdf)
- [55] Qi Y, Jafferries T N, Lyons K, Lee C M, Ahmad H, McAlpine, M C, “Piezoelectric ribbons printed onto rubber for flexible energy conversion”, Nano Letters, Vol. 10, No. 2, pp.524–528, 2010.
- [56] Chen X., Xu S., Yao N., Shi Y., “1.6V nanogenerator for mechanical energy harvesting using PZT nanofibres”, Nano Letters, Vol 10 No 6, pp 2133 – 2137, 2010.
- [57] Park K-I, L Minbaek, Liu Y, Moon S, Hwang G-T, Zhu G, Kim J E, Kim S O, Kim D Y, Wang, Z L, Lee K J, ‘Flexible nanocomposite generator made of BaTiO<sub>3</sub> nanoparticles and graphitic carbons’, Advanced Materials, Vol. 24, No. 22, pp.2999–3004, 293, 12 June 2012.
- [58] Chen Xm Yang T, Wang W, Y Xi, “Vibration energy harvesting with a clamped piezoelectric circular diaphragm”, Ceramics International, vol. 38S, pp, S271-S274, 2012.
- [59] Minazara E, Vasic D, Costa F, Poulin G, “Piezoelectric diaphragm for vibration energy harvesting”, Ultrasonics, vol. 44, pp e699-e703, 2006.
- [60] Wischke, M, Woias, P, “Power harvesting from human walking”, Proceedings Power MEMS, pages 65-68, 2007.
- [61] Kim S, Clark W, Wang Q-M, “Piezoelectric energy harvesting with a clamped circular plate : Experimental Study”, Journal of Intelligent. Material Systems and Structures, Special Issue on energy harvesting, Vol 16, No 10, pp 855-64, Oct 2005.

- [62] Palosaari J., Leinonen M., Juuti J., Hannu J. and Jantunen H., “Piezoelectric circular diaphragm with mechanically induced pre-stress for energy harvesting”, *Smart Materials and Structures*, Vol. 23 No. 8, July 2014.
- [63] Wang W, Yang T, Chen X, Yao X, “Vibration energy harvesting using a piezoelectric circular diaphragm array”, *IEEE Transactions on Ultrasonics, Ferroelectrics, and Frequency Control*, vol. 59, no. 9, September 2012.
- [64] Ericka M, Vasic D, Costa F, Poulin G, Tliba S, “Energy harvesting from vibration using a piezoelectric membrane”, *Journal de Physique IV France*, Volume 128, pp 187-93, September 2005.
- [65] Kim H W, Batra A, Priya S, Uchino K, Markley D, Newnham R E. and Hofmann H F, “Energy Harvesting Using a Piezoelectric Cymbal Transducer in Dynamic Environment”, *Japanese Journal of Applied Physics*, Vol 43, No 9A, pp. 6178 – 6183, 2004.
- [66] Wang S, Lam K H, Sun C L, Kwok K W, Chan H L W, Guo M S and Zhao X-Z, “Energy harvesting with piezoelectric drum transducer”, *Applied Physics Letters* vol. 90, 113506, 2007.
- [67] Antaki J F, Bertocci G E, Green E C, Nadeem A, Rintoul T, Kormos R L, Griffith B P. ‘A gait powered autologous battery charging system for artificial organs’, *ASAIO Journal*, , Vol. 41, No. 3, pp.M588–M595 July–September 1995.
- [68] Kymissis, J., Kendall, C., Paradiso, J. and Gershenfeld, N. ‘Parasitic power harvesting in shoes’, *Wearable Computers, Digest of Papers. Second International Symposium*, Pittsburgh, PA, USA, pp.132–39, 19–20 October 1998.
- [69] Shenck N. S., Paradiso J. A., “Energy scavenging with shoe-mounted piezoelectrics”, *IEEE Micro*, Volume 21 Issue 3, pages 30 – 42, 2001.
- [70] Pelrine , R.E. Heel Strike Generator Using Electrostrictive Polymers, Patent number: 6768246, Issue date: 27 July 2004.
- [71] <https://www.theengineer.co.uk/inspiration/trevor-baylis-to-test-electric-shoes/>

- [72] Wang Z. L., Song J., “Piezoelectric nanogenerators based on zinc oxide nanowire arrays”, *Science*, Volume 306, pages 242 – 246, 2006.
- [73] Wang X., Song J., Wang Z. L., “Nanowire and nanobelt arrays of zinc oxide from synthesis to properties and to novel devices”, *Journal of Materials Chemistry*, Volume 17, pages 711 – 720, 2007.
- [74] Von Buren T, “Body Worn Inertial Electromagnetic Microgenerators”, PhD Thesis, Swiss Federal Institute of Technology, 2006.
- [75] Liu X , “An Electromagnetic Energy Harvester for Powering Consumer Electronics”, , Masters thesis, Clemson University, August 2012.
- [76] J Zhao, Z You, “A shoe embedded piezoelectric energy harvester for wearable sensors”, *Sensors*, July 2014, Vol 14, No 7.
- [77] M Leinonen, J Palosaari, M Sobocinski, J Juuti and H Jantunen, “Energy Harvesting from Vibration and Walking with Piezoelectric Materials.”,[http://www.defmin.fi/files/1928/Energy\\_harvesting\\_from\\_vibration\\_and\\_walking\\_with\\_piezoelectric\\_materials.pdf](http://www.defmin.fi/files/1928/Energy_harvesting_from_vibration_and_walking_with_piezoelectric_materials.pdf)
- [78] [http://www.talkingelectronics.com/projects/PIC\\_LAB-1/extra\\_06.html](http://www.talkingelectronics.com/projects/PIC_LAB-1/extra_06.html)
- [79] Mohammadi S., Abdalbeigi M., “Analytical optimization of piezoelectric circular diaphragm generator”, *Advances in Materials Science and Engineering*, Volume 2013, Article ID 620231, 10 pages, <http://dx.doi.org/10.1155/2013/620231>, 2013.
- [80] Telba A. and Ali W. G., “Modelling and simulation of piezoelectric energy harvesting”, *Proceedings of the World Congress on Engineering*, Vol II, July 4-6, London U K.
- [81] Kim H. W., Priya S., Uchino K., Newnham R. E., “Piezoelectric energy harvesting under high pre-stressed cyclic vibrations”, *Journal of Electroceramics*, Vol. 15 No. 1, pp 27-34, 2005.
- [82] SR Anton, HA Sodano, “A Review of power harvesting using piezoelectric materials (2003-2006)”, *Smart Materials and Structures*, Vol. 16 No. 3, R1-R21, 2007.

- [83] HS Kim, JH Kim, J Kim, “A review of piezoelectric energy harvesting based on vibration”, *International Journal of Precision Engineering and Manufacturing*, Vol. 12 No. 6, pp 1129-1141, 2011.
- [84] W Wang, RJ Humag, CJ Huang, LF Li, “Energy harvesting array using piezoelectric circular diaphragm for rail vibration”, *Acta Mechanica Sinica*, Vol. 30 No. 6, pp 884-888, 2014.
- [85] C L Sun, K H Lam, H L W Chan, X Z Zhao, C L Choy, “A novel drum piezoelectric actuator”, *Applied Physics A*, Vol 84, Issue 4, September 2006, pp 385 - 389.
- [86] Marinkovic, B. and Koser, H., “Smart sand: a wide bandwidth vibration energy harvesting platform”, *Applied Physics Letters*, vol. 94, no. 10, pp. 103505 (3 pp).
- [87] Renaud, M., Sterken, T., Fiorini, P., Puers, R., Baert, K and van Hoof, C., “Scavenging energy from human body: design of a piezoelectric transducer”, *The Thirteenth International Conference on Solid-State Sensors and Actuators Transducers*, Seoul, Korea, 2005, pp. 784–787.
- [88] <http://www.barefootrunning.fas.harvard.edu/4BiomechanicsofFootStrike.html>
- [89] <https://en.wikipedia.org/wiki/Pedobarography>
- [90] [www.airmartechonology.com/uploads/AirPDF/airducer\\_appnotes.pdf](http://www.airmartechonology.com/uploads/AirPDF/airducer_appnotes.pdf)
- [91] Rao Y, McEhchern M, Arnold D P, “A compact human powered energy harvesting system”, *Journal of Physics: Conference Series*, Volume 476, conference 1, 2013.
- [92] Shenck, N. S., and J. A. Paradiso. "Unobtrusive Energy Scavenging Using Shoe-Mounted Piezoelectrics and Simple Power-Conditioning Electronics."
- [93] <http://www.piezo.com/tech1terms.html#capac>
- [94] Guyomar D. & Lallart M., “Recent Progress in Piezoelectric Conversion and Energy Harvesting Using Non Linear Electronic Interfaces and Issues in Small Scale Implementation”, *Micromachines* Volume 2 No 2, 2011.

- [95] Ottman G. K., Hofmann H. F., Bhatt A. C., Lesieutre G. A., “Adaptive Piezoelectric Energy Harvesting Circuit for Wireless Remote Power Supply”, IEEE Transactions On Power Electronics, Vol. 17, No. 5, 2002.
- [96] <http://www.thetaeng.com/designIdeas/FETBridge.html>
- [97] Garbuio L., Lallart M., Guyomar D., Richard C., Audigier D., “Mechanical Energy Harvester with Ultralow Threshold Rectification Based on SSHI Nonlinear Technique”, IEEE Transactions On Industrial Electronics, Vol. 56, No. 4, April 2009.
- [98] Lefeuvre, E., Sebald, G., Guyomar, D., Lallart, M., Richard, C., “Materials, structures and power interfaces for efficient piezoelectric energy harvesting”, Journal of Electroceramics, Volume 22 Issue 1, pages 171-179, 2009.
- [99] Liu, Y., Tian, G., Wang, Y., Lin, J., Zhang, Q., Hofman, H.F. “Active piezoelectric energy harvesting: general principles and experimental demonstration” Journal of Intelligent Material Systems and Structures, Vol 20 No 5, pages 575-585, 2009.
- [100] Lallart, M., Garbuio, L., Richard, C., Guyomar, D., “High efficiency, low-cost capacitor voltage inverter for outstanding performances in piezoelectric energy harvesting.” IEEE Transactions on Ultrasonics, Ferroelectrics and Frequency Control, Vol 57 No 2, pages281-291, 2010.
- [101] Lallart, M., Garbuio, L., Petit, L., Richard, C., Guyomar, D. Double Synchronized Switch Harvesting (DSSH): A new energy harvesting scheme for efficient energy extraction. IEEE Transactions on Ultrasonics, Ferroelectrics and Frequency Control, Vol 55 issue 10, pages 2119-2130, 2008.
- [102] Shen, H.; Qiu, J.; Ji, H.; Zhu, K.; Balsi, M. Enhanced synchronized switch harvesting: A new energy harvesting scheme for efficient energy extraction. Smart Mater. Struct. Vol 55, No 10, 2010, 115017.

- [103] Lallart, M., Guyomar, D., “Piezoelectric conversion and energy harvesting enhancement by initial energy injection.” Applied Physics Letters, Vol 97 issue 1, 014104, 2010.
- [104] <http://cds.linear.com/docs/en/datasheet/35881fc.pdf>
- [105] <http://cds.linear.com/docs/en/datasheet/35882fc.pdf>
- [106] [https://en.wikipedia.org/wiki/Electrolytic\\_capacitor](https://en.wikipedia.org/wiki/Electrolytic_capacitor)
- [107] <https://en.wikipedia.org/wiki/Supercapacitor>
- [108] [https://en.wikipedia.org/wiki/Lithium-ion\\_battery](https://en.wikipedia.org/wiki/Lithium-ion_battery)
- [109] [http://batteryuniversity.com/learn/article/charging\\_at\\_high\\_and\\_low\\_temperatures](http://batteryuniversity.com/learn/article/charging_at_high_and_low_temperatures)
- [110] [https://en.wikipedia.org/wiki/Nickel%E2%80%93metal\\_hydride\\_battery](https://en.wikipedia.org/wiki/Nickel%E2%80%93metal_hydride_battery)
- [111] Sodano H A, Inman D J, “Comparison piezoelectric energy harvesting devices for recharging batteries”, Journal of Intelligent Material Systems and Structures, vol. 16 no. 10, 799 – 807, 2005.
- [112] (Varta MBU20 and V80H datasheet).
- [113] Kim D G, Yun S N, Ham Y B, Park J H, “Energy harvesting strategy using piezoelectric element driven by vibration method”, Wireless Sensor Networks, Vol 2 No 2, pp 100-107, 2010.
- [114] <http://powerelectronics.com/energy-harvesting/energy-harvesting-efforts-are-picking-steam>.
- [115] <http://digital.csic.es/bitstream/10261/127788/7/D-c%20Arduino%20uno.pdf>
- [116] <https://www.arduino.cc/en/Tutorial/Blink>
- [117] <https://www.openhomeautomation.net/arduino-battery>
- [118] [https://en.wikipedia.org/wiki/RF\\_module](https://en.wikipedia.org/wiki/RF_module).

[119] <https://electrosome.com/wireless-transmitter-and-receiver-using-ask-rf-module>.

## APPENDIX A

---

### 1. Impedance analysis and $d_{33}$ measurement of 27 mm piezo buzzer

| Sample No. | Resonance frequency (kHz) | Impedance at Resonance ( $\Omega$ ) | Impedance at 40Hz (k $\Omega$ ) | Capacitance at 40Hz (nF) | $d_{33}$ (pC/N) |
|------------|---------------------------|-------------------------------------|---------------------------------|--------------------------|-----------------|
| 1          | 99                        | 7.54                                | 169.83                          | 23.44                    | 463             |
| 2          | 98                        | 7.6                                 | 156.92                          | 25.36                    | 454.33          |
| 3          | 100                       | 7.83                                | 159.92                          | 24.89                    | 461.5           |
| 4          | 99                        | 7.83                                | 164.2                           | 24.23                    | 450.5           |
| 5          | 100                       | 7.92                                | 161.54                          | 24.65                    | 465.67          |
| 6          | 100                       | 8.43                                | 156.36                          | 25.45                    | 441.83          |
| 7          | 99                        | 8.8                                 | 166.86                          | 23.86                    | 473.83          |
| 8          | 99                        | 8.75                                | 162.39                          | 24.51                    | 446.17          |
| 9          | 99                        | 9.09                                | 166.61                          | 23.89                    | 458.33          |
| 10         | 99                        | 8.08                                | 163.4                           | 25.04                    | 455.37          |



## 2. Impedance analysis and d33 measurement of 35 mm piezo buzzer

| Sample No. | Resonance frequency (kHz) | Impedance at resonance ( $\Omega$ ) | Impedance at 40Hz (k $\Omega$ ) | Capacitance at 40Hz (nF) | d33 (pC/N) |
|------------|---------------------------|-------------------------------------|---------------------------------|--------------------------|------------|
| 1          | 77                        | 12.7                                | 138.47                          | 28.74                    | 328.36     |
| 2          | 76                        | 14.91                               | 131.86                          | 30.18                    | 323.1      |
| 3          | 76                        | 24.25                               | 133.12                          | 29.9                     | 333.64     |
| 4          | 77                        | 10.91                               | 133.56                          | 29.8                     | 333.64     |
| 5          | 77                        | 20.52                               | 135.37                          | 29.4                     | 315        |
| 6          | 75                        | 17.48                               | 131.89                          | 30.18                    | 342.64     |
| 7          | 77                        | 16.37                               | 135.56                          | 29.37                    | 288.82     |
| 8          | 77                        | 19.48                               | 133.84                          | 29.73                    | 316.18     |
| 9          | 77                        | 15.19                               | 136.1                           | 29.24                    | 318.9      |
| 10         | 76                        | 20.01                               | 135.33                          | 30.22                    | 326.2      |

**3. Impedance analysis and d33 measurement of drums 27 and 35 mm**

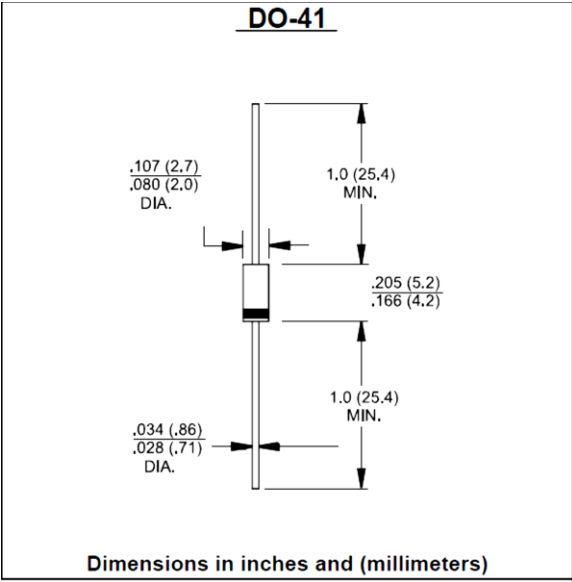
| <b>Sample No.</b> | <b>Resonance frequency (kHz)</b> | <b>Impedance at resonance (<math>\Omega</math>)</b> | <b>Impedance at 40Hz (k<math>\Omega</math>)</b> | <b>Capacitance at 40Hz (nF)</b> | <b>d33 (pC/N)</b> |
|-------------------|----------------------------------|---|---|---------------------------------|-------------------|
| 1                 | 77                               | 12.7  | 138.47  | 28.74                           | 328.36            |
| 2                 | 76                               | 14.91   | 131.86  | 30.18                           | 323.1             |
| 3                 | 76                               | 24.25   | 133.12  | 29.9                            | 333.64            |
| 4                 | 77                               | 10.91   | 133.56  | 29.8                            | 333.64            |
| 5                 | 77                               | 20.52   | 135.37  | 29.4                            | 315               |
| 6                 | 75                               | 17.48   | 131.89  | 30.18                           | 342.64            |
| 7                 | 77                               | 16.37   | 135.56  | 29.37                           | 288.82            |
| 8                 | 77                               | 19.48   | 133.84  | 29.73                           | 316.18            |
| 9                 | 77                               | 15.19   | 136.1   | 29.24                           | 318.9             |
| 10                | 76                               | 20.01   | 135.33  | 30.22                           | 326.2             |

## APPENDIX B

---

### 1. SR 110 schottky diode

| Features  | Mechanical Data   |
|---|---|
| <ul style="list-style-type: none"> <li>_ Low forward voltage drop</li> <li>_ High current capability</li> <li style="padding-left: 20px;">_ High reliability</li> <li>_ High surge current capability</li> </ul>          | <ul style="list-style-type: none"> <li>_ Cases: DO-41 molded plastic</li> <li>_ Epoxy: UL 94V-O rate flame retardant</li> <li>_ Lead: Axial leads, solderable per MILSTD-202, Method 208 guaranteed</li> <li>_ Polarity: Color band denotes cathode end</li> <li>_ High temperature soldering guaranteed: 250OC/10 seconds/.375", (9.5mm) lead lengths at 5 lbs., (2.3kg) tension</li> <li>_ Weight: 0.33 gram</li> </ul> |
| Maximum Recurrent Peak Reverse Voltage - 100 V<br>Maximum RMS Voltage - 70 V<br>Maximum DC Blocking Voltage – 100V<br>Maximum D.C. Reverse Current @ TA=25°C<br>at Rated DC Blocking Voltage – 0.05 mA                    |   |
| Typical Thermal Resistance (Note 1) R $\theta$ JA - 50 °C/W<br>Typical Junction Capacitance (Note 2) - 28 pF<br>Operating Junction Temperature Range TJ - -65 to +150 °C<br>Storage Temperature Range TSTG -65 to +150 °C |   |



**Form Factor**

**2. FDS4559**

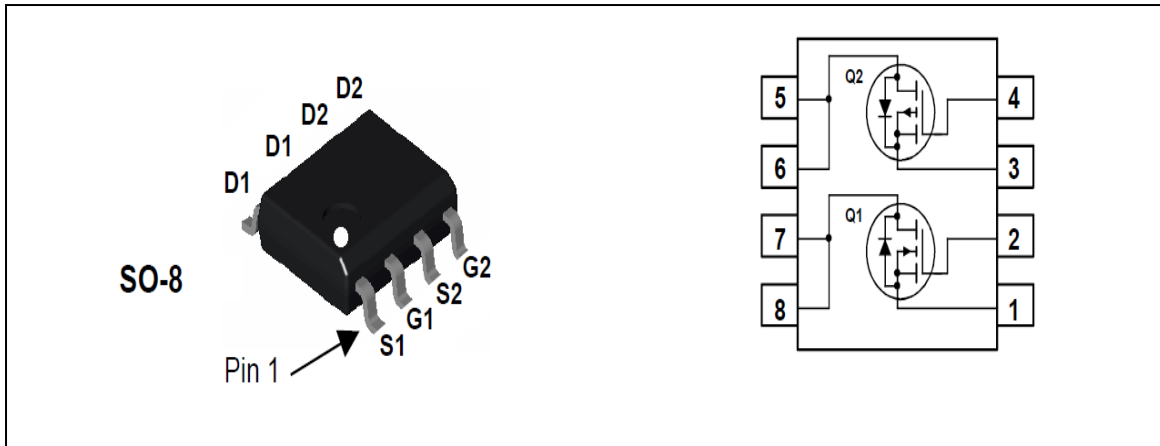
**60V Complementary PowerTrench MOSFET**

**General Description**

This complementary MOSFET device is produced using Fairchild’s advanced PowerTrench process that has been especially tailored to minimize the on-state resistance and yet maintain low gate charge for superior switching performance.

| Applications  | Features   |
|---|--|
| <ul style="list-style-type: none"> <li>• DC/DC converter</li> <li>• Power management</li> <li>• LCD backlight inverter</li> </ul> | <ul style="list-style-type: none"> <li>• <b>Q1: N-Channel</b></li> <li>4.5 A, 60 V RDS(on) = 55 mΩ @ VGS = 10V</li> <li>RDS(on) = 75 mΩ @ VGS = 4.5V</li> <li>• <b>Q2: P-Channel</b></li> <li>-3.5 A, -60 V RDS(on) = 105 mΩ @ VGS = -10V</li> <li>RDS(on) = 135 mΩ @ VGS = -4.5V</li> </ul> |

## Pin Configuration

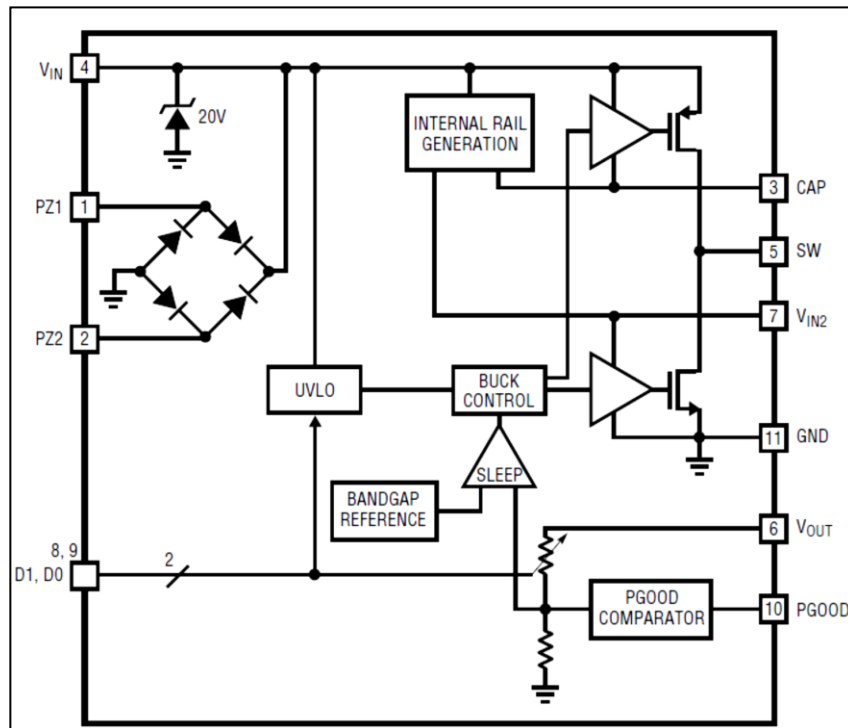


## APPENDIX C

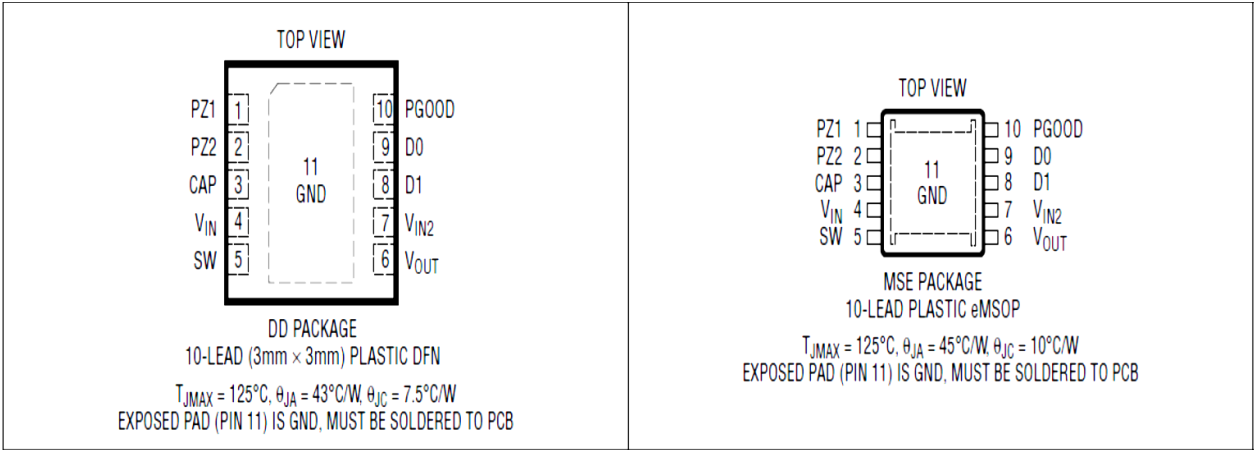
### 1. Pin logic level for controlling the voltage output of LTC 3588 in appendix.

| PIN INPUT |    | LTC 3588 – 1    |            | LTC 3588 – 2    |            |
|-----------|----|-----------------|------------|-----------------|------------|
| D1        | D0 | VOUT<br>(volts) | IVOUT (nA) | VOUT<br>(volts) | IVOUT (nA) |
| 0         | 0  | 1.8             | 44         | 3.45            | 86         |
| 0         | 1  | 2.5             | 62         | 4.1             | 101        |
| 1         | 0  | 3.3             | 81         | 4.5             | 111        |
| 1         | 1  | 3.6             | 89         | 5.0             | 125        |

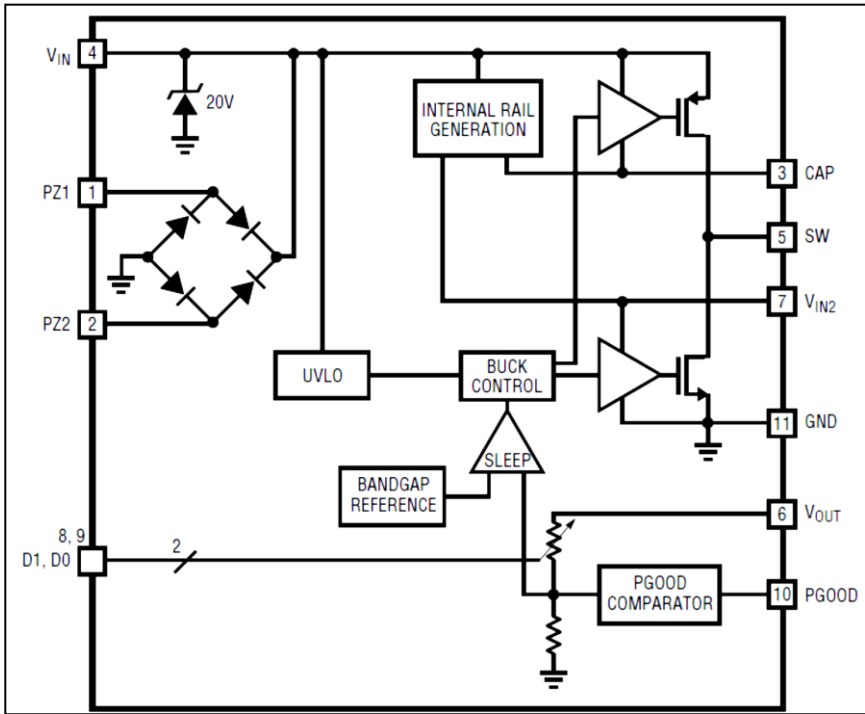
### 2. Internal block diagram and pin configuration of LTC 3588 – 1 and LTC 3588 –



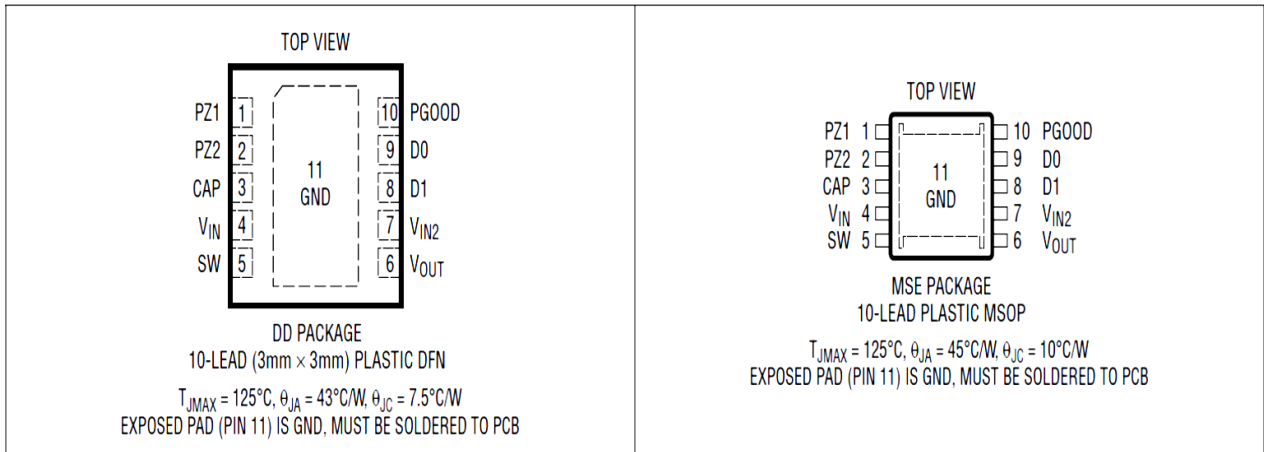
**A. Internal block diagram of LTC 3588 – 1.**



**B. Pin configuration of LTC 3588 – 1.**



**C. Internal block diagram of LTC 3588 – 2.**

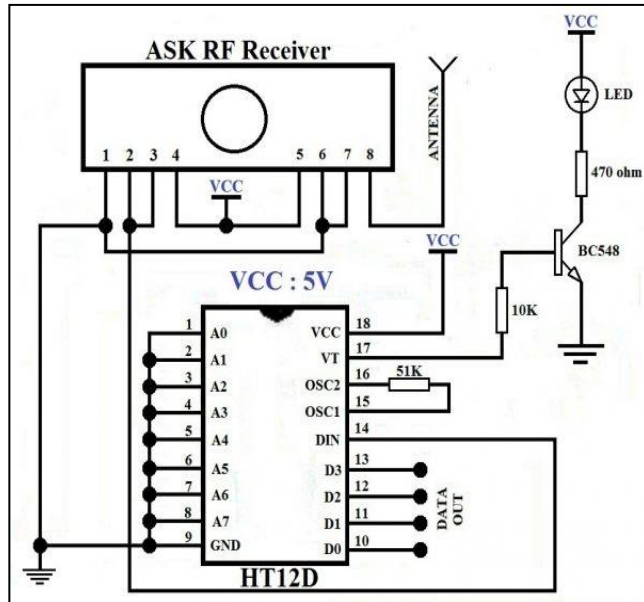


**D. Pin configuration of LTC 3588 – 2.**

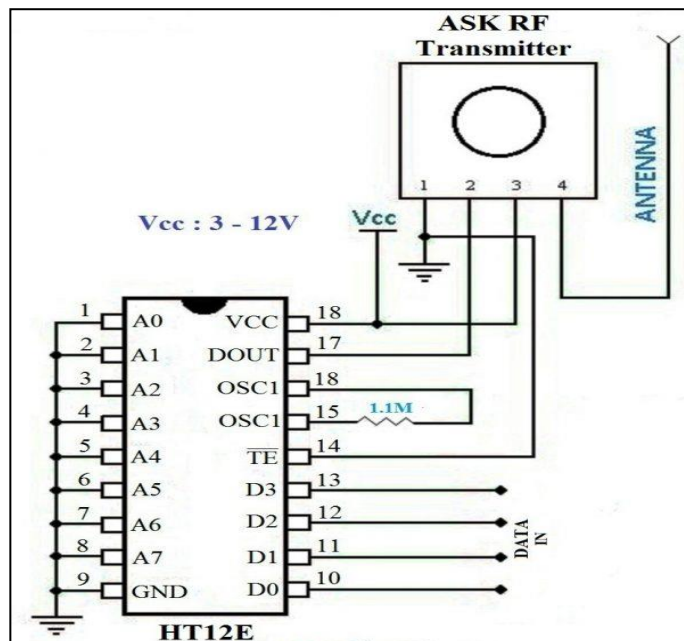


## APPENDIX D

### 1. Circuit diagram for RF transmitter module



### 2. Circuit diagram for RF receiver module



### 3. Arduino Program to flash a LED

```
void setup() {  
  
  // initialize digital pin 13 as an output.  
  
  pinMode(13, OUTPUT);  
  
}  
  
// the loop function runs over and over again forever  
  
void loop() {  
  
  digitalWrite(13, HIGH); // turn the LED on (HIGH is the voltage level)  
  
  delay(1000);           // wait for a second  
  
  digitalWrite(13, LOW); // turn the LED off by making the voltage LOW  
  
  delay(1000);           // wait for a second  
  
}
```